Low-Complexity Signal Processing Algorithms for Wireless Sensor Networks

Tong Wang

Ph.D.

University of York

Electronics

March 2012

Abstract

Recently, wireless sensor networks (WSNs) have attracted a great deal of research interest because of their unique features that allow a wide range of applications in the areas of military, environment, health and home. One of the most important constraints on WSNs is the low power consumption requirement as sensor nodes carry limited, generally irreplaceable, power sources. Therefore, low complexity and high energy efficiency are the most important design characteristics for WSNs. In this thesis, we focus on the development of low complexity signal processing algorithms for the physical layer and cross layer designs for WSNs. For the physical layer design, low-complexity set-membership (SM) channel estimation algorithms for WSNs are investigated. Two matrix-based SM algorithms are developed for the estimation of the complex matrix channel parameters. The main goal is to reduce the computational complexity significantly as compared with existing channel estimators and extend the lifetime of the WSN by reducing its power consumption. For the cross layer design, strategies to jointly design linear receivers and the power allocation parameters for WSNs via an alternating optimization approach are proposed. We firstly consider a two-hop wireless sensor network with multiple relay nodes. Two design criteria are considered: the first one minimizes the mean-square error (MMSE) and the second one maximizes the sum-rate (MSR) of the wireless sensor network. Then, in order to increase the applicability of our investigation, we develop joint strategies for general multihop WSNs. They can be considered as an extension of the strategies proposed for the two-hop WSNs and more complex mathematical derivations are presented. The major advantage is that they are applicable to general multihop WSNs which can provide larger coverage than the two-hop WSNs.

Contents

List of Figures

List of Tables

Acknowledgements

I would firstly like to gratefully acknowledge my supervisor Dr. Rodrigo C. de Lamare for his helpful support and constant encouragement. I have learned an incredible amount from him throughout my Ph.D. research. He has been actively interested in my work and has always been available to advise me. I am deeply benefited from his motivation, enthusiasm, preciseness, patience, and immense knowledge in communications that, taken together, make him a great mentor.

I would also like to thank Dr. Paul D. Mitchell and Prof. Anke Schmeink, for their help, valuable supervision and useful advice for my research, without which much of this work would not have been possible.

Further thanks go to all members of the Communications Research Group, for their help and support throughout my research.

Finally, my deep gratitude goes to my parents and my wife for their unconditional support, endless love and encouragement.

Declaration

Some of the research presented in this thesis has resulted in some publications. These publications are listed at the end of Chapter 1.

All work presented in this thesis as original is so, to the best knowledge of the author. References and acknowledgements to other researchers have been given as appropriate.

Chapter 1

Introduction

Contents

1.1 Overview

Recently, there has been a growing research interest in wireless sensor networks (WSNs) because of their unique features that allow a wide range of applications in the areas of military, environment, health and home [1]. WSNs are usually composed of a large number of densely deployed sensing devices which can transmit their data to the desired user through multihop relays [2]. Low complexity and high energy efficiency are the most important design characteristics of communication protocols [3] and physical layer techniques employed for WSNs. The performance and capacity of these networks can be significantly enhanced by exploiting the spatial diversity with cooperation between the nodes [2]. In a cooperative WSN, nodes relay signals to each other in order to propa-

gate redundant copies of the same signals to the destination nodes. Among the existing relaying schemes, the amplify-and-forward (AF) and the decode-and-forward (DF) are the most popular approaches [4]. Array processing techniques have been used for the selection and positioning of the nodes for WSNs [5, 6]. Due to limitations in sensor node power, computational capacity and memory [1], some power-constrained relay strategies [7, 8] and power allocation methods [35] have been proposed for WSNs to obtain the best possible SNR or best possible quality of service (QoS) at the destinations.

Considering the traditional wireless networks such as cellular systems, the primary goal in such systems is to provide high QoS and bandwidth efficiency. The base stations have easy access to the power supply and the mobile user can replace or recharge exhausted batteries in the handset [1]. However, power conservation is getting more important for wireless networks, especially for WSNs. It is because that one of the most important constraints on WSNs is the low power consumption requirement as sensor nodes carry limited, generally irreplaceable, power sources. Therefore, our research about WSNs will focus primarily on power conservation.

The research project can be divided into two main parts: physical layer design and cross layer design for WSNs. For the physical layer design, we focus on the low complexity channel estimation methods for WSNs. Because most of the research on other layers are based on the assumption of perfect synchronization and available channel state information (CSI) at each node [1], more accurate estimates of the CSI will bring about better performance in WSNs. We investigate the set-membership filtering (SMF) framework and incorporate it into the conventional channel estimation methods. These set-membership channel estimation methods can reduce the computational complexity significantly and extend the lifetime of the WSN by reducing its power consumption. For the cross layer design, we investigate strategies to jointly design linear receivers and the power allocation parameters for WSNs via an alternating optimization approach subject to different kinds of power constraints. These strategies are firstly considered for the two-hop WSNs for simplicity. Then, in order to increase the applicability of our investigation, we develop joint strategies in the general multihop WSNs which can provide larger coverage than the two-hop WSNs. Therefore, more general and more complex mathematical derivations are

presented.

1.2 Contributions

The major contributions in this thesis can be structured as follows:

- Two matrix-based set-membership (SM) algorithms for channel estimation in cooperative WSNs using the AF cooperation protocol are developed. It has been shown that our proposed algorithms can achieve better or similar performance to conventional NLMS and RLS channel estimation, offering reduced computational complexity. The major novelty in these algorithms presented here is that they are matrix-based SM channel estimation algorithms as opposed to vector-based SM techniques for filtering applications [9–11]. Therefore we specify a bound on the norm of the estimation error vector instead of the magnitude of the scalar estimation error. A key contribution is the consideration of techniques to reduce the complexity of the channel estimation for WSNs.

- A novel error bound function is introduced to change the error bound automatically in order to obtain optimal performance with the proposed SM channel estimation algorithms. The incorporation of the time-varying bound function makes them robust to changes in the environment.

- Analytical expressions of the steady-state output excess mean-square error (MSE) of the two SM channel estimation methods are proposed. The novelty in this analysis is that we employ the chi-square distribution to describe the probability of the update for estimating the channel matrix as opposed to the Gaussian distribution for estimating the filter vector [12–14].

- The strategies to jointly design linear receivers and the power allocation parameters via an alternating optimization approach are presented for two-hop WSNs. Two design criteria are considered: the first one minimizes the mean-square error and the second one maximizes the sum-rate of the wireless sensor network. The constrained

MMSE and constrained MSR expressions for the design of linear receivers and the power allocation parameters are derived subject to global, individual and neighbour-based power constraints. Computer simulations show good performance of our proposed methods in terms of bit error rate or sum-rate compared to the method with equal power allocation. Furthermore, the methods with neighbour-based constraints bring flexibility to balance the performance against the computational complexity and the need for feedback information which is desirable for WSNs to extend their lifetime.

- The strategies to jointly design linear receivers and the power allocation parameters via an alternating optimization approach are presented for multihop WSNs. They can be considered as the extension work of the strategies proposed for the two-hop WSNs and more complex mathematical derivations are presented. The major novelty is that they are applicable to general multihop WSNs which can provide larger coverage than the two-hop WSNs.

1.3 Thesis Outline

The structure of the thesis is as follows:

- In Chapter 2, a literature review of WSNs is presented that describes their applications, design factors, relay strategies, channel estimation techniques and power allocation methods. Also, a review of existing adaptive filtering, parameter estimation and an introduction to the set-membership filtering framework are given.

- In Chapter 3, two SM channel estimation methods are proposed based on time-varying bounds for cooperative wireless sensor networks. Analyses of the steady-state MSE and computational complexity are presented for the two channel estimation algorithms and closed-form expressions of the excess MSE and the probability of update are provided. Furthermore, the incorporation of the time-varying bound function makes it robust to changes in the environment.

- In Chapter 4, we consider a two-hop wireless sensor network with multiple relay nodes where the amplify-and-forward scheme is employed. We firstly derive constrained MMSE expressions for the design of linear receivers and power allocation parameters. The constraints include the global, individual and neighbour-based power constraints. Then, we derive constrained MSR expressions for the design of linear receivers and power allocation parameters. The constraints include the global and neighbour-based power constraints. We make use of the alternating optimization algorithms to compute these expressions of linear receivers and power allocation parameters to minimize the mean-square error or maximize the sum-rate of the WSN. Finally, computational complexity and convergence analysis of the proposed optimization algorithms are presented.

- In Chapter 5, we consider a general multihop wireless sensor network with multiple relay nodes where the amplify-and-forward scheme is employed. We firstly derive constrained MMSE expressions for the design of linear receivers and power allocation parameters. The constraints include the global, local and individual power constraints. Then, we derive constrained MSR expressions for the design of linear receivers and power allocation parameters subject to local power constraints. We make use of the alternating optimization algorithms to compute these expressions of linear receivers and power allocation parameters to minimize the mean-square error or maximize the sum-rate of the WSN. Finally, computational complexity and convergence analysis of the proposed optimization algorithms are presented.

- In Chapter 6, we present conclusions and the possible future work based on the content of the thesis.

1.4 Notation

In this thesis, we use bold upper case and lower case letters to denote matrices and vectors, respectively. Unless otherwise stated, all vectors are column vectors. The symbol $\mathbf{I}$ denotes the identity matrix of appropriate dimensions, and the boldface $\mathbf{0}$ denotes ei-

ther a zero vector or a zero matrix. The notation $\|\boldsymbol{x}\|$ denotes the Euclidean norm of a vector. $\Re(\cdot)$ and $\Im(\cdot)$ denote the real and imaginary components of a complex number, respectively. The notation $(\cdot)^*$, $(\cdot)^T$, $(\cdot)^H$ and $(\cdot)^{-1}$ denote the complex conjugate, standard transpose, Hermitian transpose and matrix inverse, respectively. $\odot$ denotes the Hadamard (element-wise) product. $E\{\cdot\}$ denotes the statistical expectation operator and $tr\{\cdot\}$ denotes the trace operator.

1.5 Publication List

Journal Papers

1. T. Wang, R. C. de Lamare, and P. D. Mitchell, "Low-Complexity Set-Membership Channel Estimation for Cooperative Wireless Sensor Networks," *IEEE Transactions on Vehicular Technology*, vol. 60, no. 6, May, 2011.

2. T. Wang, R. C. de Lamare, and A. Schmeink, "Joint Linear Receiver Design and Power Allocation Using Alternating Optimization Algorithms for Wireless Sensor Networks," *IEEE Transactions on Vehicular Technology*, 2012 (accepted).

3. T. Wang, R. C. de Lamare, and A. Schmeink, "Alternating Optimization Algorithms for Power Adjustment and Receive Filter Design in Multihop Wireless Sensor Networks," *IEEE Transactions on Wireless Communications*, 2012 (under review).

Conference Papers

1. T. Wang, R. C. de Lamare and P. D. Mitchell, "Low-Complexity Channel Estimation for Cooperative Wireless Sensor Networks Based on Data Selection," *IEEE Vehicular Technology Conference (VTC)*, May 2010.

2. T. Wang, R. C. de Lamare and P. D. Mitchell, "BEACON Channel Estimation for Cooperative Wireless Sensor Networks Based on Data Selection," *IEEE International Symposium on Wireless Communication Systems (ISWCS)*, September 2010.

3. T. Wang and R. C. de Lamare, ”Joint Receiver Design and Power Allocation Strategies for Wireless Sensor Networks,” *Sensor Signal Processing for Defence(SSPD)*, September 2011.

4. T. Wang, R. C. de Lamare and A. Schmeink, ”Joint Receiver Design and Power Allocation Strategies for Multihop Wireless Sensor Networks,” *IEEE International Symposium on Wireless Communication Systems (ISWCS)*, November 2011.

5. T. Wang, R. C. de Lamare and A. Schmeink, ”Joint Maximum Sum-rate Receiver Design and Power Allocation Strategies for Multihop Wireless Sensor Networks,” *IEEE International Conference on Acoustics, Speech, and Signal Processing (ICASSP)*, March 2012.

Chapter 2

Literature Review

Contents

2.1 Introduction

This chapter presents a literature review of the existing techniques developed for WSNs and the adaptive filtering and estimation algorithms utilized for channel estimation in this thesis. Firstly, a summary of the applications of WSNs is given alongside an introduction to their design factors. Following this, an overview and description of cooperative communication techniques, power allocation and channel estimation methods for WSNs are presented. Then, a review of existing adaptive filtering and parameter estimation al-

gorithms is introduced. Finally, an introduction to the set-membership filtering (SMF) framework which has been widely applied to the adaptive filtering techniques to reduce the computational complexity is given.

2.2 The Applications of WSNs and Design Factors

WSNs are usually composed of a large number of densely deployed sensing devices which are required to sense, compute and transmit their data to the desired users [2]. Recently, there has been a growing research interest in wireless sensor networks (WSNs) because their unique features allow a wide range of applications that include the following [1]:

- Military applications: monitoring friendly forces, equipment and ammunition; battlefield surveillance; reconnaissance of opposing forces and terrain; targeting; battle damage assessment; nuclear, biological and chemical (NBC) attack detection and reconnaissance.
- Environmental applications: forest fire detection; biocomplexity mapping of the environment; flood detection; precision agriculture.
- Health applications: telemonitoring of human physiological data; tracking and monitoring doctors and patients inside a hospital; drug administration in hospitals.
- Home applications: home automation; smart environment.
- Other commercial applications: environmental control in office buildings; interactive museums; detecting and monitoring car thefts; managing inventory control; vehicle tracking and detection.

The design of WSNs is influenced by some factors which include fault tolerance, scalability, production costs, operating environment, sensor network topology, hardware constraints, transmission media and power consumption [1]. Therefore, these factors can be considered as the guideline for our future research. Since the sensors are typically small,

power limited, and have low cost, low complexity and high energy-efficiency are the most important design characteristics of communication protocols [3,15,16] and physical layer techniques.

2.3 Cooperative Communication Techniques

Among the most promising wireless communication techniques that have emerged recently, cooperative diversity [2, 17–20] has shown great potential for improving the performance of wireless networks and meeting the demands of future wireless applications such as WSNs. Cooperative communications [4] exploit spatial diversity through cooperation among distributed antennas belonging to multiple terminals in wireless systems. Signal fading due to multipath propagation can be mitigated by enabling a set of cooperative relays to forward the received information to the destination. A key aspect of the cooperative communications is to process the signal received from the source nodes by the relay nodes [21].

2.3.1 Relay Schemes

A WSN consists of a large number of small sensors which are geographically distributed. Due to limitations in sensor nodes size, power and cost, they are only able to communicate in a short range. Therefore, many relay schemes are used to increase the transmission range [4, 7, 8]. These relay schemes can be categorized into three general groups:

- Amplify-and-Forward (AF): In the AF scheme, the relay nodes amplify the received signal and rebroadcast the amplified signals toward the destination. The advantage of the AF scheme is that it is the simplest among the three schemes. However, the relay nodes amplify not only the desired signal but also both the interference and the noise which will impair the spectrum efficiency of the WSNs.
- Decode-and-Forward (DF): In the DF scheme, the relay nodes first decode the

received signals and then regenerate new signals to the destination subsequently. Compared with the AF scheme, the DF scheme has the advantage of reducing the effect of the interference and the noise at the relay nodes while requiring a higher computational complexity. The drawback is that it entails the possibility of forwarding the incorrectly decoded signals to the destination which will lead to error propagation and the decrease in the performance of the WSNs.

- Compress-and-Forward (CF): In the CF scheme, the relay nodes compress the received signals, exploiting the statistical dependencies between the signals at the nodes and then transmit the quantized signals to the destination. It is shown in [22] that the CF scheme can be applied to a variety of wireless channels and can achieve a rate gain over direct transmission. In [23] and [24], it is shown that CF outperforms DF when the channel between the relay and destination is better than that between the source and relay or the cooperative clustered receivers are considered in the system. The standard source coding and Wyner-Ziv coding (WZC) can be employed by the relay nodes to compress the signal. Compared with the standard source coding [23], the WZC using the rate distortion theory with side information [25] could provide a higher achievable rate in theory.

Among these existing relay schemes, the AF and the DF are the most popular ones due their simplicity in terms of design [4].

2.3.2 Relay Strategies

Another advantage of the relay schemes is that they can exploit the spatial diversity to combat the fading effect of wireless links [7, 8]. This is because of that more than one relay are used to transmit the same signal that forms multiple transmission paths to the destination. In order to make use of this advantage, three distributed relay strategies are proposed which can meet different requirement of the WSNs [7]:

- MMSE strategy with no power constraints: In this method, relays can have different

power usage in order to achieve the desired QoS at the destination node. It can be used to guarantee a certain QoS when QoS has the highest priority and avoid spending more than the necessary amount of power in applications with low QoS requirements.

- Relay strategy with local power constraints: This method is practical when the power budget of each node is fixed and we want to get the best possible SNR or QoS at the destination by spending this power budget.
- Relay strategy with global power constraints: This method is suggested when we are given a global power budget and we can allocate different power shares to different nodes as long as their total power usage does not exceed the global power constraint.

In the distributed relay strategies mentioned above, the relay nodes do not need to share information about the received signals. Furthermore, a cooperative MMSE relay strategy for WSNs is proposed which employs cooperation between relay nodes to forward the signal [8]. A constraint on the global power is considered. Simulation results show that the cooperation between relays can improve the BER performance compared with noncooperative relays.

2.4 Power Allocation Algorithms

Due to the limitations in sensor node energy, computational capacity and memory [1], it is important for WSNs to allocate appropriately their limited energy, radio bandwidth and other resources to maximize the contribution of each node to the whole network. In [26], a resource allocation approach called Self-Organizing Resource Allocation (SORA) is presented which can increase the efficiency of the resource allocation compared with the method manually tuning sensor resource usage.

In WSNs, the power control is one of the most critical roles of resource allocation techniques. Some power allocation methods have been proposed for WSNs to obtain the best

possible SNR or best possible quality of service (QoS) [27, 28] at the destinations. The idea consists of formulating the power allocation problem as a centralized or distributed optimization problem subject to power constraints on certain groups of signals. By adjusting appropriately the power levels used for the links between the sources, the relays and the destinations, significant performance gains can be obtained for a given power budget. The majority of the previous literature considers a source and destination pair, with one or more randomly placed relay nodes. These relay nodes are usually placed with uniform distribution [29], equal distance [30], or in line [31] with the source and destination. The reason for these simple considerations is that they can simplify complex problems and obtain closed-form solutions.

The power allocation for WSNs can be approached in a centralized or a distributed manner. For the centralized approaches [32, 33], a network controller is required which is responsible for monitoring the information of the whole network such as the CSI and SNR, calculating the optimum power allocation parameters of each link and sending them to all nodes via feedback channels. This approach considers all the available links but it has two major drawbacks. The first one is the high computational burden and storage demand at the network controller. The second one is that it requires a significant amount of control information provided by feedback channels which leads to the loss in bandwidth efficiency. For the distributed approaches [34], each node only needs to have the knowledge of its 'partner' information and calculate its own power allocation parameter. Therefore, this approach requires less control information and is ideally suited to distributed WSNs. However, the performance of the distributed approaches is inferior to the centralized approaches.

Most of the research on power allocation for WSNs are based on the assumption of perfect synchronization and available CSI at each node. A WSN is said to have full CSI when all of its nodes have access to accurate and instantaneous CSI. When full CSI is available to all the nodes, the power of each node can be optimally allocated to improve the system efficiency and lower the outage probability [35] or BER [36]. However, it is often difficult to have full CSI in a WSN since the channel state changes frequently and is difficult to be tracked continuously. To address this issue, optimization techniques based

on mean channel gains are known as partial CSI which is easier to obtain in practice. A single relay AF system using mean channel gain CSI is analyzed in [37], where the outage probability is the criterion used for optimization. For DF systems, a near-optimal power allocation strategy called the Fixed-Sum-Power with Equal-Ratio (FSP-ER) scheme based on partial CSI has been developed in [29]. This near-optimal scheme allocates one half of the total power to the source node and splits the remaining half equally among selected relay nodes. A node is selected for relay if its mean channel gain to the destination is above a threshold. Simulation results show that this scheme significantly outperforms two traditional power allocation schemes. One is the 'Constant-Power scheme' where all nodes serve as relay nodes and all nodes including the source node and relay nodes transmit with the same power. The other one is the 'Best-Select scheme' where only one node with the largest mean channel gain to the destination is chosen as the relay node.

Due to the inherent limitations in sensor node size, power and cost [1], they are only able to communicate in a short range. Therefore, multihop communication [38] is employed to provide a large coverage area of the WSNs. By using multihop transmission, the rapid decay of the received signal which is caused by the increased transmission distance can be overcome. Moreover, the pathways around the obstacles between the source and destination can be provided to avoid the signal fading [39]. Several works about the power allocation of the multihop transmission systems have been proposed in [40]- [44]. The work reported in [40] develops a cross-layer model for multihop communication and analyzes the energy consumption of multihop topologies with equal distance and optimal node spacing. The centralized and the distributed schemes for power allocation are presented to minimize the total transmission power under the constraint on the BER at the destination in [41] and [42]. In [43], two optimal power allocation schemes are proposed to maximize the instantaneous received SNR under short-term and long-term power constraints. In [44], the outage probability is considered as the optimization criterion to derive the optimal power allocation schemes under a given power budget for both regenerative and non-regenerative systems.

The BER performance [33, 35], capacity [45] and outage probability [46, 47] are often used as the optimization criterion for the power allocation performance. In [48], a power

allocation method is proposed to maximize the Effective Configuration Duration (ECD) in WSNs. It aims to minimize the signalling overhead for performing relay nodes selection and power allocation which can save power and thus significantly extend the lifetime. Compared with traditional power allocation schemes, this method jointly considers the residual energy of sensors and the mean channel gains. Therefore, the feedback burden is limited and the stability of the topology is increased.

2.5 Channel Estimation Techniques

Power allocation for WSNs has been studied under different CSI assumptions in section 2.4. It indicates that more accurate estimates of the CSI will bring about better performance in WSNs. Moreover, most of the research on other layers are based on the assumption of perfect synchronization and available CSI at each node [1]. Therefore, the method used to estimate the channel coefficients of the WSNs need to be considered.

2.5.1 Conventional LS and MMSE Channel Estimation

Consider a channel estimation problem where the output error is defined as:

$$\mathbf{e} = \mathbf{r} - \mathbf{H}\mathbf{s}, \tag{2.1}$$

where $\mathbf{s}$ is the training sequence symbol vector, $\mathbf{H}$ is the estimated channel matrix and $\mathbf{r}$ is the received signal vector at the destination. Conventional channel estimation schemes seek to find the channel matrix $\mathbf{H}$ by minimizing a cost function which is a suitable objective function of the output error vector $\mathbf{e}$. Among them, the LS and MMSE are the two most widely applied channel estimation algorithms reported for WSNs in [49] and [50].

The LS Channel Estimator

The least squares (LS) channel estimation algorithm minimizes the weighted sum of the squared norm of the error vector $\|\mathbf{e}\|^2$ which can be described as the following optimization problem:

$$\mathbf{H}_{LS}(n) = \arg\min_{\mathbf{H}(n)} \sum_{l=1}^{n} \lambda^{n-l} \|\mathbf{r}(l) - \mathbf{H}(n)\mathbf{s}(l)\|^2, \tag{2.2}$$

where λ denotes the forgetting factor. Computing the gradient of the argument and equating it to a zero matrix, we obtain the LS channel estimator as given by [76]:

$$\mathbf{H}_{LS}(n) = \left[\sum_{l=1}^{n} \lambda^{n-l} \mathbf{r}(l)\mathbf{s}^H(l)\right] \left[\sum_{l=1}^{n} \lambda^{n-l} \mathbf{s}(l)\mathbf{s}^H(l)\right]^{-1}, \tag{2.3}$$

where $(\cdot)^H$ and $(\cdot)^{-1}$ denote the complex-conjugate (Hermitian) transpose and the inverse respectively. The LS estimator has a cubic cost with the number of parameters. A complexity reduction is possible by using a recursive procedure that yields the RLS algorithm which has a quadratic cost [65].

The MMSE Channel Estimator

The minimum mean square error (MMSE) channel estimation algorithm minimizes the expected value of the squared norm of the error vector $\|\mathbf{e}\|^2$ which can be described as the following optimization problem:

$$\mathbf{H}_{MMSE} = \arg\min_{\mathbf{H}} E[\|\mathbf{r} - \mathbf{H}\mathbf{s}\|^2]. \tag{2.4}$$

After some derivation, the MMSE channel estimator is given by [77]:

$$\mathbf{H}_{MMSE} = \frac{\rho}{M}\mathbf{R}\mathbf{S}^H \left(E[\mathbf{H}^H\mathbf{H}]^{-1} + \frac{\rho}{M}\mathbf{S}\mathbf{S}^H\right)^{-1}, \tag{2.5}$$

where ρ is the signal to noise ratio (SNR), $\mathbf{S}$ and $\mathbf{R}$ are the training sequence symbol matrix and the received symbol matrix, respectively, during a training period with length M. The MMSE channel estimator requires the full a priori knowledge of the channel correlation matrix and the SNR and has a cubic cost with the number of parameters.

2.5.2 Channel Estimation for WSNs

Two different pilot-symbol-assisted channel estimation methods are proposed based on the two-hop AF relay network [49]:

- The first estimation method is the cascaded channel estimation (C-CE). It estimates the source-to-relay channel and the relay-to-destination channel together as a cascaded channel at the destination.
- The second estimation method is the disintegrated channel estimation (D-CE). It estimates the source-to-relay channel and the relay-to-destination channel at the relay and destination, respectively. This method feeds forward a quantized version of the source-to-relay channel estimate to the destination.

Simulation results demonstrate that C-CE outperforms D-CE when the number of quantization bits is small. As the number of employed quantization bits increase, D-CE will outperform C-CE. It should be also noted that compared with D-CE, C-CE has an inherent advantage which is the lower cost of equipping the relay with a channel estimator and a vector quantizer. Therefore, C-CE becomes particularly attractive for WSNs.

The optimal training (pilot-symbol) design for channel estimation has been introduced in [51] to improve the performance of cascaded channel estimation. It shows that the optimal training can be achieved from an arbitrary sequence and a set of well designed precoding matrices for all relay nodes. The whole design process is efficiently conducted by dividing it into a convex optimization problem plus a matrix calculation problem. Also, some popular space time coding (STC) techniques [52, 53] are applied in [51] to simplify the relay design. Besides these direct training-based methods, a semi-blind method which only employs a very short training sequence is proposed in [54]. This efficient channel estimation is analyzed theoretically and verified by simulations. They show that it can achieve high estimation accuracy and outperform the direct training-based channel estimation.

2.6 Adaptive Filtering and Estimation Algorithms

A filter (or estimator) is a system which is designed to extract the desired information contained in the input signal by mapping it to the output signal. Therefore, filtering is a signal processing operation that processes the signal to manipulate the information contained in the signal.

Figure 2.1 illustrates the block diagram of the general adaptive filtering system, where n denotes the number of iterations. $\mathbf{x}(n) = [x_1(n), x_2(n), ..., x_N(n)]^H$ is the input signal vector. $y(n)$ and $d(n)$ are the output signal and desired signal, respectively. $e(n)$ is the error signal which is calculated by $d(n) - y(n)$.

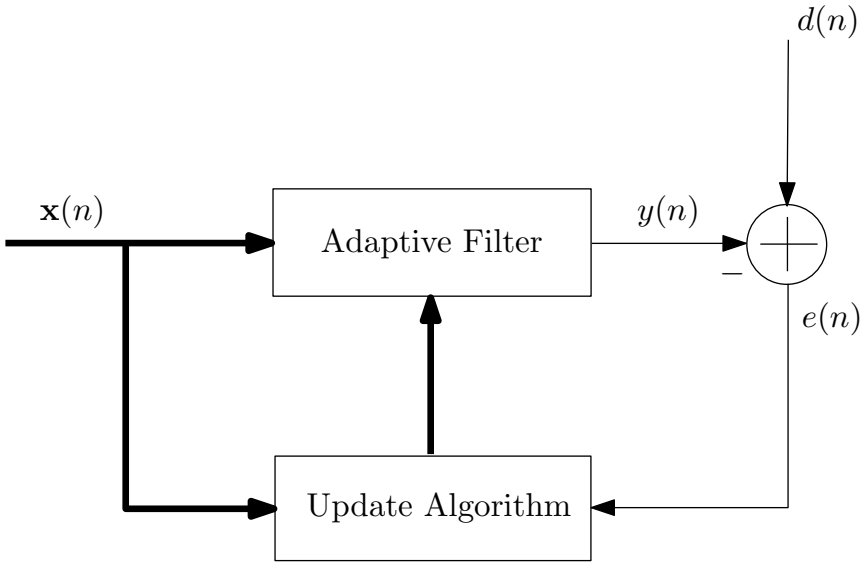

Figure 2.1: Block diagram of the general adaptive filter

The classical applications of the adaptive filtering include system identification, beamforming, interference cancelation, channel equalization and channel estimation [55]- [61].

2.6.1 Wiener Filter

The Wiener filter is a widely used filter which represents the optimal solution for the parameters of the adaptive filter. It employs the mean-square error (MSE) cost function defined as

$$\begin{aligned} J_{\mathrm{MSE}}(n) = E[|e(n)|^2] &= E[|d(n) - y(n)|^2] \\ &= E[|d(n) - \mathbf{w}^H(n)\mathbf{x}(n)|^2]. \end{aligned} \tag{2.6}$$

The aim of the Wiener filter is to minimize the MSE. Therefore, by setting the gradient of J_{MSE} in (2.6) with respect to the filter $\mathbf{w}(n)$ equal to zero:

$$\frac{\partial J_{\mathrm{MSE}}(n)}{\partial \mathbf{w}(n)} = -2\mathbf{p} + 2\mathbf{R}\mathbf{w}(n) = \mathbf{0}, \tag{2.7}$$

where $\mathbf{R} = E[\mathbf{x}(n)\mathbf{x}^H(n)]$ is the autocorrelation of the input signal, $\mathbf{p} = E[\mathbf{x}(n)d^*(n)]$ is the cross-correlation between the input signal and the desired signal. $(.)^*$ denotes the complex conjugate. Then, we get the Wiener (optimal) solution

$$\mathbf{w}_{\mathrm{MMSE}}(n) = \mathbf{R}^{-1}\mathbf{p}, \tag{2.8}$$

In practice, the perfect estimates of $\mathbf{R}$ and $\mathbf{p}$ are not available because they are statistical values. When the input signals and desired signals are ergodic, the values of $\mathbf{R}$ and $\mathbf{p}$ can be estimated by using time averages.

2.6.2 Least-Mean-Square Algorithm

As mentioned above, the parameters that determine the Wiener solution are not available in practice. An alternative method is to estimate these parameters using known signals and make use of these estimates to search the optimal values using the adaptive algorithms. As a result, adaptive filter coefficients can converge to the Wiener solution in some sense. Some classical searching methods of optimization theory [62]- [64] such as the Newton and steepest-descent algorithms have been investigated for the adaptive filtering.

A steepest-descent-based algorithm can be used to search the Wiener solution in (2.8) as follows:

$$\mathbf{w}(n+1) = \mathbf{w}(n+1) + \mu[-2\hat{\mathbf{p}}(n) + 2\hat{\mathbf{R}}(n)\mathbf{w}(n)], \tag{2.9}$$

where μ is the step size of the algorithm that controls the speed of the updating. $\hat{\mathbf{R}}(n)$ and $\hat{\mathbf{p}}(n)$ denote the estimates of $\mathbf{R}$ and $\mathbf{p}$ at time instance n which can be obtained as follows:

$$\hat{\mathbf{R}}(n) = \mathbf{x}(n)\mathbf{x}^H(n) \tag{2.10}$$

$$\hat{\mathbf{p}}(n) = \mathbf{x}(n)d^*(n) \tag{2.11}$$

By substituting (2.10) and (2.11) into (2.9), we get

$$\begin{aligned} \mathbf{w}(n+1) &= \mathbf{w}(n) + \mu[-2\mathbf{x}(n)d^*(n) + 2\mathbf{x}(n)\mathbf{x}^H(n)\mathbf{w}(n)] \\ &= \mathbf{w}(n) + 2\mu\mathbf{x}(n)[d^*(n) - \mathbf{x}^H(n)\mathbf{w}(n)] \\ &= \mathbf{w}(n) + 2\mu\mathbf{x}(n)e^*(n). \end{aligned} \tag{2.12}$$

Equation (2.12) is the updating equation of the gradient-based algorithm known as the least-mean-square (LMS) algorithm.

The LMS algorithm is one of the most widely used algorithms in adaptive filtering. The main advantage of it is the low computational complexity because it does not require computing the correlation functions and the matrix inversion.

2.6.3 Least Squares Algorithm

Besides the MSE, the least squares (LS) error is another way to define the cost function that satisfies the optimality. For the LS algorithms, the cost function is given by

$$\begin{aligned} J_{\mathrm{LS}}(n) &= \sum_{i=0}^{n} \lambda^{n-i}\epsilon(i)^2 \\ &= \sum_{i=0}^{n} \lambda^{n-i}[d(i) - \mathbf{w}^H(n)\mathbf{x}(i)]^2, \end{aligned} \tag{2.13}$$

where λ is an exponential weighting factor called forgetting factor and $\epsilon(i)$ is the a posteriori output error at time instant i which is computed after the adaptive filter coefficient is updated. By setting the gradient of J_{LS} in (2.13) with respect to the filter $\mathbf{w}(n)$ equal to zero, we obtain

$$\frac{\partial J_{\mathrm{LS}}(n)}{\partial \mathbf{w}(n)} = -2\sum_{i=0}^{n} \lambda^{n-i}\mathbf{x}(i)[d^*(i) - \mathbf{x}^H(i)\mathbf{w}(n)] = \mathbf{0}. \tag{2.14}$$

Therefore, the expression for the optimal coefficient vector $\mathbf{w}(n)$ that minimizes the LS error is given by

$$\mathbf{w}_{\mathrm{LS}}(n) = \left[\sum_{i=0}^{n} \lambda^{n-i}\mathbf{x}(i)^H\mathbf{x}(i)\right]^{-1} \sum_{i=0}^{n} \lambda^{n-i}\mathbf{x}(i)d^*(i) \tag{2.15}$$

When $\lambda = 1$ and n tends to infinity, it can be seen from (2.15) that the LS solution will tend to the Wiener solution.

2.6.4 Recursive Least-Squares Algorithm

The main drawback of the LS algorithm is the high computational complexity caused by the matrix inversion. In practice, the computation of the inverse matrix can be avoided by employing the matrix inverse lemma [65] which reduces the computational complexity. As a result, the LS solution can be computed in an recursive form resulting in the recursive least-squares (RLS) algorithm.

Let

$$\boldsymbol{\phi}(n) = \sum_{i=0}^{n} \lambda^{n-i}\mathbf{x}(i)^H\mathbf{x}(i) \tag{2.16}$$

and

$$\mathbf{z}(n) = \sum_{i=0}^{n} \lambda^{n-i}\mathbf{x}(i)d^*(i) \tag{2.17}$$

Eqation (2.15) becomes:

$$\mathbf{w}(n) = \boldsymbol{\phi}^{-1}(n)\mathbf{z}(n) \tag{2.18}$$

Isolating the term corresponding to $i = n$ from the rest of the summation on the right-hand side of (2.16), we may write:

$$\boldsymbol{\phi}(n) = \lambda\left[\sum_{i=0}^{n-1} \lambda^{n-1-i}\mathbf{x}(i)\mathbf{x}^H(i)\right] + \mathbf{x}(n)\mathbf{x}^H(n) \tag{2.19}$$

The expression inside the brackets on the right-hand side of (2.19) equals $\boldsymbol{\phi}(n-1)$. Hence, we have the following recursion for updating the value of $\boldsymbol{\phi}(n)$:

$$\boldsymbol{\phi}(n) = \lambda\boldsymbol{\phi}(n-1) + \mathbf{x}(n)\mathbf{x}^H(n) \tag{2.20}$$

Similarly, we may use (2.17) to derive the following recursion for updating $\mathbf{z}(n)$:

$$\mathbf{z}(n) = \lambda \mathbf{z}(n-1) + \mathbf{x}(i)d^*(i) \tag{2.21}$$

Then, using the matrix inversion lemma, we obtain the following recursive equation for the inverse of $\boldsymbol{\phi}(n)$:

$$\boldsymbol{\phi}^{-1}(n) = \lambda^{-1}\boldsymbol{\phi}^{-1}(n-1) - \frac{\lambda^{-2}\boldsymbol{\phi}^{-1}(n-1)\mathbf{x}(n)\mathbf{x}^H(n)\boldsymbol{\phi}^{-1}(n-1)}{1+\lambda^{-1}\mathbf{x}^H(n)\boldsymbol{\phi}^{-1}(n-1)\mathbf{x}(n)} \tag{2.22}$$

For convenience of computation, let:

$$\mathbf{P}(n) = \boldsymbol{\phi}^{-1}(n) \tag{2.23}$$

and

$$\mathbf{k}(n) = \frac{\lambda^{-1}\mathbf{P}(n-1)\mathbf{x}(n)}{1+\lambda^{-1}\mathbf{x}^H(n)\mathbf{P}(n-1)\mathbf{x}(n)} \tag{2.24}$$

Therefore, we may rewrite (2.18) and (2.22) as:

$$\mathbf{w}(n) = \mathbf{P}(n)\mathbf{z}(n) \tag{2.25}$$

$$\mathbf{P}(n) = \lambda^{-1}\mathbf{P}(n-1) - \lambda^{-1}\mathbf{k}(n)\mathbf{x}^H(n)\mathbf{P}(n-1) \tag{2.26}$$

Then we substitute (2.21) and (2.26) into (2.25) to obtain a recursive equation for updating the adaptive filter coefficient $\mathbf{w}(n)$:

$$\mathbf{w}(n) = \mathbf{w}(n-1) - \mathbf{k}(n)\mathbf{x}^H(n)\mathbf{w}(n-1) + \mathbf{P}(n)\mathbf{x}(n)d^*(n) \tag{2.27}$$

By rearranging (2.24) , we can get:

$$\begin{aligned}\mathbf{k}(n) &= [\lambda^{-1}\mathbf{P}(n-1) - \lambda^{-1}\mathbf{k}(n)\mathbf{x}^H(n)\mathbf{P}(n-1)]\mathbf{x}(n) \\ &= \mathbf{P}(n)\mathbf{x}(n)\end{aligned} \tag{2.28}$$

Using (2.28) above, we get the desired recursive equation for updating $\mathbf{w}(n)$:

$$\mathbf{w}(n) = \mathbf{w}(n-1) + \mathbf{k}(n)\xi^*(n) \tag{2.29}$$

where $\xi(n) = d(n) - \mathbf{w}^H(n-1)\mathbf{x}(n)$ denotes the a priori output error at time instant n. Table 2.1 and table 2.2 show the summary of the LMS and the RLS algorithms.

Table 2.1: Summary of the LMS Algorithm

Initialize the algorithm by setting

$$\mathbf{w}(0) = 0$$

For each instant of time, n=0, 1, 2, ..., compute

$$e(n) = d(n) - \mathbf{w}^H(n)\mathbf{x}(n)$$

$$\mathbf{w}(n+1) = \mathbf{w}(n) + 2\mu\mathbf{x}(n)e^*(n)$$

Table 2.2: Summary of the RLS Algorithm

Initialize the algorithm by setting

$$\mathbf{w}(0) = 0$$

$$\mathbf{P}(0) = \mathbf{I}$$

For each instant of time, n=1, 2, ..., compute

$$\xi(n) = d(n) - \mathbf{w}^H(n-1)\mathbf{x}(n)$$

$$\mathbf{k}(n) = \frac{\lambda^{-1}\mathbf{P}(n-1)\mathbf{x}(n)}{1+\lambda^{-1}\mathbf{x}^H(n)\mathbf{P}(n-1)\mathbf{x}(n)}$$

$$\mathbf{w}(n) = \mathbf{w}(n-1) + \mathbf{k}(n)\xi^*(n)$$

$$\mathbf{P}(n) = \lambda^{-1}\mathbf{P}(n-1) - \lambda^{-1}\mathbf{k}(n)\mathbf{x}^H(n)\mathbf{P}(n-1)$$

2.7 Set-membership Filtering

Set-membership filtering (SMF) represents a class of recursive estimation algorithms which have been applied to the conventional system identification problem in order to improve the performance in terms of high convergence speed, low misadjustment and a reduced number of updates.

Consider a general adaptive filter where the estimation error is defined as

$$e(n) = d(n) - \mathbf{w}^H(n)\mathbf{x}(n), \tag{2.30}$$

where $\mathbf{x}(n) = [x_1(n), x_2(n), ..., x_N(n)]^H$ denotes the input signal vector, $\mathbf{w}(n) = [w_1(n), w_2(n), ..., w_N(n)]^H$ denotes the parameter vector and $d(n)$ denotes the desired signal sequence. The SMF specifies an upper bound γ on the magnitude of the estimation output error over a model space of interest which is denoted as S, comprising all possible input-desired signal pairs $(\mathbf{x}, d)$. The set-membership (SM) criterion corresponds to

finding **w** that satisfies

$$|e(n)|^2 \leq \gamma^2 \quad \forall(\mathbf{x}, d) \in S. \tag{2.31}$$

The set of all possible **w** that satisfy (2.31) is referred to as the feasibility set and can be expressed as

$$\Theta = \bigcap_{(\mathbf{x},d)\in S} \left\{\mathbf{w} \in C^N : |d - \mathbf{w}^H\mathbf{x}| \leq \gamma\right\}. \tag{2.32}$$

At time instant n, the constraint set C_n is defined as the set of all $\mathbf{w}(n)$ that satisfy (2.31) for the input-desired signal pairs $(\mathbf{x}(n), d(n))$

$$C_n = \left\{\mathbf{w}(n) \in C^N : |d(n) - \mathbf{w}^H(n)\mathbf{x}(n)| \leq \gamma\right\}. \tag{2.33}$$

where $\mathbf{w}(n)$ denotes a specific instance of **w**. It can be depicted in Figure 2.2 where C_n comprises the region between the two lines $d(n) - \mathbf{w}^H(n)\mathbf{x}(n) = \pm\gamma$. The intersection of the constraint sets C_n over all time instants i=1,2,...,n is called the exact membership set and is given by

$$\psi(n) = \bigcap_{i=1}^{n} C_i. \tag{2.34}$$

It can be seen that the feasibility set Θ is a subset of the exact membership set $\psi(n)$ at any given time instant.

The key strategy of the formulation is to find a feasibility set such that the bounded error specification is met for any member of this set. As a result, the SMF is aimed at estimating the feasibility set itself or a member of this set [61]. It employs a deterministic objective function related to a bounded error constraint on the filter output to make sure that all the updates belong to a set of feasible solutions. Any update whose output estimation error is smaller than the given bounds is an acceptable solution. Therefore,

$$d(n) - \mathbf{w}^H(n)\mathbf{x}(n) = \gamma$$

$$C_n$$

$$d(n) - \mathbf{w}^H(n)\mathbf{x}(n) = -\gamma$$

Figure 2.2: Constraint set C_n about $\mathbf{w}(n)$

SMF-based designs allow the reduction of computational complexity in detection, estimation and filtering operations, as it updates the parameters only when the output error is higher than a pre-determined upper bound.

The SMF framework has been applied to adaptive filtering algorithms widely. The algorithms include the set-membership normalized LMS algorithm (SM-NLMS) [66], the BEACON algorithm [10, 67], the set-membership affine projection algorithm (SM-AP) [68] and the set-membership binormalized data-reusing LMS algorithms (SM-BNDRLMS) [69]. As compared with their competing algorithms [65], these set-membership algorithms offer a number of advantages. First, they are able to achieve good convergence and tracking performance. Second, they can save a large number of filter updates due to the data-selective updating. This allows a substantial reduction in complexity and an extension of battery life, without performance degradation which is desirable for the WSNs. Therefore, the SM-based algorithms can be also considered for the receiver design, interference cancelation and channel estimation for the WSNs.

An open issue for the SM algorithms is the appropriate selection of the error bound, because it has a critical effect on their performance. The extreme settings of the bound, namely, overbounding (the error bound being too large) and underbounding (the error bound being too small) will result in performance degradation [71, 72]. In practice, the bound depends on the environmental parameters such as the SNR. It is very difficult to determine the optimal error bound accurately because there is usually insufficient knowledge about the underlying system. The required error bound may be time variant due to changing environmental conditions. The parameter-dependent error bound [67, 71] and an adaptive error bound [73] have been proposed to reduce the risk of overbounding and underbounding of the SM algorithms.

Chapter 3

Low-Complexity Set-Membership Channel Estimation for Cooperative WSNs

Contents

3.1 Introduction

Due to limitations in sensor node power, computational capacity and memory [1], some power-constrained relay strategies [7, 8] and power allocation methods [35] have been proposed for WSNs to obtain the best possible SNR or best possible quality of service

(QoS) at the destinations. Most of these ideas are based on the assumption of perfect synchronization and available channel state information (CSI) at each node [1]. This shows the importance of channel estimation and suggests that more accurate estimates of the CSI will bring about better performance in WSNs.

The normalized least mean squares (NLMS) estimation method is appropriate for WSNs due to its simplicity. However, the main problem of the NLMS is that the tradeoff between convergence speed and steady state performance is achieved through the introduction of a step size [65]. It is not possible to achieve the best solution on these two aspects using a conventional NLMS estimation method. Channel estimation with the NLMS algorithm can be improved by introducing the set-membership filtering (SMF) framework [67] which modifies the objective function of the NLMS algorithm. It specifies an error bound on the magnitude of the estimation error, which can make the step size adaptive. Therefore the SM-NLMS channel estimation method can achieve good convergence and tracking performance for each update. An SM-NLMS channel estimation algorithm for cooperative WSNs is proposed in [74]. Compared with the NLMS channel estimation method, the RLS channel estimator can provide better performance in terms of the convergence speed and steady state [65]. However, it is not suitable for WSNs due to its high computational complexity [65]. In order to overcome this shortcoming, the SMF framework can be employed to devise a computationally efficient version of the conventional RLS channel estimation method, called BEACON channel estimation. It can be considered as a constrained optimization problem where the objective function is the least squares (LS) cost function and the constraint is a bound on the magnitude of the estimation error. As a result, an adaptive forgetting factor can be derived to achieve the optimal performance for each update. Most importantly, the set-membership (SM) algorithms possess a feature that allows updating for only a small fraction of the time, expressed as the update rate (UR). Therefore, the UR of the two SM channel estimation algorithms decreases due to the data-selective update which can reduce the computational complexity significantly and extend the lifetime of the WSN by reducing its power consumption.

The biggest issue for the SM channel estimation is the appropriate selection of the er-

ror bound, because it has a critical effect on the estimation performance. For SM-NLMS channel estimation, the extreme settings of the bound, namely, overbounding (the error bound being too large) and underbounding (the error bound being too small) will result in performance degradation [71, 72]. In practice, the bound depends on the environmental parameters such as the SNR. It is very difficult to determine the optimal error bound accurately because there is usually insufficient knowledge about the underlying system. For the BEACON channel estimation, the value of the error bound can be varied to trade off achievable performance against computational complexity [10]. A higher error bound would result in lower UR but worse performance. For WSNs the aim is to achieve an acceptable CSI quickly with low power consumption. Therefore, the bound for BEACON channel estimation should be adjusted to ensure good estimation performance, lower computational complexity and a low UR. Also, the required error bound may be time variant due to changing environmental conditions.

In this chapter, we develop two matrix-based SM algorithms for channel estimation in cooperative WSNs using the AF cooperation protocol. The major novelty in these algorithms presented here is that they are matrix-based SM channel estimation algorithms as opposed to vector-based SM techniques for filtering applications [9–11]. Therefore we specify a bound on the norm of the estimation error vector instead of the magnitude of the scalar estimation error. Then, a novel error bound function is introduced to change the error bound automatically in order to obtain optimal performance with the proposed SM channel estimation. Furthermore, we propose analytical expressions of the steady-state output excess mean-square error (MSE) of the two SM channel estimation methods. Further novelty in this analysis is that we employ the chi-square distribution to describe the probability of the update for estimating the channel matrix as opposed to the Gaussian distribution for estimating the filter vector [12–14]. A key contribution of this work is the consideration of techniques to reduce the complexity of the channel estimation for WSNs.

This chapter is organized as follows. Section 3.2 describes the general cooperative WSN system model and its constrained form. Section 3.3 proposes two channel estimation methods using the SMF framework and presents an error bound function which tunes the error bound automatically. Section 3.4 contains the analysis of the steady-state output

excess MSE and the computational complexity. Section 3.5 presents and discusses the simulation results, while Section 3.6 provides some concluding remarks.

3.2 Cooperative WSN System Model

Consider a general m-hop wireless sensor network (WSN) with multiple parallel relay nodes for each hop, as shown in Figure 3.1. The WSN consists of N_s sources, N_d destinations and N_r relays which are separated into $m-1$ groups: $N_{r(1)}$,$N_{r(2)}$, ... ,$N_{r(m-1)}$. All these nodes are assumed to be within communication range. We will concentrate on a time division scheme with perfect synchronization, for which all signals are transmitted and received in separate time slots. The sources first broadcast the $N_s \times 1$ signal vector $\mathbf{s}$ to the destinations and all groups of relays. We consider an amplify-and-forward (AF) cooperation protocol in this work. Each group of relays receives the signal from the sources and the previous groups of relays, amplifies and rebroadcasts them to the next groups of relays and the destinations. In practice, we need to consider the constraints on the transmission policy. For example, each transmitting node would transmit during only one phase. In our WSN system, we assume that each group of relays transmits the signal to the nearest group of relays and the destinations directly. We can use a block diagram to indicate the cooperative WSN system with these transmission constraints as shown in Figure 3.2.

Let $\mathbf{H}_{s,r(i)}$ denote the $N_{r(i)} \times N_s$ channel matrix between the sources and the ith group of relays, $\mathbf{H}_{r(i),d}$ denote the $N_d \times N_{r(i)}$ channel matrix between the ith group of relays and destinations, and $\mathbf{H}_{r(i-1),r(i)}$ denote the $N_{r(i)} \times N_{r(i-1)}$ channel matrix between two groups of relays. The received signal at the ith group of relays ($\mathbf{x}_i$) and destinations ($\mathbf{d}$) for each phase can be expressed as:

Phase 1:

$$\mathbf{x}_1 = \mathbf{H}_{s,r(1)}\mathbf{s} + \mathbf{v}_{r(1)}, \tag{3.1}$$

$$\mathbf{d}^1 = \mathbf{H}_{s,d}\mathbf{s} + \mathbf{v}_d^1, \tag{3.2}$$

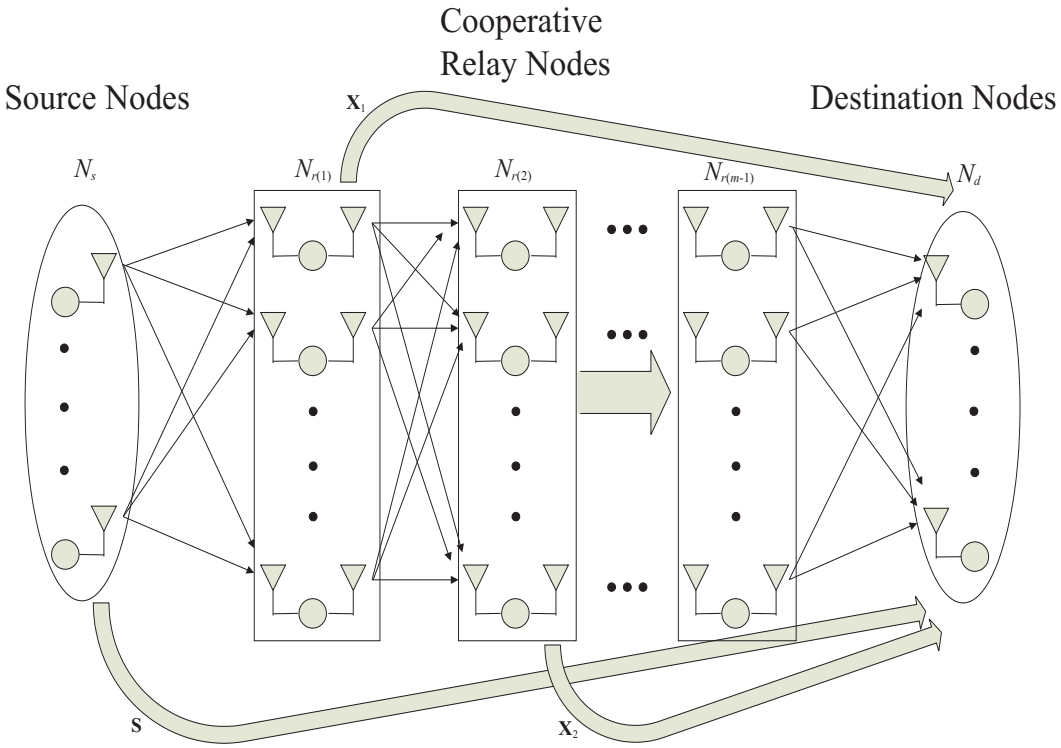

Figure 3.1: An m-hop cooperative WSN with N_s sources, N_d destinations and N_r relays.

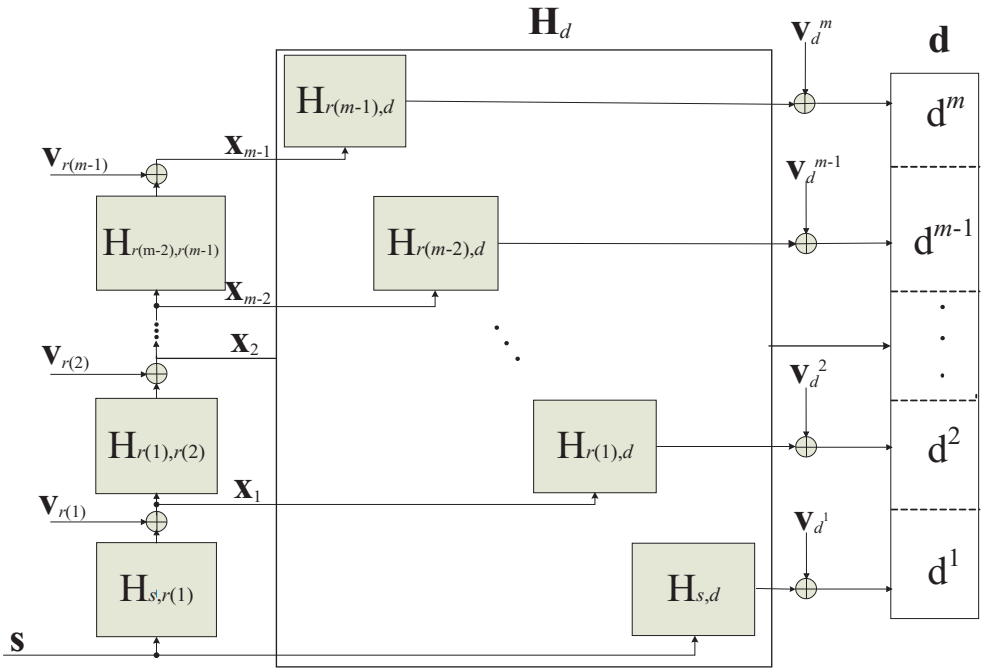

Figure 3.2: Block diagram of the cooperative WSN system with transmission constraints.

Phase 2:

$$\mathbf{x}_2 = \mathbf{H}_{r(1),r(2)}\mathbf{A}_1\mathbf{x}_1 + \mathbf{v}_{r(2)}, \tag{3.3}$$

$$\mathbf{d}^2 = \mathbf{H}_{r(1),d}\mathbf{A}_1\mathbf{x}_1 + \mathbf{v}_d^2, \tag{3.4}$$

$\vdots$

Phase i: $(i = 3, 4, ..., m-1)$

$$\mathbf{x}_i = \mathbf{H}_{r(i-1),r(i)}\mathbf{A}_{i-1}\mathbf{x}_{i-1} + \mathbf{v}_{r(i)}, \tag{3.5}$$

$$\mathbf{d}^i = \mathbf{H}_{r(i-1),d}\mathbf{A}_{i-1}\mathbf{x}_{i-1} + \mathbf{v}_d^i, \tag{3.6}$$

$\vdots$

Phase m:

$$\mathbf{d}^m = \mathbf{H}_{r(m-1),d}\mathbf{A}_{m-1}\mathbf{x}_{m-1} + \mathbf{v}_d^m, \tag{3.7}$$

where $\mathbf{v}$ is a zero-mean circularly symmetric complex additive white Gaussian noise (AWGN) vector with covariance matrix $\sigma^2\mathbf{I}$. $\mathbf{A}_i$ is a diagonal matrix whose elements represent the amplification coefficient of each relay of the ith group. The vectors $\mathbf{d}^i$ and $\mathbf{v}_d^i$ denote the received signal and noise at the destination nodes during the ith phase, respectively. At the destination nodes, the received signal can be expressed as:

$$\mathbf{d} = \mathbf{H}_d\mathbf{A}\mathbf{y} + \mathbf{v}_d, \tag{3.8}$$

where,

$$\mathbf{d} = \begin{bmatrix} \mathbf{d}^m \\ - - - \\ \mathbf{d}^{m-1} \\ - - - \\ \vdots \\ - - - \\ \mathbf{d}^2 \\ - - - \\ \mathbf{d}^1 \end{bmatrix}, \quad \mathbf{v}_d = \begin{bmatrix} \mathbf{v}_d^m \\ - - - \\ \mathbf{v}_d^{m-1} \\ - - - \\ \vdots \\ - - - \\ \mathbf{v}_d^2 \\ - - - \\ \mathbf{v}_d^1 \end{bmatrix}, \quad \mathbf{y} = \begin{bmatrix} \mathbf{x}_{m-1} \\ - - - \\ \mathbf{x}_{m-2} \\ - - - \\ \vdots \\ - - - \\ \mathbf{x}_1 \\ - - - \\ \mathbf{s} \end{bmatrix}, \tag{3.9}$$

$(mN_d \times 1) \qquad (mN_d \times 1) \qquad ((N_r + N_s) \times 1)$

$$\mathbf{H}_d = \begin{bmatrix} \mathbf{H}_{r(m-1),d} & & \cdots & & \mathbf{0} \\ & \mathbf{H}_{r(m-2),d} & & & \\ \vdots & & \ddots & & \vdots \\ & & & \mathbf{H}_{r(1),d} & \\ \mathbf{0} & & \cdots & & \mathbf{H}_{s,d} \end{bmatrix}, \tag{3.10}$$

$$(mN_d \times (N_r + N_s))$$

$$\mathbf{A} = \begin{bmatrix} \mathbf{A}_{m-1} & & \cdots & & 0 \\ & \mathbf{A}_{m-2} & & & \\ \vdots & & \ddots & & \vdots \\ & & & \mathbf{A}_1 & \\ 0 & & \cdots & & \mathbf{I} \end{bmatrix}. \tag{3.11}$$

$$((N_r + N_s) \times (N_r + N_s))$$

Here, we use dashed lines to separate the vectors $\mathbf{d}$, $\mathbf{v}_d$ and $\mathbf{y}$ in order to distinguish between transmissions to the destinations in m different time slots. The matrix $\mathbf{H}_d$ consists of all the channels between each group of relays and destinations. The matrix $\mathbf{A}$ consists of the amplification coefficients of all relays.

In our transmission scheme, all the data packets transmitted from the source nodes and relay nodes contain two parts: a preamble part with training sequence symbols and another part with data symbols. Please see Figure 3.3. The source nodes transmit packets and the relay nodes retransmit those packets that contain the identical training sequence symbols which are known at the destination nodes. Therefore, we can make use of them for channel estimation at the destination nodes. Moreover, the decision directed channel estimation (DD-CE) is exploited in our system by a scheme detailed in Figure 3.4 which is located at the final destination. We consider an MMSE detector whose formula can be expressed as $\mathbf{W}_{MMSE}(n) = [\mathbf{H}(n)\mathbf{H}^H(n) + \frac{\sigma_n^2}{\sigma_s^2}\mathbf{I}]^{-1}\mathbf{H}(n)$ [65], where $\mathbf{H}(n)$ is the estimated channel coefficient at time instant n which can be received from the channel estimator. The block marked with a Q[$\cdot$] represents a decision device. After the training sequence, the channel estimation algorithm is switched to decision directed mode [75]

and the detected data symbols are fed to the channel estimator. It can continue to estimate and track the channel. Therefore, the channel variation can be tracked after the training phase and this can yield better results. Furthermore, this decision directed approach can reduce the length of the training sequence which increases the bandwidth efficiency of the WSNs.

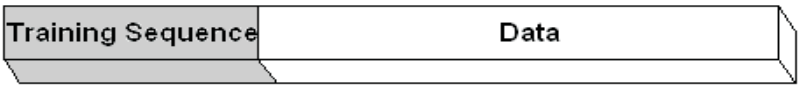

Figure 3.3: The structure of the packet transmitted from source nodes and relay nodes

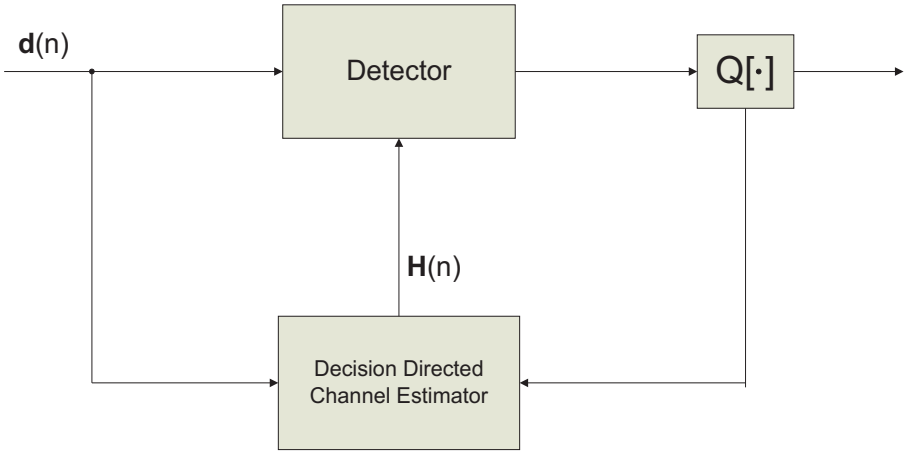

Figure 3.4: The structure of the decision directed channel estimation at the destination

3.3 Set-Membership Channel Estimation

In contrast with the two conventional channel estimation methods introduced in section 2.5.1, set-membership (SM) channel estimation specifies an upper bound γ on the norm of the estimation error vector over a model space of interest which is denoted as S, comprising all possible received signal pairs $(\mathbf{s}, \mathbf{r})$. The SM criterion corresponds to finding $\mathbf{H}$ that satisfies:

$$\|\mathbf{e}(\mathbf{H})\|^2 \leq \gamma^2, \forall(\mathbf{s}, \mathbf{r}) \in S. \tag{3.12}$$

where $\mathbf{e}(\mathbf{H}) = \mathbf{r} - \mathbf{Hs}$. The set of all possible $\mathbf{H}$ that satisfy (3.12) is referred to as the feasibility set and can be expressed as:

$$\Theta = \bigcap_{(\mathbf{s},\mathbf{r})\in S} \left\{\mathbf{H} \in C^{M\times N} : \|\mathbf{r} - \mathbf{Hs}\| \leq \gamma\right\}. \tag{3.13}$$

At time instant n, the constraint set C_n is defined as the set of all $\mathbf{H}(n)$ that satisfy (3.12) for the received signal pairs $(\mathbf{s}(n), \mathbf{r}(n))$:

$$C_n = \left\{\mathbf{H}(n) \in C^{M\times N} : \|\mathbf{r}(n) - \mathbf{H}(n)\mathbf{s}(n)\| \leq \gamma\right\}. \tag{3.14}$$

The idea behind the SM channel estimation is that if the estimated channel at a time instant lies outside the constraint set C_n, the estimated channel at the next time instant will lie on the closest boundary of C_n. Otherwise, there is no need to compute and the power consumption can be significantly reduced. This SM approach makes the estimator adapt only in the direction that is necessary.

3.3.1 Proposed SM-NLMS Channel Estimation

The basic update in the LMS Channel Estimation can be written as:

$$\mathbf{H}(n+1) = \mathbf{H}(n) + \mu(n)\mathbf{e}(n)\mathbf{s}^H(n), \tag{3.15}$$

where $\mathbf{e}(n) = \mathbf{r}(n) - \mathbf{H}(n)\mathbf{s}(n)$ denotes the a priori error vector at time instant n, and $\mu(n)$ is the time-dependent step size. Then we can get a posterior error vector:

$$\mathbf{g}(n) = \mathbf{r}(n) - \mathbf{H}(n+1)\mathbf{s}(n). \tag{3.16}$$

By substituting (3.15) into (3.16), we have:

$$\begin{aligned}\mathbf{g}(n) &= \mathbf{r}(n) - \left(\mathbf{H}(n) + \mu(n)\mathbf{e}(n)\mathbf{s}^H(n)\right)\mathbf{s}(n) \\ &= (\mathbf{r}(n) - \mathbf{H}(n)\mathbf{s}(n)) - \mu(n)\mathbf{e}(n)\mathbf{s}^H(n)\mathbf{s}(n) \\ &= \mathbf{e}(n) - \mu(n)\mathbf{e}(n)\mathbf{s}^{\mathbf{H}}(n)\mathbf{s}(n).\end{aligned} \tag{3.17}$$

The constraint set is described as:

$$\|\mathbf{g}(n)\| = \|\mathbf{e}(n) - \mu(n)\mathbf{e}(n)\mathbf{s}^H(n)\mathbf{s}(n)\| \leq \gamma. \tag{3.18}$$

If $\|\mathbf{e}(n)\| > \gamma$, then the previous solution lies outside the constraint set. We can choose the constraint value $\|\mathbf{g}(n)\|$ equal to γ so that the new solution lies on the closest boundary of the constraint set. Therefore:

$$\|\mathbf{g}(n)\| = \|\mathbf{e}(n)\| \left|1 - \mu(n)\mathbf{s}^H(n)\mathbf{s}(n)\right| = \gamma. \tag{3.19}$$

Hence the step size at the nth iteration $\mu(n)$ can be expressed as:

$$\mu(n) = \frac{1}{\mathbf{s}^H(n)\mathbf{s}(n)} \left(1 - \frac{\gamma}{\|\mathbf{e}(n)\|}\right). \tag{3.20}$$

Finally, we can write the update equation as:

$$\mathbf{H}(n+1) = \mathbf{H}(n) + \mu(n)\mathbf{e}(n)\mathbf{s}^H(n), \tag{3.21}$$

where

$$\mu(n) = \begin{cases} \frac{1}{\mathbf{s}^H(n)\mathbf{s}(n)} \left(1 - \frac{\gamma}{\|\mathbf{e}(n)\|}\right), & \text{if } \|\mathbf{e}(n)\| > \gamma, \\ 0, & \text{otherwise.} \end{cases} \tag{3.22}$$

Equation (3.22) shows that the estimated channel matrix updates with a specified step size, only when the norm of the estimation error vector is larger than a fixed error bound which we set. Otherwise, the step sizes are zeros which means there is no update at these time instants.

3.3.2 Proposed BEACON Channel Estimation

Here, we propose BEACON channel estimation can be considered as the following optimization problem:

$$\begin{gathered} \mathbf{H}(n)_{\text{opt}} = \arg\min_{\mathbf{H}(n)} \sum_{l=1}^{n-1} \lambda(n)^{n-l} \|\mathbf{r}(l) - \mathbf{H}(n)\mathbf{s}(l)\|^2, \\ \text{subject to } \|\mathbf{r}(n) - \mathbf{H}(n)\mathbf{s}(n)\|^2 = \gamma^2. \end{gathered} \tag{3.23}$$

It is a computationally efficient modified version of an optimal bounding ellipsoidal (OBE) algorithm [10], which is closely related to a constrained LS algorithm. To solve this constrained optimization problem, we can modify the LS cost function using the method of Lagrange multipliers which yields the following Lagrangian function:

$$\mathcal{L} = \sum_{l=1}^{n-1} \lambda(n)^{n-l} \|\mathbf{r}(l) - \mathbf{H}(n)\mathbf{s}(l)\|^2 + \lambda(n) \left[\|\mathbf{r}(n) - \mathbf{H}(n)\mathbf{s}(n)\|^2 - \gamma^2\right], \tag{3.24}$$

where $\lambda(n)$ plays the role of both the Lagrange multiplier and the forgetting factor of the LS cost function [67]. By setting the gradient of $\mathcal{L}$ with respect to $\mathbf{H}(n)$ equal to zero, after some mathematical manipulations (see Appendix A), we get the desired recursive equation for updating the channel matrix $\mathbf{H}(n)$:

$$\mathbf{H}(n) = \mathbf{H}(n-1) + \lambda(n)\boldsymbol{\epsilon}(n)\mathbf{k}(n), \tag{3.25}$$

where $\boldsymbol{\epsilon}(n) = \mathbf{r}(n) - \mathbf{H}(n-1)\mathbf{s}(n)$ denotes the prediction error vector at time instant n and the recursive equation for updating the gain vector $\mathbf{k}(n)$ is

$$\mathbf{k}(n) = \frac{\mathbf{s}^H(n)\mathbf{P}(n-1)}{1 + \lambda(n)\mathbf{s}^H(n)\mathbf{P}(n-1)\mathbf{s}(n)}, \tag{3.26}$$

where

$$\mathbf{P}(n) = \mathbf{P}(n-1) - \lambda(n)\mathbf{P}(n-1)\mathbf{s}(n)\mathbf{k}(n). \tag{3.27}$$

The error vector is

$$\mathbf{e}(n) = \mathbf{r}(n) - \mathbf{H}(n)\mathbf{s}(n). \tag{3.28}$$

By substituting (3.25) into (3.28), we have:

$$\begin{aligned}
\mathbf{e}(n) &= \mathbf{r}(n) - \left[\mathbf{H}(n-1) + \lambda(n)\boldsymbol{\epsilon}(n)\mathbf{k}(n)\right]\mathbf{s}(n) \\
&= \mathbf{r}(n) - \mathbf{H}(n-1)\mathbf{s}(n) - \lambda(n)\boldsymbol{\epsilon}(n)\mathbf{k}(n)\mathbf{s}(n) \\
&= \boldsymbol{\epsilon}(n) - \lambda(n)\boldsymbol{\epsilon}(n)\frac{\mathbf{s}^H(n)\mathbf{P}(n-1)\mathbf{s}(n)}{1 + \lambda(n)\mathbf{s}^H(n)\mathbf{P}(n-1)\mathbf{s}(n)} \\
&= \boldsymbol{\epsilon}(n) - \lambda(n)\boldsymbol{\epsilon}(n)\frac{G(n)}{1 + \lambda(n)G(n)} \\
&= \boldsymbol{\epsilon}(n)\left[1 - \frac{\lambda(n)G(n)}{1 + \lambda(n)G(n)}\right] \\
&= \boldsymbol{\epsilon}(n)\frac{1}{1 + \lambda(n)G(n)},
\end{aligned} \tag{3.29}$$

where $G(n) = \mathbf{s}^H(n)\mathbf{P}(n-1)\mathbf{s}(n)$. The constraint set is described as:

$$\|\mathbf{e}(n)\| = \|\boldsymbol{\epsilon}(n)\frac{1}{1 + \lambda(n)G(n)}\| \leq \gamma. \tag{3.30}$$

If $\|\boldsymbol{\epsilon}(n)\| > \gamma$, then the previous solution lies outside the constraint set. We can choose the constraint value $\|\mathbf{e}(n)\|$ equal to γ so that the new solution lies on the closest boundary of the constraint set. Therefore:

$$\|\mathbf{e}(n)\| = \|\boldsymbol{\epsilon}(n)\|\frac{1}{|1 + \lambda(n)G(n)|} = \gamma. \tag{3.31}$$

Table 3.1: Summary of the BEACON Channel Estimation Algorithm

Initialize the algorithm by setting

$$\mathbf{H}(0) = 0$$

$$\mathbf{P}(0) = \mathbf{I}$$

For each instant of time, n=1, 2, ..., compute

$$\boldsymbol{\epsilon}(n) = \mathbf{r}(n) - \mathbf{H}(n-1)\mathbf{s}(n)$$

$$\lambda(n) = \begin{cases} \frac{1}{G(n)}\left(\frac{\|\boldsymbol{\epsilon}(n)\|}{\gamma} - 1\right), & \text{if } \|\boldsymbol{\epsilon}(n)\| > \gamma, \\ 0, & \text{otherwise.} \end{cases}$$

$$\text{where } G(n) = \mathbf{s}^H(n)\mathbf{P}(n-1)\mathbf{s}(n)$$

$$\mathbf{k}(n) = \frac{\mathbf{s}^H(n)\mathbf{P}(n-1)}{1+\lambda(n)G(n)}$$

$$\mathbf{H}(n) = \mathbf{H}(n-1) + \lambda(n)\boldsymbol{\epsilon}(n)\mathbf{k}(n)$$

$$\mathbf{P}(n) = \mathbf{P}(n-1) - \lambda(n)\mathbf{P}(n-1)\mathbf{s}(n)\mathbf{k}(n)$$

Hence the optimal forgetting factor at the nth iteration can be expressed as:

$$\lambda(n) = \frac{1}{G(n)}\left(\frac{\|\boldsymbol{\epsilon}(n)\|}{\gamma} - 1\right). \tag{3.32}$$

Table 3.1 shows a summary of the BEACON channel estimation algorithm which will be used for the simulations.

3.3.3 Time-Varying Bound

In order to obtain the optimal error bound at each time instant, in this section we introduce an error bound function which can adjust the error bound automatically with the update of the channel estimate. A similar bound for the SM filtering techniques has been described in [67]. For channel estimation, the bound is heuristic and employs the CSI parameter matrix and the noise variance that should be related with the estimates of interest. It can be expressed as:

$$\gamma(n+1) = (1-\beta)\gamma(n) + \beta\sqrt{\alpha\|\mathbf{H}(n)\|^2\sigma^2}, \tag{3.33}$$

where β is the forgetting factor, α is the tuning parameter, and σ^2 is the variance of the noise which is assumed to be known at the destinations. This time-varying bound is recursive so that it can be used to avoid too high or low values of $\|\mathbf{H}(n)\|^2$.

3.4 Analysis of the Proposed Algorithms

In this section, the analysis of the steady-state output MSE and the computational complexity of the two SM algorithms are developed.

3.4.1 Steady-State Output MSE Analysis

In this subsection, we investigate the output MSE in the SM-NLMS and the BEACON channel estimation. The received signal at time instant n is given by:

$$\mathbf{r}(n) = \mathbf{H}_0\mathbf{s}(n) + \mathbf{n}(n), \tag{3.34}$$

where $\mathbf{H}_0$ $(M \times N)$ is the channel matrix needed to be estimated and $\mathbf{n}(n)$ is the measurement noise which is assumed here to be Gaussian with zero mean and variance σ_n^2. Defining the channel estimation error matrix as:

$$\Delta\mathbf{H}(n) = \mathbf{H}_0 - \mathbf{H}(n). \tag{3.35}$$

We can express the output error vector as:

$$\begin{aligned}\mathbf{e}(n) &= \mathbf{r}(n) - \mathbf{H}(n)\mathbf{s}(n) \\ &= \mathbf{r}(n) - [\mathbf{H}_0 - \Delta\mathbf{H}(n)]\mathbf{s}(n) \\ &= \mathbf{r}(n) - \mathbf{H}_0\mathbf{s}(n) + \Delta\mathbf{H}(n)\mathbf{s}(n) \\ &= \mathbf{n}(n) + \Delta\mathbf{H}(n)\mathbf{s}(n).\end{aligned} \tag{3.36}$$

Therefore, the output MSE expression can be derived as:

$$\begin{aligned}J(n) &= E[\|\mathbf{e}(n)\|^2] \\ &= E[\mathbf{e}^H(n)\mathbf{e}(n)] \\ &= E\{[\mathbf{n}^H(n) + \mathbf{s}^H(n)\Delta\mathbf{H}^H(n)][\mathbf{n}(n) + \Delta\mathbf{H}(n)\mathbf{s}(n)]\} \\ &= E[\|\mathbf{n}(n)\|^2] + E[\mathbf{s}^H(n)\Delta\mathbf{H}^H(n)\Delta\mathbf{H}(n)\mathbf{s}(n)] \\ &= M\sigma_n^2 + E\{tr[\mathbf{s}^H(n)\Delta\mathbf{H}^H(n)\Delta\mathbf{H}(n)\mathbf{s}(n)]\} \\ &= M\sigma_n^2 + tr\{E[\mathbf{s}^H(n)\Delta\mathbf{H}^H(n)\Delta\mathbf{H}(n)\mathbf{s}(n)]\},\end{aligned} \tag{3.37}$$

where $tr(\cdot)$ denotes the trace of a matrix. The property of the matrix trace $tr(\mathbf{XY}) = tr(\mathbf{YX})$ will be used in the following derivation. From (3.37), we can define the output excess MSE as:

$$\begin{aligned} J_{ex}(n) &= tr\{E[\mathbf{s}^H(n)\Delta\mathbf{H}^H(n)\Delta\mathbf{H}(n)\mathbf{s}(n)]\} \\ &= tr\{E[\mathbf{s}(n)\mathbf{s}^H(n)\Delta\mathbf{H}^H(n)\Delta\mathbf{H}(n)]\}. \end{aligned} \tag{3.38}$$

For the SM-NLMS

The update equations for the SM-NLMS channel estimation are given by (3.21) and (3.22). In (3.22) $\mathbf{s}^H(n)\mathbf{s}(n)$ is equal to $N\sigma_s^2$, where σ_s^2 is the variance of the pilot signal. By substituting (3.22) into (3.21), we can achieve an alternative update equation:

$$\mathbf{H}(n+1) = \mathbf{H}(n) + \frac{1}{N\sigma_s^2}\left(1 - \frac{\gamma}{\|\mathbf{e}_0(n)\|}\right)\mathbf{e}(n)\mathbf{s}^H(n), \tag{3.39}$$

where

$$\|\mathbf{e}_0(n)\| = \begin{cases} \|\mathbf{e}(n)\|, & \text{if } \|\mathbf{e}(n)\| > \gamma, \\ \gamma, & \text{otherwise.} \end{cases} \tag{3.40}$$

As a consequence, the update equation of the channel estimation error can be expressed as:

$$\begin{aligned} \Delta\mathbf{H}(n+1) =& \Delta\mathbf{H}(n) - \frac{1}{N\sigma_s^2}\left(1 - \frac{\gamma}{\|\mathbf{e}_0(n)\|}\right)\mathbf{e}(n)\mathbf{s}^H(n) \\ =& \Delta\mathbf{H}(n) - \frac{1}{N\sigma_s^2}\mathbf{e}(n)\mathbf{s}^H(n) + \frac{\gamma}{N\sigma_s^2}\frac{\mathbf{e}(n)}{\|\mathbf{e}_0(n)\|}\mathbf{s}^H(n). \end{aligned} \tag{3.41}$$

Then, we can use (3.41) to derive the update equation of the output excess MSE in (3.38) (see Appendix B):

$$J_{ex}(n+1) = M\sigma_n^2 + 2\gamma E\left[\frac{1}{\|\mathbf{e}_0(n)\|}\right]J_{ex}(n) - 2\gamma E\left[\frac{\|\mathbf{e}(n)\|^2}{\|\mathbf{e}_0(n)\|}\right] + \gamma^2 E\left[\frac{\|\mathbf{e}(n)\|^2}{\|\mathbf{e}_0(n)\|^2}\right]. \tag{3.42}$$

From (3.40), the three expected values in (3.42) can be expressed as:

$$E\left[\frac{1}{\|\mathbf{e}_0(n)\|}\right] = E\left[\frac{1}{\|\mathbf{e}(n)\|}\middle|\|\mathbf{e}(n)\| > \gamma\right]P_{up} + \frac{1}{\gamma}(1 - P_{up}), \tag{3.43}$$

$$E\left[\frac{\|\mathbf{e}(n)\|^2}{\|\mathbf{e}_0(n)\|}\right] = E\left[\|\mathbf{e}(n)\|\middle|\|\mathbf{e}(n)\| > \gamma\right]P_{up} + \frac{1}{\gamma}E\left[\|\mathbf{e}(n)\|^2\middle|\|\mathbf{e}(n)\| \le \gamma\right](1 - P_{up}), \tag{3.44}$$

$$E\left[\frac{\|\mathbf{e}(n)\|^2}{\|\mathbf{e}_0(n)\|^2}\right] = P_{up} + \frac{1}{\gamma^2}E\left[\|\mathbf{e}(n)\|^2\big|\|\mathbf{e}(n)\| \leq \gamma\right](1-P_{up}), \tag{3.45}$$

where $E[\cdot\big|\cdot]$ denotes the conditional expected value and P_{up} stands for the probability of update in each recursion. Let:

$$X_1 = E\left[\frac{1}{\|\mathbf{e}(n)\|}\bigg|\|\mathbf{e}(n)\| > \gamma\right], \tag{3.46}$$

$$Y_1 = E\left[\|\mathbf{e}(n)\|\big|\|\mathbf{e}(n)\| > \gamma\right], \tag{3.47}$$

$$Z_1 = E\left[\|\mathbf{e}(n)\|^2\big|\|\mathbf{e}(n)\| \leq \gamma\right]. \tag{3.48}$$

By substituting (3.43)-(3.45) into (3.42), we can get

$$\begin{aligned} J_{ex}(n+1) =& M\sigma_n^2 + [2\gamma X_1 P_{up} + 2(1-P_{up})]J_{ex}(n) - 2\gamma Y_1 P_{up} - 2Z_1(1-P_{up}) \\ &+ \gamma^2 P_{up} + Z_1(1-P_{up}) \\ =& [2\gamma X_1 P_{up} + 2 - 2P_{up}]J_{ex}(n) - 2\gamma Y_1 P_{up} - Z_1(1-P_{up}) + M\sigma_n^2 + \gamma^2 P_{up}. \end{aligned} \tag{3.49}$$

During the steady state, $J_{ex}(n+1) \to J_{ex}(n)$. Therefore, the steady-state output excess MSE expression of the SM-NLMS channel estimation is:

$$J_{ex}(n) = \frac{2\gamma Y_1 P_{up} + Z_1(1-P_{up}) - M\sigma_n^2 - \gamma^2 P_{up}}{2\gamma X_1 P_{up} - 2P_{up} + 1}. \tag{3.50}$$

For the BEACON

According to Table 3.1, we can get the update equation of the channel estimation error for the BEACON channel estimation which is very similar to (3.41):

$$\Delta\mathbf{H}(n) = \Delta\mathbf{H}(n-1) - \frac{\boldsymbol{\epsilon}(n)\mathbf{s}^H(n)\mathbf{P}(n-1)}{G(n)} + \gamma\frac{\boldsymbol{\epsilon}(n)}{\|\boldsymbol{\epsilon}_0(n)\|}\frac{\mathbf{s}^H(n)\mathbf{P}(n-1)}{G(n)}, \tag{3.51}$$

where

$$\|\boldsymbol{\epsilon}_0(n)\| = \begin{cases} \|\boldsymbol{\epsilon}(n)\|, & \text{if } \|\boldsymbol{\epsilon}(n)\| > \gamma, \\ \gamma, & \text{otherwise.} \end{cases} \tag{3.52}$$

Following the same steps described for the SM-NLMS channel estimation in the Appendix, we find that the steady-state output excess MSE expression of the BEACON channel estimation has the same style as (3.50):

$$J_{ex}(n) = \frac{2\gamma Y_2 P_{up} + Z_2(1-P_{up}) - M\sigma_n^2 - \gamma^2 P_{up}}{2\gamma X_2 P_{up} - 2P_{up} + 1}, \tag{3.53}$$

where

$$X_2 = E\left[\frac{1}{\|\boldsymbol{\epsilon}(n)\|}\middle|\|\boldsymbol{\epsilon}(n)\| > \gamma\right], \tag{3.54}$$

$$Y_2 = E\left[\|\boldsymbol{\epsilon}(n)\|\middle|\|\boldsymbol{\epsilon}(n)\| > \gamma\right], \tag{3.55}$$

$$Z_2 = E\left[\|\boldsymbol{\epsilon}(n)\|^2\middle|\|\boldsymbol{\epsilon}(n)\| \leq \gamma\right]. \tag{3.56}$$

The Probability of Update P_{up}

From (3.22), we can get the relation about the probability of update of the SM-NLMS channel estimation:

$$P_{up} = Pr\{\|\mathbf{e}(n)\| > \gamma\} = Pr\{\|\mathbf{e}(n)\|^2 > \gamma^2\}. \tag{3.57}$$

Similarly, for the BEACON channel estimation we just need to use $\boldsymbol{\epsilon}(n)$ instead of $\mathbf{e}(n)$. It is easy to see that P_{up} depends on the distribution of $\|\mathbf{e}(n)\|^2$. For the estimated channel matrix $\mathbf{H}_0$ with size $M \times N$:

$$\begin{aligned}\|\mathbf{e}(n)\|^2 &= \sum_{i=1}^{M}(\Re^2[e_i(n)] + \Im^2[e_i(n)]) \\ &= \frac{\sigma_n^2}{2}\sum_{i=1}^{M}(\frac{\Re^2[e_i(n)]}{\sigma_n^2/2} + \frac{\Im^2[e_i(n)]}{\sigma_n^2/2}).\end{aligned} \tag{3.58}$$

During the steady state, assuming $\Delta\mathbf{H}(n) \rightarrow 0$, the linear relationship between $\mathbf{e}(n)$,$\Delta\mathbf{H}(n)$ and $\mathbf{n}(n)$ in (3.36) shows that the distribution of $\mathbf{e}(n)$ is typically Gaussian unless a jamming or other interference signal with another distribution is present. Therefore, the elements of the error vector $\mathbf{e}(n)$ have the same distribution as the elements of the noise vector $\mathbf{n}(n)$. Recalling that $\Re[n_i(n)]$ and $\Im[n_i(n)] \sim \mathcal{N}(0, \frac{\sigma_n^2}{2})$, we can express the distribution of (3.58) by a chi-square random variable with $2M$ degrees of freedom as follows:

$$\|\mathbf{e}(n)\|^2 \sim \frac{\sigma_n^2}{2}\mathcal{X}_{2M}^2. \tag{3.59}$$

Therefore, (3.57) becomes:

$$\begin{aligned} P_{up} =& Pr\left\{\sum_{i=1}^{M}(\frac{\Re^2[e_i(n)]}{\sigma_n^2/2}+\frac{\Im^2[e_i(n)]}{\sigma_n^2/2})>\gamma^2\frac{2}{\sigma_n^2}\right\} \\ =& 1-Pr\left\{\sum_{i=1}^{M}(\frac{\Re^2[e_i(n)]}{\sigma_n^2/2}+\frac{\Im^2[e_i(n)]}{\sigma_n^2/2})\leq\gamma^2\frac{2}{\sigma_n^2}\right\} \\ =& 1-F\left(\gamma^2\frac{2}{\sigma_n^2};2M\right), \end{aligned} \tag{3.60}$$

where $F(\cdot)$ is the chi-square cumulative distribution function (CDF) [78] defined by:

$$F(x;l)=\frac{\Gamma_L(l/2,x/2)}{\Gamma(l/2)}. \tag{3.61}$$

In (3.61) $\Gamma_L(s,x)$ is the lower incomplete Gamma function:

$$\Gamma_L(s,x)=\int_0^x t^{s-1}e^{-t}dt, \tag{3.62}$$

and $\Gamma(x)$ is the gamma function:

$$\Gamma(x)=\int_0^\infty t^{x-1}e^{-t}dt. \tag{3.63}$$

By substituting (3.62) and (3.63) into (3.61), we can finally obtain:

$$F(x;l)=\frac{\int_0^{\frac{x}{2}}t^{\frac{l}{2}-1}e^{-t}dt}{\int_0^\infty t^{\frac{l}{2}-1}e^{-t}dt}, \tag{3.64}$$

where l denotes the number of degrees of freedom.

3.4.2 Computational Complexity Analysis

Table 3.2 lists the computational complexity per update in terms of the number of multiplications, additions and divisions for the SM-NLMS and BEACON algorithms and their competing algorithms. The size of the estimated channel matrix is $M \times N$. For our cooperative WSN system model, when $\mathbf{H}_d$ is chosen as the estimated channel, we can get:

$$M = mN_d, \tag{3.65}$$

and

$$N = N_r + N_s. \tag{3.66}$$

Table 3.2: Computational Complexity per Update

Algorithm	Multiplication	Addition	Division
NLMS	$2MN + N + min\{M, N\}$	$2MN + N - 1$	1
SM-NLMS	$MN + M + P_{up}(MN + N + min\{M, N\})$	$MN + M - 1 + P_{up}(MN + N)$	2
RLS	$4N^2 + 2MN + N$	$3N^2 + 2MN - N$	2
BEACON	$N^2 + MN + M + N$	$N^2 + MN + M - 2$	2
	$+P_{up}(2N^2 + MN + N + min\{M, N\})$	$+P_{up}(2N^2 + MN - N + 2)$	

Because the multiplication dominates the computational complexity of the algorithms, in order to compare the computational complexity of our proposed algorithms with their competing algorithms, the number of multiplications versus the size of the channel matrix performance for each update is displayed in Figure 3.5. For the purpose of illustration, we set M equal to N. It can be seen that our proposed SM-NLMS and BEACON channel estimation algorithms have a significant complexity reduction compared with the conventional NLMS and RLS channel estimation algorithms. Obviously, a lower P_{up} will cause a lower computational complexity. Furthermore, assuming the linear MMSE detectors are used in the destination nodes which require cubic complexity, we can get the conclusion that the power used for our proposed channel estimation is only a small fraction of the power budget of these nodes.

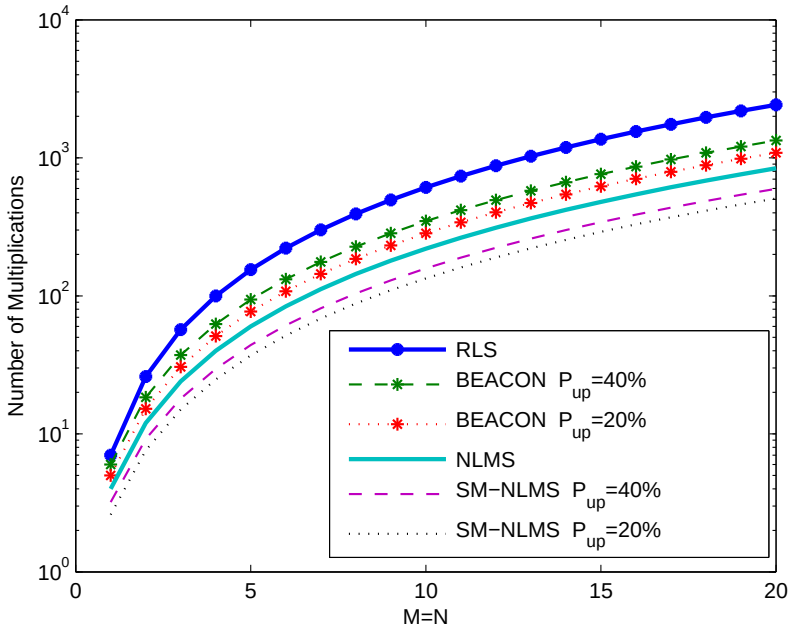

Figure 3.5: The number of multiplications versus the size of the channel matrix.

3.5 Simulations

In this section, we numerically study the performance of our two proposed SM estimation methods as well as the design of the optimal error bound. We consider a 3-hop (m=3) wireless sensor network. The number of source nodes (N_s), two groups of relay nodes ($N_{r(1)}, N_{r(2)}$) and destination nodes (N_d) are 2, 4, 4, 3, respectively. We consider an AF cooperation protocol and the amplification coefficient of each relay is set to 1 for the purpose of simplification. We choose $\mathbf{H}_d$ as our estimated channel because it is the most significant and most complex channel among all channels of the WSN system. The quasi-static fading channel (block fading channel) is considered in our simulations whose elements are Rayleigh random variables (with zero mean and unit variance) and assumed to be invariant during the transmission of each packet. Also, in order to test our proposed channel estimation algorithms in a time-varying environment, we consider a typical fading channel for wireless communications systems, a Rayleigh fading channel which is modeled according to Clarke's Model [79]. According to the transmission scheme introduced in Section 3.2, during each phase, the sources and each group of relays transmit the QPSK modulated packets with n_p symbols among which n_t are training symbols and n_d are data symbols (Note that $n_p = n_t + n_d$). The quantities n_p, n_t and n_d will be specified in the following simulations. The noise at the destination nodes is modeled as circularly symmetric complex Gaussian random variables with zero mean. The SNR is fixed at 10 dB.

3.5.1 MSE performance

Figure 3.6 and Figure 3.7 show the channel matrix mean square error (MSE) performance of our proposed SM-NLMS and BEACON channel estimation methods for the quasi-static fading channel, and compare them with the conventional NLMS and RLS channel estimation algorithms. For the SM-NLMS estimator, we transmit packets with 1000 (n_p) symbols among which 100 (n_t) are training symbols and 900 (n_d) are data symbols. We choose five fixed error bounds (γ) ranging from 0.3 to 1.1. It can be seen that increasing

the error bound makes the update rate (UR) decrease. It means the update is selective which can reduce the computational complexity and power consumption. In the case of an error bound equal to 1.1, the UR can fall dramatically to 0.0868. As the error bound increases, the MSE performance first becomes better and then becomes worse. The optimal error bound appears between 0.7 and 0.9. In that situation, the SM-NLMS channel estimation achieves the fastest convergence speed and lowest steady states. Otherwise, the performance degrades due to overbounding or underbounding. For the BEACON estimator, we transmit packets with 2000 (n_p) symbols among which 100 (n_t) are training symbols and 1900 (n_d) are data symbols. We choose four fixed error bounds ranging from 0.6 to 0.9. Also, the minimum-mean-square error (MMSE) channel estimator which requires the full a priori knowledge of the channel correlation matrix and the noise variance is used here for reference. It can be seen that a higher value of γ results in worse MSE performance but a lower UR. In the case of an error bound equal to 0.6, the BEACON algorithm outperforms the conventional RLS algorithm (with a forgetting factor of 0.998) in terms of convergence speed and steady state with a slightly reduced UR (0.9128). When the error bound is increased to 0.8, although its convergence speed is slower than RLS channel estimation, the final MSE is comparable with a much lower UR (0.4356). Figure 3.8 and Figure 3.9 illustrate the performance when we apply the time-varying bound (TVB) into the SM-NLMS and BEACON channel estimation. For the SM-NLMS estimator, we set α to 1.5 and β to 0.01. The curve of our proposed algorithm lies on the optimal position which is very close to the curve of the SM-NLMS with fixed error bound 0.8. Also, its update rate decreases further which is our expectation. For the BEACON estimator, we set α to 3 and β to 0.001. Our proposed algorithm can achieve very similar performance to the conventional RLS channel estimation with a substantial reduction in the UR. Therefore, the computational complexity is significantly reduced. The MSE versus SNR performance of the SM-NLMS and BEACON channel estimation methods are displayed with fixed error bounds and the proposed time-varying error bounds in Figure 3.10 and Figure 3.11. In the cases of fixed error bounds, the MSE is lower bounded at different values for different error bounds. For the SM-NLMS estimator, a higher SNR needs a specified lower error bound to achieve the optimal MSE performance. When the time-varying error bound is applied, the MSE remains very close to the optimal values for all SNRs. For the BEACON estimator, when the SNR is larger than a specified value,

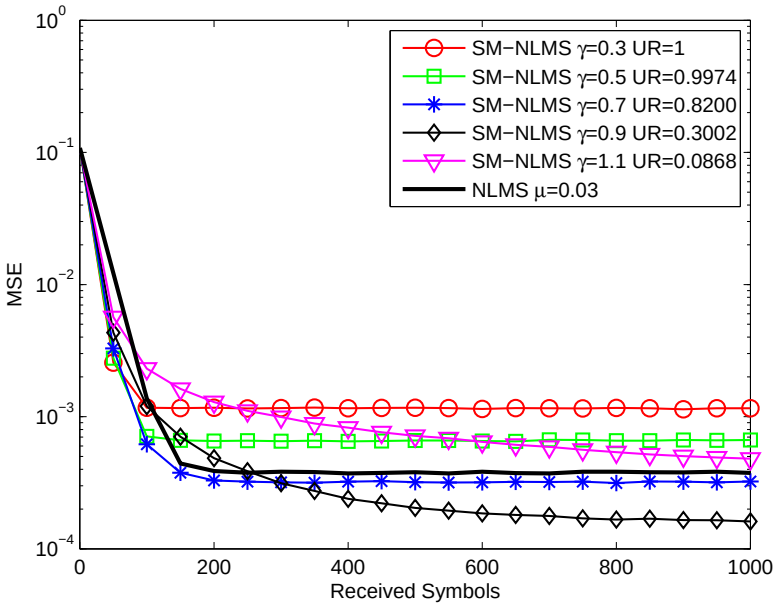

Figure 3.6: MSE performance of the SM-NLMS channel estimation of $\mathbf{H}_d$ for quasi-static fading channel compared with the NLMS channel estimation. n_p=1000, n_t=100 and n_d=900.

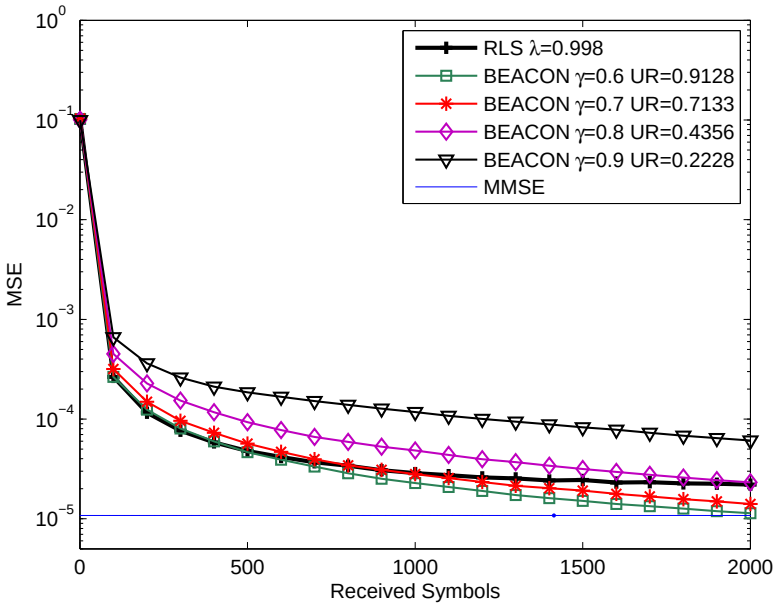

Figure 3.7: MSE performance of the BEACON channel estimation of $\mathbf{H}_d$ for quasi-static fading channel compared with the RLS channel estimation. n_p=2000, n_t=100 and n_d=1900.

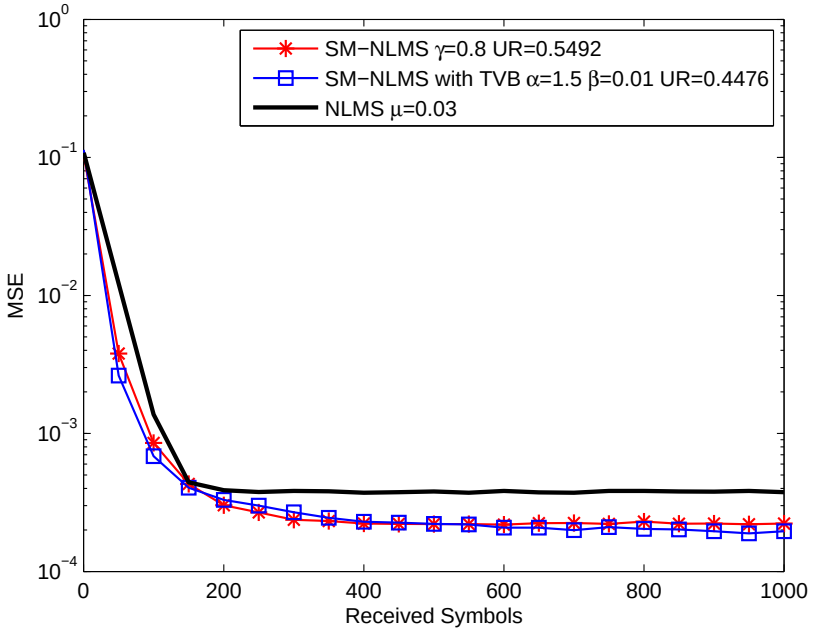

Figure 3.8: MSE performance of the SM-NLMS channel estimation with a time-varying bound for quasi-static fading channel. n_p=1000, n_t=100 and n_d=900.

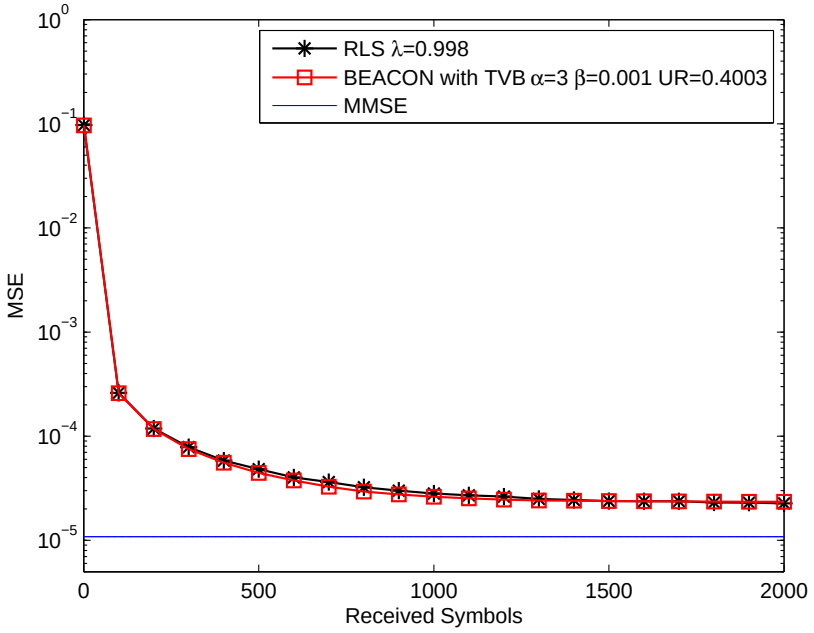

Figure 3.9: MSE performance of the BEACON channel estimation with a time-varying bound for quasi-static fading channel. n_p=2000, n_t=100 and n_d=1900.

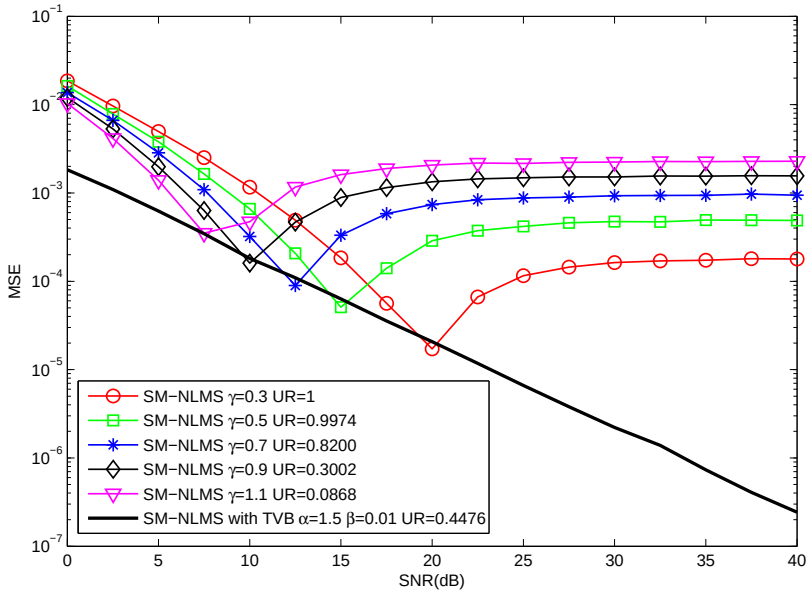

Figure 3.10: SM-NLMS channel estimation MSEs versus SNR for both the fixed bound and time-varying bound for quasi-static fading channel. n_p=1000, n_t=100 and n_d=900.

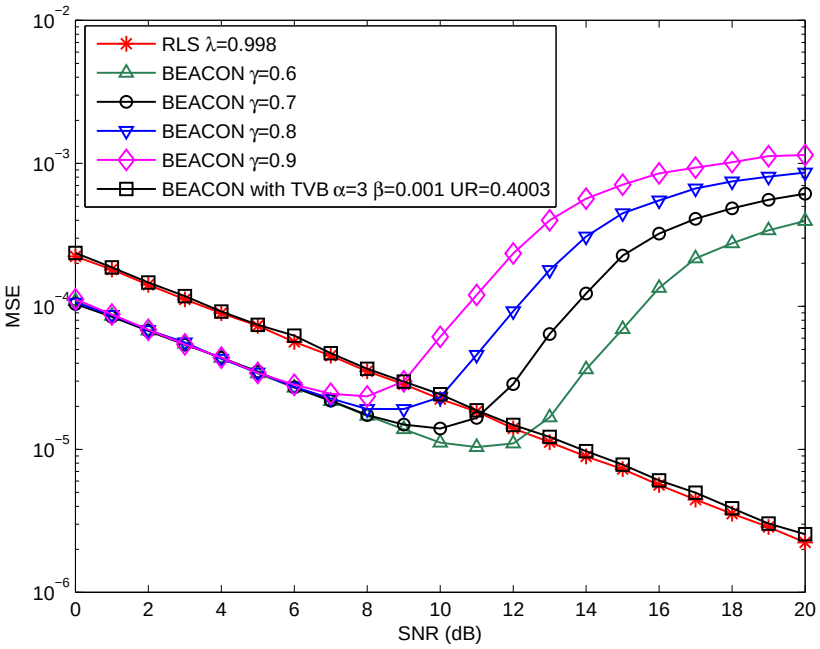

Figure 3.11: BEACON channel estimation MSEs versus SNR for both the fixed bound and time-varying bound for quasi-static fading channel. n_p=2000, n_t=100 and n_d=1900.

its MSE will become worse. However, when the time-varying error bound (TVB) is applied, it can be observed that the MSE keeps on decreasing along with the increase of the SNR. We can notice from Figure 3.11 that when the SNR is low, setting fixed bounds can achieve better performance than setting time-varying bound. Therefore, it would be possible to devise a "hybrid" BEACON channel estimation that switches between fixed and time-varying bounds depending on the SNR. These two figures show the robustness to the SNR variation of our proposed algorithms for the quasi-static fading channel.

Figure 3.12 and Figure 3.13 show the MSE performance of our proposed channel estimation algorithms for the time-varying fading channel and three different fading rates (normalized Doppler frequency f_dT, where T is the symbol duration) are used in the simulations: 10^{-5}, 5×10^{-5}, and 10^{-4}. Because of the requirements of low power consumption and the fact that a fast convergence speed of the proposed algorithms might help reducing the need for long training sequences for the WSNs, we focus on the performance of packets with 500 (n_p) symbols among which 50 (n_t) are training symbols and 450 (n_d) are data symbols. For the SM-NLMS estimator, our proposed algorithm can achieve better performance than the conventional NLMS algorithms for all the three fading rates. Along with the increase of the fading rate, the advantage becomes less pronounced and the update rate becomes higher. For the BEACON estimator, our proposed algorithm can achieve very similar performance to the conventional RLS algorithms for all the three fading rate. (Note that for the conventional RLS algorithms, when increasing the fading rate, we have to lower the forgetting factor to get the optimal performance.) Along with the increasing of the fading rate, the update rate becomes higher. In order to show the performance tendency for higher f_dT, we extend its range up to 5×10^{-3}. The performance curves are shown in Figure 3.14 which includes the MSE performance versus f_dT and update rate (UR) versus f_dT of SM-NLMS and BEACON channel estimation for Rayleigh fading channels. (Note that the MSE values we used in this figure are chosen from the MSE when receiving 500 symbols.) This figure indicates that the performance of our proposed algorithms is comparable to the existing NLMS and RLS algorithms even for the fast fading channels. Therefore, we can conclude that our proposed channel estimation algorithms can work well for the time-varying fading channel and for a wide range of values of f_dT.

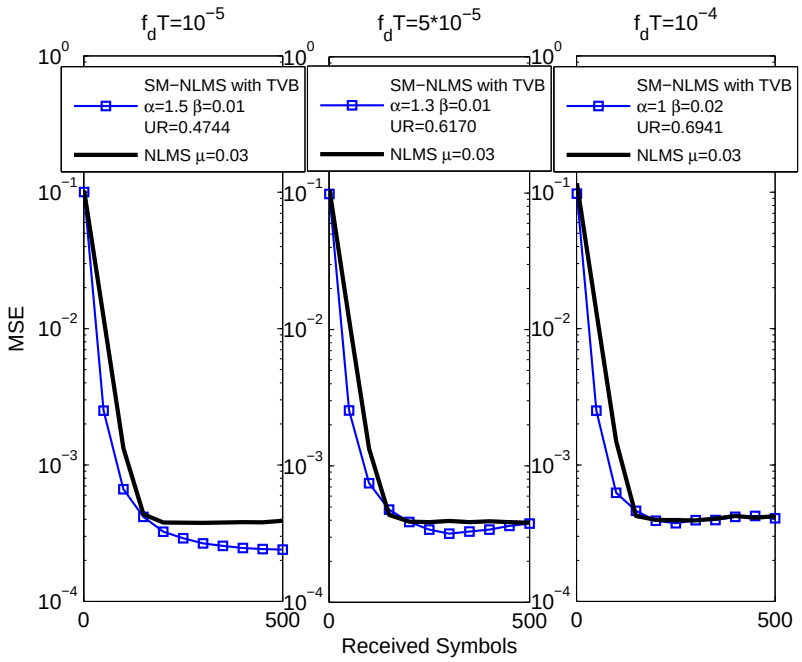

Figure 3.12: MSE performance of the SM-NLMS channel estimation for Rayleigh fading channels compared with the NLMS channel estimation. n_p=500, n_t=50 and n_d=450.

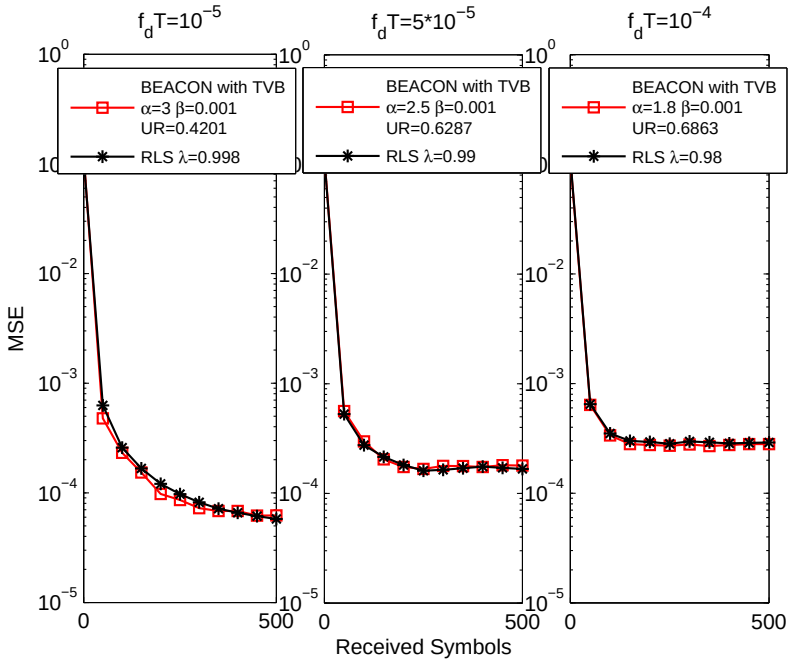

Figure 3.13: MSE performance of the BEACON channel estimation for Rayleigh fading channels compared with the RLS channel estimation. n_p=500, n_t=50 and n_d=450.

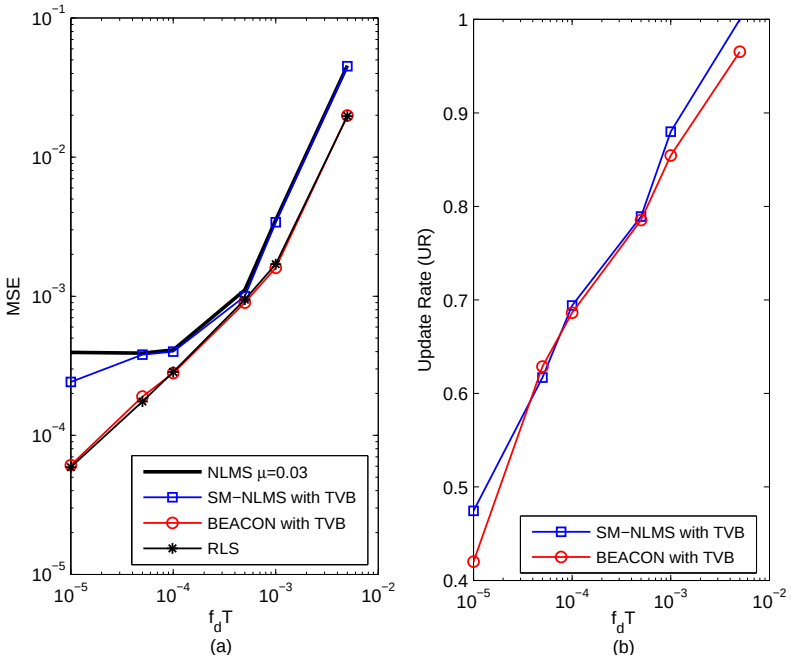

Figure 3.14: (a) MSE performance versus f_dT and (b) UR versus f_dT of SM-NLMS and BEACON channel estimation for Rayleigh fading channels.

3.5.2 BER performance

The MSE performance is very useful to give designers an idea of how well channel estimators perform, whereas bit error rate (BER) performance is more meaningful in practice to assess the performance of the data transmission. Therefore, in this subsection we focus on the BER performance of our proposed algorithms. We consider a simulation where the data packets transmitted at the sources nodes have 1000 (n_p) symbols and trained with 100 (n_t) symbols. Linear MMSE detectors are used at the destination nodes. We choose $\mathbf{H}_d$ as our estimated channel and other channels are assumed to be known. Quasi-static fading channel and Rayleigh fading channel are considered. And for the Rayleigh fading channel, the SNR is fixed at 5dB. It can be seen from Figure 3.15 that our two proposed SM channel estimation algorithms with time varying bound can achieve a similar BER performance to their competing algorithms no matter in a Quasi-static fading channel or Rayleigh fading channel with a wide range values of fading rate. Also, the BEACON channel estimator has lower BER than the SM-NLMS channel estimator due to the higher computational complexity and the use of the second-order statistics.

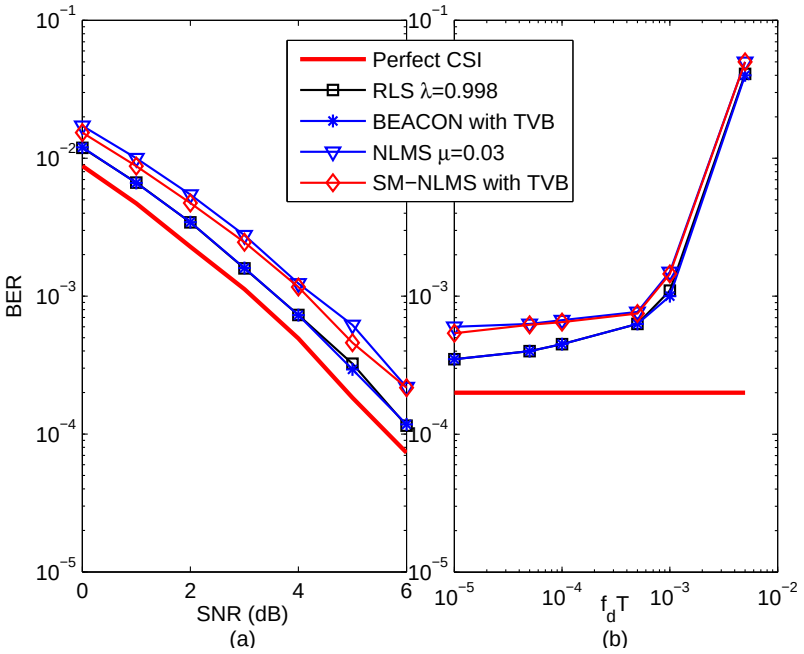

Figure 3.15: (a) BER performance versus SNR for quasi-static fading channel and (b) BER performance versus f_dT (SNR=5dB) for Rayleigh fading channel. n_p=1000, n_t=100 and n_d=900.

3.5.3 Verification of the Analysis

In this subsection, experiments were conducted to validate our analysis of the SM-NLMS and BEACON algorithms. The basic idea is to evaluate the formulas derived in section 3.4 by comparing the analytical results with that obtained by computer simulations. From (3.65) and (3.66), the two variables M and N used in section 3.4 can be obtained. M=9 and N=10. First of all, the analysis of the probability of update is verified using (3.60). It can be seen from Figure 3.16 that the P_{up} in simulations of the SM-NLMS and BEACON channel estimation is close to and lower bounded by the P_{up} from our analysis. The gap between the analytical curve and the simulations of two SM channel estimation is due to the approximation made in the analysis. In section 3.4, we assume that the channel matrix error $\Delta\mathbf{H}$ approaches zero during the steady-state. However, for the SM algorithms it is not accurate because the bound set for the output estimation error would enlarge the $\Delta\mathbf{H}$. During the steady-state, the SM-NLMS channel estimation has a larger $\Delta\mathbf{H}$ than the BEACON channel estimation which therefore causes a larger

gap between the analytical curve and the simulation. After that we continue to verify the analysis of the steady-state output excess MSE using (3.50) and (3.53). Because it is difficult to obtain the full-analytical expressions of the conditional expected values $X_1, Y_1, Z_1, X_2, Y_2, Z_2$, a semi-analytical method is used here. It means that the data from the simulations is used to calculate these conditional expected values in (3.50) and (3.53). In order to lower the effect of the difference between the analytical P_{up} and the simulation P_{up} of the SM-NLMS channel estimation, $1.1\sigma_n^2$ is chosen approximately to take the place of σ_n^2 in (3.60) which would produce a more accurate $\Delta\mathbf{H}$ and P_{up} for the SM-NLMS channel estimation. Figure 3.17 and Figure 3.18 show the steady-state output excess MSE versus $\gamma^2/(mN_d\sigma_n^2)$ of the two channel estimation algorithms. From the figures, it can be seen that the semi-analytical curves can match the simulation curves well. Therefore, it can be stated that our analysis is able to predict accurately the output steady-state excess MSE for different choices of bound γ.

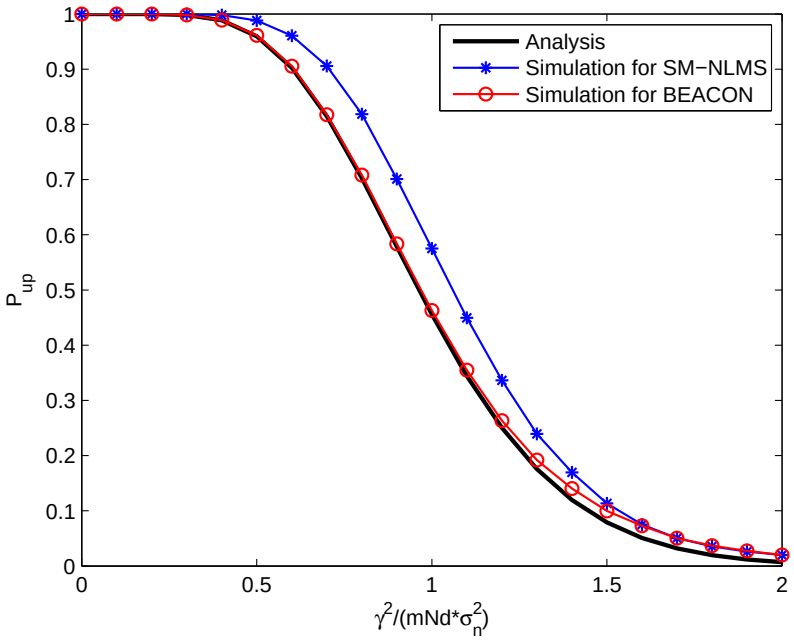

Figure 3.16: Analysis of the probability of the update P_{up}.

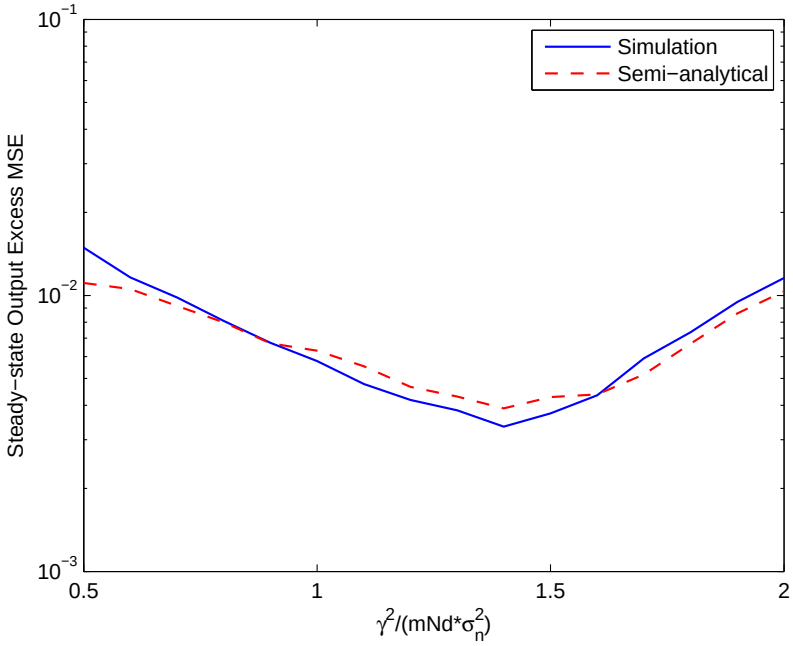

Figure 3.17: Steady-state excess MSE analysis for the SM-NLMS channel estimation.

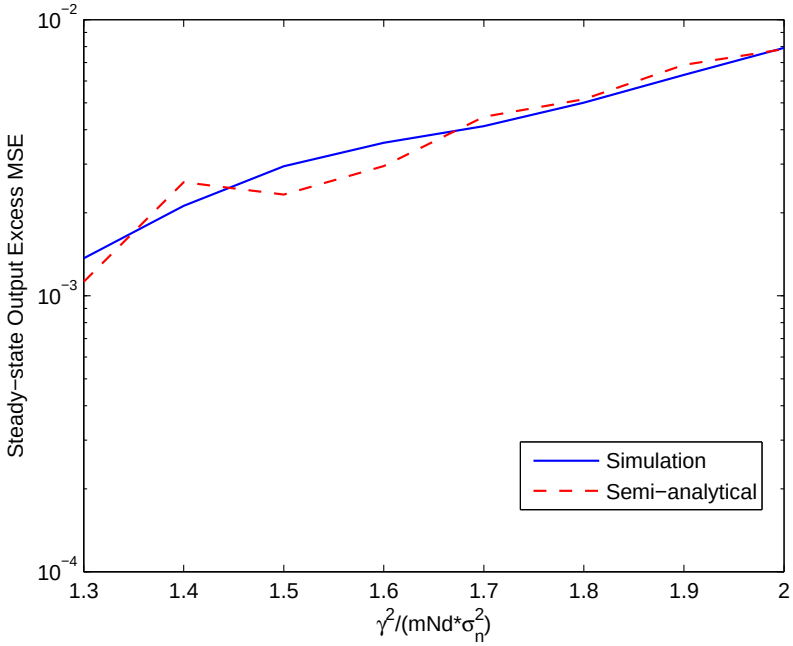

Figure 3.18: Steady-state excess MSE analysis for the BEACON channel estimation.

3.6 Summary

Two SM channel estimation methods have been proposed based on time-varying bound for cooperative wireless sensor networks. It has been shown that our proposed methods can achieve better or similar performance to conventional NLMS and RLS channel estimation, offering reduced computational complexity. Analyses of the steady-state MSE and computational complexity are presented for the two channel estimation and closed-form expressions of the excess MSE and the probability of update are provided. Furthermore, the incorporation of the time-varying bound function makes it robust to changes in the environment. These features are desirable for WSNs and bring about a significant reduction in energy consumption.

Chapter 4

Joint Linear Receiver Design and Power Allocation Using Alternating Optimization Algorithms for Two-Hop WSNs

Contents

4.1 Introduction

In this chapter, we consider a general two-hop wireless sensor network where the AF relaying scheme is employed. Our strategy is to jointly design the linear receivers and the power allocation parameter vector that contains the optimal complex amplification coefficients for each relay node via an alternating optimization approach. Two kinds of receivers are designed, the minimum mean-square error (MMSE) receiver and the maximum sum-rate (MSR) receiver. They can be considered as solutions to constrained optimization problems where the objective function is the mean-square error (MSE) cost function or the sum-rate (SR) and the constraint is a bound on the power levels among the relay nodes. Then, the constrained MMSE or MSR expressions for the linear receiver and the power allocation parameter can be derived. For the MMSE receiver, a closed form solution for the Lagrangian multiplier (λ) that arises in the expressions of the power allocation parameter can be achieved. For the MSR receiver, the novelty is that we make use of the Generalized Rayleigh Quotient [83] to solve the optimization problem in an alternating fashion. Finally, the optimal amplification coefficients are transmitted to the relay nodes through the feedback channel. In this work, we first present the strategies where the power allocation is considered for all of the relay nodes. They are subject to the global or individual power constraints. Next, to reduce the computational complexity for the power allocation, we choose the relay nodes which have good channel coefficients (when a channel power gain is above a threshold) between them and the destination nodes called neighbour relay nodes. Only the power allocation for these nodes are required and the remaining nodes use the equal power allocation method [29]. Therefore, the computational complexity and feedback burden can be reduced.

The main contributions of this chapter can be summarized as:

1) Constrained MMSE expressions for the design of linear receivers and power allocation parameters. The constraints include the global, individual and neighbour-based power constraints.

2) Constrained MSR expressions for the design of linear receivers and power allocation

parameters. The constraints include the global and neighbour-based power constraints.

3) Alternating optimization algorithms that compute the linear receivers and power allocation parameters in 1) and 2) to minimize the mean-square error or maximize the sum-rate of the WSN.

4) Computational complexity and convergence analysis of the proposed optimization algorithms.

The rest of this chapter is organized as follows. Section 4.2 describes the general two-hop WSN system model. Section 4.3 develops three joint MMSE receiver design and power allocation strategies subject to three different power constraints. Section 4.4 develops two joint MSR receiver design and power allocation strategies subject to two different power constraints. Section 4.5 contains the analysis of the computational complexity and the convergence. Section 4.6 presents and discusses the simulation results, while Section 4.7 provides some concluding remarks.

4.2 Two-Hop WSN System Model

Consider a general two-hop wireless sensor network (WSN) with multiple parallel relay nodes, as shown in Figure 4.1. The WSN consists of N_s source nodes, N_d destination nodes and N_r relay nodes. We concentrate on a time division scheme with perfect synchronization, for which all signals are transmitted and received in separate time slots. The sources first broadcast the $N_s \times 1$ signal vector $\mathbf{s}$ to all relay nodes. We consider an amplify-and-forward (AF) cooperation protocol in this work. Each relay node receives the signal, amplifies and rebroadcasts them to the destination nodes. In practice, we need to consider the constraints on the transmission policy. For example, each transmitting node would transmit during only one phase. Let $\mathbf{H}_s$ denote the $N_r \times N_s$ channel matrix between the source nodes and the relay nodes and $\mathbf{H}_d$ denote the $N_d \times N_r$ channel matrix

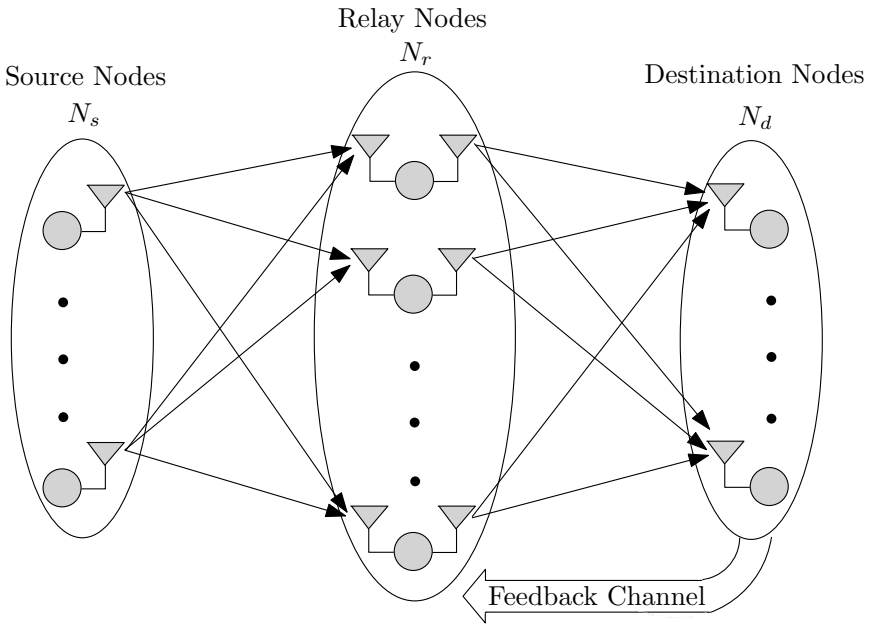

Figure 4.1: A two-hop cooperative WSN with N_s source nodes, N_d destination nodes and N_r relay nodes.

between the relay nodes and the destination nodes as given by

$$\mathbf{H}_s = \begin{bmatrix} \mathbf{h}_{s,1} \\ \mathbf{h}_{s,2} \\ \vdots \\ \mathbf{h}_{s,N_r} \end{bmatrix}, \qquad \mathbf{H}_d = \begin{bmatrix} \mathbf{h}_{d,1} \\ \mathbf{h}_{d,2} \\ \vdots \\ \mathbf{h}_{d,N_d} \end{bmatrix}, \tag{4.1}$$

where $\mathbf{h}_{s,i} = [h_{s,i,1}, h_{s,i,2}, ..., h_{s,i,N_s}]$ for $i = 1, 2, ..., N_r$ denotes the channel coefficients between the source nodes and the ith relay node, and $\mathbf{h}_{d,i} = [h_{d,i,1}, h_{d,i,2}, ..., h_{d,i,N_r}]$ for $i = 1, 2, ..., N_d$ denotes the channel coefficients between the relay nodes and the ith destination node. The received signal at the relay nodes can be expressed as

$$\mathbf{x} = \mathbf{H}_s\mathbf{s} + \mathbf{v}_r, \tag{4.2}$$

$$\mathbf{y} = \mathbf{F}\mathbf{x}, \tag{4.3}$$

where $\mathbf{v}$ is a zero-mean circularly symmetric complex additive white Gaussian noise (AWGN) vector with covariance matrix $\sigma_n^2\mathbf{I}$, and $\mathbf{F} = \text{diag}\left\{(\sigma_s^2|\mathbf{h}_{s,1}|^2 + \sigma_n^2), (\sigma_s^2|\mathbf{h}_{s,2}|^2 + \sigma_n^2), ..., (\sigma_s^2|\mathbf{h}_{s,N_r}|^2 + \sigma_n^2)\right\}^{-\frac{1}{2}}$ denotes the normalization matrix which can normalize the power of the received signal for each relay node.

At the destination nodes, the received signal can be expressed as

$$\mathbf{d} = \mathbf{H}_d\mathbf{A}\mathbf{y} + \mathbf{v}_d, \tag{4.4}$$

where $\mathbf{A} = \mathrm{diag}\{a_1, a_2, ..., a_{N_r}\}$ is a diagonal matrix whose elements represent the amplification coefficient of each relay node. Please note that the property of the matrix vector multiplication $\mathbf{Ay} = \mathbf{Ya}$ will be used in the next section, where $\mathbf{Y}$ is the diagonal matrix form of the vector $\mathbf{y}$ and $\mathbf{a}$ is the vector form of the diagonal matrix $\mathbf{A}$. In our proposed designs, the full CSI of the system is assumed to be known at all the destination nodes. In practice, a fusion centre [80] which contains the destination nodes is responsible for gathering the CSI, computing the optimal linear filters and the optimal amplification coefficients. The fusion centre also recovers the transmitted signal of the source nodes and transmits the optimal amplification coefficients to the relay nodes via a feedback channel.

4.3 Proposed Joint MMSE Design of the Receiver and Power Allocation

In this section, three constrained optimization problems are proposed to describe the joint design of the MMSE linear receiver ($\mathbf{W}$) and the power allocation parameter ($\mathbf{a}$) subject to a global, individual and neighbour-based power constraints.

4.3.1 MMSE Design with a Global Power Constraint

We first consider the case where the total power of all the relay nodes is limited to P_T. The proposed method can be considered as the following optimization problem

$$\begin{aligned}[\mathbf{W}_{opt}, \mathbf{a}_{opt}] \ &= \arg\min_{\mathbf{W},\mathbf{a}} E[\|\mathbf{s} - \mathbf{W}^H\mathbf{d}\|^2], \\ &\text{subject to } N_d\mathbf{a}^H\mathbf{a} = P_T.\end{aligned} \tag{4.5}$$

where $(\cdot)^H$ denotes the complex-conjugate (Hermitian) transpose. To solve this constrained optimization problem, we modify the MSE cost function using the method of

Lagrange multipliers [65] which yields the following Lagrangian function

$$\begin{aligned}\mathcal{L} =&E[\|\mathbf{s}-\mathbf{W}^H\mathbf{d}\|^2]+\lambda(N_d\mathbf{a}^H\mathbf{a}-P_T)\\ =&E(\mathbf{s}^H\mathbf{s})-E(\mathbf{d}^H\mathbf{W}\mathbf{s})-E(\mathbf{s}^H\mathbf{W}^H\mathbf{d})+E(\mathbf{d}^H\mathbf{W}\mathbf{W}^H\mathbf{d})+\lambda(N_d\mathbf{a}^H\mathbf{a}-P_T).\end{aligned} \tag{4.6}$$

By fixing $\mathbf{a}$ and setting the gradient of $\mathcal{L}$ in (4.6) with respect to the conjugate of the filter $\mathbf{W}$ equal to zero, we get

$$\begin{aligned}\mathbf{W}_{\text{opt}} &= [E(\mathbf{d}\mathbf{d}^H)]^{-1}E(\mathbf{d}\mathbf{s}^H)\\ &= \left[\mathbf{H}_d\mathbf{A}E(\mathbf{y}\mathbf{y}^H)\mathbf{A}^H\mathbf{H}_d^H+\sigma_n^2\mathbf{I}\right]^{-1}\mathbf{H}_d\mathbf{A}E(\mathbf{y}\mathbf{s}^H).\end{aligned} \tag{4.7}$$

The optimal expression for the power allocation vector $\mathbf{a}$ is obtained by equating the partial derivative of $\mathcal{L}$ with respect to $\mathbf{a}^*$ to zero

$$\begin{aligned}\frac{\partial\mathcal{L}}{\partial\mathbf{a}^*} =&-E\left(\frac{\partial\mathbf{d}^H}{\partial\mathbf{a}^*}\mathbf{W}\mathbf{s}\right)+E\left(\frac{\partial\mathbf{d}^H}{\partial\mathbf{a}^*}\mathbf{W}\mathbf{W}^H\mathbf{d}\right)+N_d\lambda\mathbf{a}\\ =&-E(\mathbf{Y}^H\mathbf{H}_d^H\mathbf{W}\mathbf{s})+E[\mathbf{Y}^H\mathbf{H}_d^H\mathbf{W}\mathbf{W}^H(\mathbf{H}_d\mathbf{Y}\mathbf{a}+\mathbf{v}_d)]+N_d\lambda\mathbf{a}\\ =&\mathbf{0}.\end{aligned} \tag{4.8}$$

where $(\cdot)^*$ denotes the complex-conjugate. Therefore, we get

$$\begin{aligned}\mathbf{a}_{\text{opt}} =&[E(\mathbf{Y}^H\mathbf{H}_d^H\mathbf{W}\mathbf{W}^H\mathbf{H}_d\mathbf{Y})+N_d\lambda\mathbf{I}]^{-1}E(\mathbf{Y}^H\mathbf{H}_d^H\mathbf{W}\mathbf{s})\\ =&[\mathbf{H}_d^H\mathbf{W}\mathbf{W}^H\mathbf{H}_d\odot E(\mathbf{y}\mathbf{y}^H)^*+N_d\lambda\mathbf{I}]^{-1}[\mathbf{H}_d^H\mathbf{W}\odot E(\mathbf{y}\mathbf{s}^H)^*\mathbf{u}]\end{aligned} \tag{4.9}$$

where $\odot$ denotes the Hadamard (element-wise) product and $\mathbf{u}=[1,1,...,1]^T$. The expressions in (4.7) and (4.9) depend on each other. Thus, it is necessary to iterate them with an initial value of $\mathbf{a}$ to obtain the solutions.

The Lagrange multiplier λ can be determined by solving

$$N_d\mathbf{a}_{\text{opt}}^H\mathbf{a}_{\text{opt}}=P_T. \tag{4.10}$$

Let

$$\boldsymbol{\phi}=E(\mathbf{Y}^H\mathbf{H}_d^H\mathbf{W}\mathbf{W}^H\mathbf{H}_d\mathbf{Y}) \tag{4.11}$$

and

$$\mathbf{z}=E(\mathbf{Y}^H\mathbf{H}_d^H\mathbf{W}\mathbf{s}). \tag{4.12}$$

Equation (4.10) becomes

$$N_d\mathbf{z}^H(\boldsymbol{\phi}+N_d\lambda\mathbf{I})^{-1}(\boldsymbol{\phi}+N_d\lambda\mathbf{I})^{-1}\mathbf{z}=P_T. \tag{4.13}$$

Using an eigenvalue decomposition (EVD), we have

$$\boldsymbol{\phi} = \mathbf{Q}\boldsymbol{\Lambda}\mathbf{Q}^{-1} \tag{4.14}$$

where $\boldsymbol{\Lambda} = \text{diag}\{\alpha_1, \alpha_2, ..., \alpha_M, 0, ..., 0\}$ consists of eigenvalues of $\boldsymbol{\phi}$, and $M = \min\{N_s, N_r, N_d\}$. Then, we get

$$\boldsymbol{\phi} + N_d\lambda\mathbf{I} = \mathbf{Q}(\boldsymbol{\Lambda} + N_d\lambda\mathbf{I})\mathbf{Q}^{-1}. \tag{4.15}$$

Therefore, (4.13) can be expressed as

$$N_d\mathbf{z}^H\mathbf{Q}(\boldsymbol{\Lambda} + N_d\lambda\mathbf{I})^{-2}\mathbf{Q}^{-1}\mathbf{z} = P_T. \tag{4.16}$$

Using the properties of the trace operation, (4.16) can be written as

$$N_d tr\left\{(\boldsymbol{\Lambda} + N_d\lambda\mathbf{I})^{-2}\mathbf{Q}^{-1}\mathbf{z}\mathbf{z}^H\mathbf{Q}\right\} = P_T. \tag{4.17}$$

Defining $\mathbf{C} = \mathbf{Q}^{-1}\mathbf{z}\mathbf{z}^H\mathbf{Q}$, (4.17) becomes

$$N_d\sum_{i=1}^{N_r}(\boldsymbol{\Lambda}(i,i) + N_d\lambda)^{-2}\mathbf{C}(i,i) = P_T. \tag{4.18}$$

Since $\boldsymbol{\phi}$ is a matrix with at most rank M, only the first M columns of $\mathbf{Q}$ span the column space of $E(\mathbf{Y}^H\mathbf{H}_d^H\mathbf{W}\mathbf{s})^H$ which causes the last $(N_r - M)$ columns of $\mathbf{z}^H\mathbf{Q}$ to become zero vectors, and thus the last $(N_r - M)$ diagonal elements of $\mathbf{C}$ are zero. Therefore, we obtain the $\{2M\}$th-order polynomial in λ

$$N_d\sum_{i=1}^{M}(\alpha_i + N_d\lambda)^{-2}\mathbf{C}(i,i) = P_T. \tag{4.19}$$

4.3.2 MMSE Design with Individual Power Constraints

Secondly, we consider the case where the power of each relay node is limited to some value $P_{T,i}$. The proposed method can be considered as the following optimization problem

$$\begin{gathered}[\mathbf{W}_{\text{opt}}, \mathbf{a}_{\text{opt}}] = \arg\min_{\mathbf{W}, a_1, ..., a_{N_r}} E[\|\mathbf{s} - \mathbf{W}^H\mathbf{d}\|^2], \\ \text{subject to } P_i = P_{T,i},\ i = 1, 2, ..., N_r,\end{gathered} \tag{4.20}$$

where P_i is the transmitted power of the ith relay node, and $P_i = N_d a_i^* a_i$. Using the method of Lagrange multipliers, we have the following Lagrangian function

$$\mathcal{L} = E[\|\mathbf{s} - \mathbf{W}^H \mathbf{d}\|^2] + \sum_{i=1}^{N_r} \lambda_i (N_d a_i^* a_i - P_{T,i}). \tag{4.21}$$

Following the same steps as described in Section 4.3.1, we get the same optimal expression for the $\mathbf{W}$ as in (4.7), and the optimal expression for the a_i

$$a_{i,\text{opt}} = [\boldsymbol{\phi}(i,i) + N_d \lambda_i]^{-1} [\mathbf{z}(i) - \sum_{l \in I, l \neq i} \boldsymbol{\phi}(i,l) a_l] \tag{4.22}$$

where $I = \{1, 2, ..., N_r\}$, $\boldsymbol{\phi}$ and $\mathbf{z}$ have the same expression as in (4.11) and (4.12). The Lagrange multiplier λ_i can be determined by solving

$$N_d a_{i,\text{opt}}^* a_{i,\text{opt}} = P_{T,i} \;\; i = 1, 2, ..., N_r. \tag{4.23}$$

4.3.3 MMSE Design with a Neighbour-based Power Constraint

In order to reduce the computational complexity for power allocation and the need for feedback, we choose the relay nodes which have good channel coefficients between them and the destination nodes called neighbour relay nodes. Only the power allocation for these nodes are required and the remaining nodes employ the equal power allocation method. Therefore, the computational complexity and feedback burden can be reduced. The received signal at the destination nodes can be rewritten as

$$\begin{aligned} \mathbf{d} &= \mathbf{H}_d \mathbf{A} \mathbf{y} + \mathbf{v}_d \\ &= \mathbf{H}_N \mathbf{A}_N \mathbf{y}_N + \mathbf{H}_o \mathbf{A}_o \mathbf{y}_o + \mathbf{v}_d, \end{aligned} \tag{4.24}$$

where $\mathbf{A}_N$ and $\mathbf{y}_N$ denote the amplification matrix and normalized signal for the neighbour relay nodes, $\mathbf{A}_o$ and $\mathbf{y}_o$ denote the amplification matrix and normalized signal for the non-neighbour relay nodes, respectively.

We consider the case where the total power of all the neighbour relay nodes is limited to P_N and $P_N + N_d \mathbf{a}_o^H \mathbf{a}_o = P_T$. The proposed method can be considered as the following

optimization problem

$$\begin{aligned}[\mathbf{W}_{\text{opt}}, \mathbf{a}_{N,\text{opt}}] &= \arg\min_{\mathbf{W},\mathbf{a}_N} E[\|\mathbf{s} - \mathbf{W}^H\mathbf{d}\|^2], \\ &\text{subject to } N_d\mathbf{a}_N^H\mathbf{a}_N = P_N.\end{aligned} \tag{4.25}$$

Using the method of Lagrange multipliers, we have the following Lagrangian function

$$\mathcal{L} = E[\|\mathbf{s} - \mathbf{W}^H\mathbf{d}\|^2] + \lambda_N(N_d\mathbf{a}_N^H\mathbf{a}_N - P_N). \tag{4.26}$$

Following the same steps as described in Section 4.3.1, we get the same optimal expression for $\mathbf{W}$ as in (4.7). Substituting (4.24) into (4.26), equating the partial derivative of $\mathcal{L}$ with respect to $\mathbf{a}_N^*$ to zero gives

$$\begin{aligned}\frac{\partial\mathcal{L}}{\partial\mathbf{a}_N^*} =& - E(\mathbf{Y}_N^H\mathbf{H}_N^H\mathbf{W}\mathbf{s}) + E(\mathbf{Y}_N^H\mathbf{H}_N^H\mathbf{W}\mathbf{W}^H\mathbf{H}_N\mathbf{Y}_N)\mathbf{a}_N \\ &+ E(\mathbf{Y}_N^H\mathbf{H}_N^H\mathbf{W}\mathbf{W}^H\mathbf{H}_o\mathbf{Y}_o\mathbf{a}_o) + N_d\lambda_N\mathbf{a}_N \\ =&\mathbf{0}.\end{aligned} \tag{4.27}$$

Therefore, we obtain the optimal expression for $\mathbf{a}_N$

$$\mathbf{a}_{N,\text{opt}} = [E(\mathbf{Y}_N^H\mathbf{H}_N^H\mathbf{W}\mathbf{W}^H\mathbf{H}_N\mathbf{Y}_N) + N_d\lambda_N\mathbf{I}]^{-1}[E(\mathbf{Y}_N^H\mathbf{H}_N^H\mathbf{W}\mathbf{s}) - E(\mathbf{Y}_N^H\mathbf{H}_N^H\mathbf{W}\mathbf{W}^H\mathbf{H}_o\mathbf{Y}_o\mathbf{a}_o)]. \tag{4.28}$$

The Lagrange multiplier λ_N can be determined by solving

$$N_d\mathbf{a}_{N,\text{opt}}^H\mathbf{a}_{N,\text{opt}} = P_N. \tag{4.29}$$

Let

$$\boldsymbol{\phi}_N = E(\mathbf{Y}_N^H\mathbf{H}_N^H\mathbf{W}\mathbf{W}^H\mathbf{H}_N\mathbf{Y}_N) \tag{4.30}$$

and

$$\mathbf{z}_N = E(\mathbf{Y}_N^H\mathbf{H}_N^H\mathbf{W}\mathbf{s}) - E(\mathbf{Y}_N^H\mathbf{H}_N^H\mathbf{W}\mathbf{W}^H\mathbf{H}_o\mathbf{Y}_o\mathbf{a}_o). \tag{4.31}$$

Equation (4.29) becomes

$$N_d\mathbf{z}_N^H(\boldsymbol{\phi}_N + N_d\lambda_N\mathbf{I})^{-1}(\boldsymbol{\phi}_N + N_d\lambda_N\mathbf{I})^{-1}\mathbf{z}_N = P_N. \tag{4.32}$$

Using an EVD,

$$\boldsymbol{\phi}_N = \mathbf{Q}_N\boldsymbol{\Lambda}_N\mathbf{Q}_N^{-1} \tag{4.33}$$

where $\mathbf{\Lambda}_N = \mathrm{diag}\{\alpha_1, \alpha_2, ..., \alpha_M, 0, ..., 0\}$ consists of the eigenvalues of $\boldsymbol{\phi}_N$, and $M_N = \min\{N_s, N_N, N_d\}$ (N_N is the number of neighbour relay nodes), we get

$$\boldsymbol{\phi}_N + N_d\lambda_N\mathbf{I} = \mathbf{Q}_N(\mathbf{\Lambda}_N + N_d\lambda_N\mathbf{I})\mathbf{Q}_N^{-1}. \tag{4.34}$$

Therefore, (4.32) can be expressed as

$$N_d\mathbf{z}_N^H\mathbf{Q}_N(\mathbf{\Lambda}_N + N_d\lambda_N\mathbf{I})^{-2}\mathbf{Q}_N^{-1}\mathbf{z}_N = P_N. \tag{4.35}$$

Using the properties of the trace operation, (4.35) can be written as

$$N_d tr\left\{(\mathbf{\Lambda}_N + N_d\lambda_N\mathbf{I})^{-2}\mathbf{Q}_N^{-1}\mathbf{z}_N\mathbf{z}_N^H\mathbf{Q}_N\right\} = P_N. \tag{4.36}$$

Defining $\mathbf{C}_N = \mathbf{Q}_N^{-1}\mathbf{z}_N\mathbf{z}_N^H\mathbf{Q}_N$, (4.36) becomes

$$N_d\sum_{i=1}^{N_N}(\mathbf{\Lambda}_N(i,i) + N_d\lambda_N)^{-2}\mathbf{C}_N(i,i) = P_N. \tag{4.37}$$

Since $\boldsymbol{\phi}_N$ is a matrix with at most rank M_N, only the first M_N columns of $\mathbf{Q}_N$ span the column space of $E(\mathbf{Y}_N^H\mathbf{H}_N^H\mathbf{W}\mathbf{s})^H$ and $E(\mathbf{Y}_N^H\mathbf{H}_N^H\mathbf{W}\mathbf{W}^H\mathbf{H}_o\mathbf{Y}_o\mathbf{a}_o)^H$ which cause the last $(N_N - M_N)$ columns of $\mathbf{z}_N^H\mathbf{Q}_N$ to become zero vectors and thus the last $(N_N - M_N)$ diagonal elements of $\mathbf{C}_N$ are zero. Therefore, we can obtain the $\{2M\}$th-order polynomial in λ_N

$$N_d\sum_{i=1}^{M_N}(\alpha_i + N_d\lambda_N)^{-2}\mathbf{C}_N(i,i) = P_N. \tag{4.38}$$

We notice from the equations in this section that when all the relay nodes are chosen as the neighbour relay nodes, the MMSE design with a neighbour-based power constraint is equivalent to the MMSE design with a global power constraint. Therefore, the global approach can be considered as a specific case of the neighbour-based approach. Table 4.1 shows a summary of our proposed MMSE design with global, individual and neighbour-based power constraints which will be used for the simulations. If the quasi-static fading channel (block fading) is considered in the simulations, we only need two iterations.

Table 4.1: Summary of the Proposed MMSE Design with Global, Individual and Neighbour-based Power Constraints for two-Hop WSNs

Global Constraint	Individual Constraints	Neighbour-based Constraint
Initialize the algorithm by setting: $\mathbf{A} = \sqrt{\frac{P_T}{N_r N_d}}\mathbf{I}$	Initialize the algorithm by setting: $a_i = \sqrt{\frac{P_{T,i}}{N_d}}$ for $i = 1, 2, ..., N_r$	Initialize the algorithm by setting: $\mathbf{A} = \sqrt{\frac{P_T}{N_r N_d}}\mathbf{I}$
For each iteration:	For each iteration:	For each iteration:
1. Compute $\mathbf{W}_{\text{opt}}$ in (4.7).	1. Compute $\mathbf{W}_{\text{opt}}$ in (4.7).	1. Compute $\mathbf{W}_{\text{opt}}$ in (4.7).
2. Compute $\boldsymbol{\phi}$ and $\mathbf{z}$ in (4.11) and (4.12).	2. Compute $\boldsymbol{\phi}$ and $\mathbf{z}$ in (4.11) and (4.12).	2. Compute $\boldsymbol{\phi}_N$ and $\mathbf{z}_N$ in (4.30) and (4.31).
3. Calculate the EVD of $\boldsymbol{\phi}$ in (4.14).	3. For $i = 1, 2, ..., N_r$	3. Calculate the EVD of $\boldsymbol{\phi}_N$ in (4.33).
4. Solve λ in (4.19).	a)Solve λ_i in (4.23).	4. Solve λ_N in (4.38)
5. Compute $\mathbf{a}_{\text{opt}}$ in (4.9).	b) Compute $a_{i,\text{opt}}$ in (4.22).	5. Compute $\mathbf{a}_{N,\text{opt}}$ in (4.28).

4.4 Proposed Joint Maximum Sum-Rate Design of the Receiver and Power Allocation

In this section, two constrained optimization problems are proposed to describe the joint MSR design of the linear receiver ($\mathbf{w}$) and power allocation parameter ($\mathbf{a}$) subject to a global and neighbour-based power constraints. By the MSR designs, the best possible SNR and QoS can be obtained at the destinations. They will improve the spectrum efficiency which is desirable for the WSNs with the limitation in the sensor node computational capacity. The individual power constraints are not considered here, because of the MSR receiver we make use of the Generalized Rayleigh Quotient which is only suitable to solve optimization problems for vectors.

4.4.1 MSR Design with a Global Power Constraint

We first consider the case where the total power of all the relay nodes is limited to P_T. By substituting (4.2) and (4.3) into (4.4), we get

$$\mathbf{d} = \mathbf{H}_d\mathbf{A}\mathbf{F}\mathbf{H}_s\mathbf{s} + \mathbf{H}_d\mathbf{A}\mathbf{F}\mathbf{v}_r + \mathbf{v}_d. \tag{4.39}$$

We focus on a system with one source node for simplicity. Therefore, the expression of the SR in terms of bps/Hz for our two-hop WSN is

$$\mathrm{SR} = \frac{1}{2}\log_2\left[1 + \frac{\sigma_s^2}{\sigma_n^2}\frac{\mathbf{w}^H\mathbf{H}_d\mathbf{A}\mathbf{F}\mathbf{H}_s\mathbf{H}_s^H\mathbf{F}^H\mathbf{A}^H\mathbf{H}_d^H\mathbf{w}}{\mathbf{w}^H(\mathbf{H}_d\mathbf{A}\mathbf{F}\mathbf{F}^H\mathbf{A}^H\mathbf{H}_d^H + \mathbf{I})\mathbf{w}}\right] \text{ (bps/Hz)}, \tag{4.40}$$

where $\mathbf{w}$ is the linear receiver. Let

$$\mathbf{\Phi} = \mathbf{H}_d\mathbf{A}\mathbf{F}\mathbf{H}_s\mathbf{H}_s^H\mathbf{F}^H\mathbf{A}^H\mathbf{H}_d^H, \tag{4.41}$$

and

$$\mathbf{Z} = \mathbf{H}_d\mathbf{A}\mathbf{F}\mathbf{F}^H\mathbf{A}^H\mathbf{H}_d^H + \mathbf{I}. \tag{4.42}$$

Equation (4.40) becomes

$$\mathrm{SR} = \frac{1}{2}\log_2\left(1 + \frac{\sigma_s^2}{\sigma_n^2}\frac{\mathbf{w}^H\mathbf{\Phi}\mathbf{w}}{\mathbf{w}^H\mathbf{Z}\mathbf{w}}\right) = \frac{1}{2}\log_2(1+ax), \tag{4.43}$$

where

$$a = \frac{\sigma_s^2}{\sigma_n^2} \tag{4.44}$$

and

$$x = \frac{\mathbf{w}^H\mathbf{\Phi}\mathbf{w}}{\mathbf{w}^H\mathbf{Z}\mathbf{w}}. \tag{4.45}$$

Since $\frac{1}{2}\log_2(1+ax)$ is a monotonically increasing function of x ($a > 0$), the problem of maximizing the sum-rate is equivalent to maximizing x. Therefore, the proposed method can be considered as the following optimization problem:

$$\begin{aligned}[\mathbf{w}_{\mathrm{opt}}, \mathbf{a}_{\mathrm{opt}}] \ &= \arg\max_{\mathbf{w},\mathbf{a}} \frac{\mathbf{w}^H\mathbf{\Phi}\mathbf{w}}{\mathbf{w}^H\mathbf{Z}\mathbf{w}}, \\ &\text{subject to } N_d\mathbf{a}^H\mathbf{a} = P_T.\end{aligned} \tag{4.46}$$

We note that the expression $\frac{\mathbf{w}^H\mathbf{\Phi}\mathbf{w}}{\mathbf{w}^H\mathbf{Z}\mathbf{w}}$ in (4.46) is the Generalized Rayleigh Quotient. Thus, the optimal solution of our maximization problem can be solved: $\mathbf{w}_{\mathrm{opt}}$ is any eigenvector corresponding to the dominant eigenvalue of $\mathbf{Z}^{-1}\mathbf{\Phi}$.

In order to obtain the optimal power allocation vector $\mathbf{a}_{\text{opt}}$, we rewrite $\frac{\mathbf{w}^H\mathbf{\Phi}\mathbf{w}}{\mathbf{w}^H\mathbf{Z}\mathbf{w}}$ and the expression is given by

$$\frac{\mathbf{w}^H\mathbf{\Phi}\mathbf{w}}{\mathbf{w}^H\mathbf{Z}\mathbf{w}} = \frac{\mathbf{a}^H\text{diag}\{\mathbf{w}^H\mathbf{H}_d\mathbf{F}\}\mathbf{H}_s\mathbf{H}_s^H\text{diag}\{\mathbf{F}^H\mathbf{H}_d^H\mathbf{w}\}\mathbf{a}}{\mathbf{a}^H\text{diag}\{\mathbf{w}^H\mathbf{H}_d\mathbf{F}\}\text{diag}\{\mathbf{F}^H\mathbf{H}_d^H\mathbf{w}\}\mathbf{a} + \mathbf{w}^H\mathbf{w}}. \tag{4.47}$$

Since the multiplication of any constant value and an eigenvector is still an eigenvector of the matrix, we express the receive filter as

$$\mathbf{w} = \frac{\mathbf{w}_{\text{opt}}}{\sqrt{\mathbf{w}_{\text{opt}}^H\mathbf{w}_{\text{opt}}}}. \tag{4.48}$$

Hence, we obtain

$$\mathbf{w}^H\mathbf{w} = 1 = \frac{N_d\mathbf{a}^H\mathbf{a}}{P_T}. \tag{4.49}$$

By substituting (4.49) into (4.47), we get

$$\frac{\mathbf{w}^H\mathbf{\Phi}\mathbf{w}}{\mathbf{w}^H\mathbf{Z}\mathbf{w}} = \frac{\mathbf{a}^H\text{diag}\{\mathbf{w}^H\mathbf{H}_d\mathbf{F}\}\mathbf{H}_s\mathbf{H}_s^H\text{diag}\{\mathbf{F}^H\mathbf{H}_d^H\mathbf{w}\}\mathbf{a}}{\mathbf{a}^H(\text{diag}\{\mathbf{w}^H\mathbf{H}_d\mathbf{F}\}\text{diag}\{\mathbf{F}^H\mathbf{H}_d^H\mathbf{w}\} + \frac{N_d}{P_T}\mathbf{I})\mathbf{a}}. \tag{4.50}$$

Let

$$\mathbf{M} = \text{diag}\{\mathbf{w}^H\mathbf{H}_d\mathbf{F}\}\mathbf{H}_s\mathbf{H}_s^H\text{diag}\{\mathbf{F}^H\mathbf{H}_d^H\mathbf{w}\}, \tag{4.51}$$

and

$$\mathbf{N} = \text{diag}\{\mathbf{w}^H\mathbf{H}_d\mathbf{F}\}\text{diag}\{\mathbf{F}^H\mathbf{H}_d^H\mathbf{w}\} + \frac{N_d}{P_T}\mathbf{I}. \tag{4.52}$$

Equation (4.50) becomes

$$\frac{\mathbf{w}^H\mathbf{\Phi}\mathbf{w}}{\mathbf{w}^H\mathbf{Z}\mathbf{w}} = \frac{\mathbf{a}^H\mathbf{M}\mathbf{a}}{\mathbf{a}^H\mathbf{N}\mathbf{a}}. \tag{4.53}$$

Likewise, we note that the expression $\frac{\mathbf{a}^H\mathbf{M}\mathbf{a}}{\mathbf{a}^H\mathbf{N}\mathbf{a}}$ in (4.53) is the Generalized Rayleigh Quotient. Thus, the optimal solution of our maximization problem can be solved: $\mathbf{a}_{\text{opt}}$ is any eigenvector corresponding to the dominant eigenvalue of $\mathbf{N}^{-1}\mathbf{M}$, and satisfying $\mathbf{a}_{\text{opt}}^H\mathbf{a}_{\text{opt}} = \frac{P_T}{N_d}$. The solutions of $\mathbf{w}_{\text{opt}}$ and $\mathbf{a}_{\text{opt}}$ depend on each other. Thus, it is necessary to iterate them with an initial value of $\mathbf{a}$ to obtain the optimum solutions.

4.4.2 MSR Design with a Neighbour-based Power Constraint

Similarly to the steps described in Section 4.3.3, we separate the relay nodes into neighbour relay nodes and non-neighbour nodes in the expressions of the system model. Therefore, (4.2) and (4.3) can be rewritten as

$$\mathbf{x}_N = \mathbf{H}_{s,N}\mathbf{s} + \mathbf{v}_N, \tag{4.54}$$

$$\mathbf{x}_o = \mathbf{H}_{s,o}\mathbf{s} + \mathbf{v}_o, \tag{4.55}$$

$$\mathbf{y}_N = \mathbf{F}_N\mathbf{x}_N, \tag{4.56}$$

$$\mathbf{y}_o = \mathbf{F}_o\mathbf{x}_o, \tag{4.57}$$

where the subscript N is denoted for the neighbour relay nodes and the subscript o is used for the non-neighbour relay nodes. By substituting (4.54)-(4.57) into (4.24), we get

$$\mathbf{d} = (\mathbf{H}_N\mathbf{A}_N\mathbf{F}_N\mathbf{H}_{s,N} + \mathbf{H}_o\mathbf{A}_o\mathbf{F}_o\mathbf{H}_{s,o})\mathbf{s} + \mathbf{H}_N\mathbf{A}_N\mathbf{F}_N\mathbf{v}_N + \mathbf{H}_o\mathbf{A}_o\mathbf{F}_o\mathbf{v}_o + \mathbf{v}_d. \tag{4.58}$$

We focus on the system which consists of one source node. Therefore, the expression of the SR in terms of bps/Hz for our two-hop WSN is

$$\mathrm{SR} = \frac{1}{2}\log_2\left[1 + \frac{\sigma_s^2}{\sigma_n^2}\frac{\mathbf{w}^H(\mathbf{H}_N\mathbf{A}_N\mathbf{F}_N\mathbf{H}_{s,N} + \mathbf{H}_o\mathbf{A}_o\mathbf{F}_o\mathbf{H}_{s,o})(\mathbf{H}_N\mathbf{A}_N\mathbf{F}_N\mathbf{H}_{s,N} + \mathbf{H}_o\mathbf{A}_o\mathbf{F}_o\mathbf{H}_{s,o})^H\mathbf{w}}{\mathbf{w}^H(\mathbf{H}_N\mathbf{A}_N\mathbf{F}_N\mathbf{F}_N^H\mathbf{A}_N^H\mathbf{H}_N^H + \mathbf{H}_o\mathbf{A}_o\mathbf{F}_o\mathbf{F}_o^H\mathbf{A}_o^H\mathbf{H}_o^H + \mathbf{I})\mathbf{w}}\right]. \tag{4.59}$$

Let

$$\mathbf{\Phi} = (\mathbf{H}_N\mathbf{A}_N\mathbf{F}_N\mathbf{H}_{s,N} + \mathbf{H}_o\mathbf{A}_o\mathbf{F}_o\mathbf{H}_{s,o})(\mathbf{H}_N\mathbf{A}_N\mathbf{F}_N\mathbf{H}_{s,N} + \mathbf{H}_o\mathbf{A}_o\mathbf{F}_o\mathbf{H}_{s,o})^H, \tag{4.60}$$

and

$$\mathbf{Z} = \mathbf{H}_N\mathbf{A}_N\mathbf{F}_N\mathbf{F}_N^H\mathbf{A}_N^H\mathbf{H}_N^H + \mathbf{H}_o\mathbf{A}_o\mathbf{F}_o\mathbf{F}_o^H\mathbf{A}_o^H\mathbf{H}_o^H + \mathbf{I}. \tag{4.61}$$

Equation (4.59) becomes

$$\mathrm{SR} = \frac{1}{2}\log_2\left(1 + \frac{\sigma_s^2}{\sigma_n^2}\frac{\mathbf{w}^H\mathbf{\Phi}\mathbf{w}}{\mathbf{w}^H\mathbf{Z}\mathbf{w}}\right) \text{ (bps/Hz)}. \tag{4.62}$$

We consider the case where the total power of all the neighbour relay nodes is limited to P_N and $P_N + N_d\mathbf{a}_o^H\mathbf{a}_o = P_T$. Following the same steps as described in Section 4.4.1, the proposed method can be considered as the following optimization problem

$$\begin{aligned}[\mathbf{w}_{\mathrm{opt}}, \mathbf{a}_{N,\mathrm{opt}}] &= \arg\max_{\mathbf{w},\mathbf{a}_N}\frac{\mathbf{w}^H\mathbf{\Phi}\mathbf{w}}{\mathbf{w}^H\mathbf{Z}\mathbf{w}}, \\ &\text{subject to } N_d\mathbf{a}_N^H\mathbf{a}_N = P_N.\end{aligned} \tag{4.63}$$

We note that the expression $\frac{\mathbf{w}^H\mathbf{\Phi}\mathbf{w}}{\mathbf{w}^H\mathbf{Z}\mathbf{w}}$ in (4.63) is the Generalized Rayleigh Quotient. Thus, the optimal solution of our maximization problem can be solved: $\mathbf{w}_{\mathrm{opt}}$ is any eigenvector corresponding to the dominant eigenvalue of $\mathbf{Z}^{-1}\mathbf{\Phi}$.

In order to obtain the optimal power allocation vector for the neighbour relay nodes $\mathbf{a}_{N,\mathrm{opt}}$, we rewrite $\frac{\mathbf{w}^H\mathbf{\Phi}\mathbf{w}}{\mathbf{w}^H\mathbf{Z}\mathbf{w}}$

$$\frac{\mathbf{w}^H\mathbf{\Phi}\mathbf{w}}{\mathbf{w}^H\mathbf{Z}\mathbf{w}} = \frac{\mathbf{a}_N^H\mathbf{M}_1\mathbf{a}_N + \mathbf{a}_N^H\mathbf{M}_2\mathbf{a}_o + \mathbf{a}_o^H\mathbf{M}_3\mathbf{a}_N + \mathbf{a}_o^H\mathbf{M}_4\mathbf{a}_o}{\mathbf{a}_N^H\mathrm{diag}\{\mathbf{w}^H\mathbf{H}_N\mathbf{F}_N\}\mathrm{diag}\{\mathbf{F}_N^H\mathbf{H}_N^H\mathbf{w}\}\mathbf{a}_N + \mathbf{w}^H(\mathbf{H}_o\mathbf{A}_o\mathbf{F}_o\mathbf{F}_o^H\mathbf{A}_o^H\mathbf{H}_o^H + \mathbf{I})\mathbf{w}} \tag{4.64}$$

where

$$\mathbf{M}_1 = \mathrm{diag}\{\mathbf{w}^H\mathbf{H}_N\mathbf{F}_N\}\mathbf{H}_{s,N}\mathbf{H}_{s,N}^H\mathrm{diag}\{\mathbf{F}_N^H\mathbf{H}_N^H\mathbf{w}\}, \tag{4.65}$$

$$\mathbf{M}_2 = \mathrm{diag}\{\mathbf{w}^H\mathbf{H}_N\mathbf{F}_N\}\mathbf{H}_{s,N}\mathbf{H}_{s,o}^H\mathrm{diag}\{\mathbf{F}_o^H\mathbf{H}_o^H\mathbf{w}\}, \tag{4.66}$$

$$\mathbf{M}_3 = \mathrm{diag}\{\mathbf{w}^H\mathbf{H}_o\mathbf{F}_o\}\mathbf{H}_{s,o}\mathbf{H}_{s,N}^H\mathrm{diag}\{\mathbf{F}_N^H\mathbf{H}_N^H\mathbf{w}\}, \tag{4.67}$$

$$\mathbf{M}_4 = \mathrm{diag}\{\mathbf{w}^H\mathbf{H}_o\mathbf{F}_o\}\mathbf{H}_{s,o}\mathbf{H}_{s,o}^H\mathrm{diag}\{\mathbf{F}_o^H\mathbf{H}_o^H\mathbf{w}\}. \tag{4.68}$$

Since the multiplication of any constant value and an eigenvector is still an eigenvector of the matrix, we express the receive filter as

$$\mathbf{w} = \frac{\mathbf{w}_{opt}}{\sqrt{\mathbf{w}_{opt}^H(\mathbf{H}_o\mathbf{A}_o\mathbf{F}_o\mathbf{F}_o^H\mathbf{A}_o^H\mathbf{H}_o^H + \mathbf{I})\mathbf{w}_{opt}}}. \tag{4.69}$$

Therefore, we obtain

$$\mathbf{w}^H(\mathbf{H}_o\mathbf{A}_o\mathbf{F}_o\mathbf{F}_o^H\mathbf{A}_o^H\mathbf{H}_o^H + \mathbf{I})\mathbf{w} = 1 = \frac{N_d}{P_N}\mathbf{a}_N^H\mathbf{a}_N. \tag{4.70}$$

By substituting (4.70) into (4.64), we obtain

$$\frac{\mathbf{w}^H\mathbf{\Phi}\mathbf{w}}{\mathbf{w}^H\mathbf{Z}\mathbf{w}} = \frac{\mathbf{a}_N^H\mathbf{M}_1\mathbf{a}_N + \mathbf{a}_N^H\mathbf{M}_2\mathbf{a}_o + \mathbf{a}_o^H\mathbf{M}_3\mathbf{a}_N + \mathbf{a}_o^H\mathbf{M}_4\mathbf{a}_o}{\mathbf{a}_N^H\mathbf{N}\mathbf{a}_N}, \tag{4.71}$$

where

$$\mathbf{N} = \mathrm{diag}\{\mathbf{w}^H\mathbf{H}_N\mathbf{F}_N\}\mathrm{diag}\{\mathbf{F}_N^H\mathbf{H}_N^H\mathbf{w}\} + \frac{N_d}{P_N}\mathbf{I}. \tag{4.72}$$

The expression $\frac{\mathbf{a}^H\mathbf{M}\mathbf{a}}{\mathbf{a}^H\mathbf{N}\mathbf{a}}$ in (4.71) can be divided into four terms and only the first term is the Generalized Rayleigh Quotient. In order to make use of the Generalized Rayleigh Quotient to solve the optimization problem, our aim is to transform the remaining three terms into the Generalized Rayleigh Quotient. For the fourth term, we have

$$\begin{aligned}\mathbf{a}_o^H\mathbf{M}_4\mathbf{a}_o &= \mathbf{a}_o^H\mathbf{M}_4\mathbf{a}_o\frac{N_d\mathbf{a}_N^H\mathbf{a}_N}{P_N} \\ &= \mathbf{a}_N^H\left(\frac{N_d\mathbf{a}_o^H\mathbf{M}_4\mathbf{a}_o}{P_N}\mathbf{I}\right)\mathbf{a}_N.\end{aligned} \tag{4.73}$$

For the second and third terms, we can achieve the Generalized Rayleigh Quotient by solving the following optimization problem:

$$\begin{aligned}[\mathbf{T}_{\text{opt}}, \mathbf{a}_{N,\text{opt}}] &= \arg\min_{\mathbf{T},\mathbf{a}_N} (\mathbf{a}_N^H \mathbf{M}_2 \mathbf{a}_o + \mathbf{a}_o^H \mathbf{M}_3 \mathbf{a}_N - \mathbf{a}_N^H \mathbf{T} \mathbf{a}_N)^2, \\ &\text{subject to } N_d \mathbf{a}_N^H \mathbf{a}_N = P_N.\end{aligned} \tag{4.74}$$

By fixing $\mathbf{a}_N$, we obtain

$$\mathbf{T} = \frac{N_d}{P_N}(\mathbf{M}_2 \mathbf{a}_o \mathbf{a}_N^H + \mathbf{a}_N \mathbf{a}_o^H \mathbf{M}_3) \tag{4.75}$$

which satisfies the following equation

$$\mathbf{a}_N^H \mathbf{M}_2 \mathbf{a}_o + \mathbf{a}_o^H \mathbf{M}_3 \mathbf{a}_N = \mathbf{a}_N^H \mathbf{T} \mathbf{a}_N \tag{4.76}$$

for any value of $\mathbf{a}_N$. Let us define

$$\mathbf{M} = \mathbf{M}_1 + \mathbf{T} + \frac{N_d \mathbf{a}_o^H \mathbf{M}_4 \mathbf{a}_o}{P_N} \mathbf{I}. \tag{4.77}$$

Then, equation (4.71) becomes

$$\frac{\mathbf{w}^H \mathbf{\Phi} \mathbf{w}}{\mathbf{w}^H \mathbf{Z} \mathbf{w}} = \frac{\mathbf{a}_N^H \mathbf{M} \mathbf{a}_N}{\mathbf{a}_N^H \mathbf{N} \mathbf{a}_N}, \tag{4.78}$$

which is a Generalized Rayleigh Quotient. Therefore, the optimal solution of our maximization problem can be solved: $\mathbf{a}_{N,\text{opt}}$ is any eigenvector corresponding to the dominant eigenvalue of $\mathbf{N}^{-1}\mathbf{M}$ and satisfies $\mathbf{a}_{N,\text{opt}}^H \mathbf{a}_{N,\text{opt}} = \frac{P_N}{N_d}$.

In this section, two methods are employed to calculate the dominant eigenvectors. The first one is the QR algorithm [87] which calculates all the eigenvalues and eigenvectors of a matrix. We can choose the dominant eigenvector among them. The second one is the power method [87] which only calculates the dominant eigenvector of a matrix. Hence, the computational complexity can be reduced. Table 4.2 shows a summary of our proposed MSR design with global and neighbour-based power constraints which will be used for the simulations. If the quasi-static fading channel (block fading) is considered in the simulations, we only need two iterations.

Table 4.2: Summary of the Proposed MSR Design with Global and Neighbour-based Power Constraints for two-Hop WSNs

Global Power Constraint	Neighbour-based Power Constraint
Initialize the algorithm by setting:	Initialize the algorithm by setting:
$\mathbf{A} = \sqrt{\frac{P_T}{N_r N_d}}\mathbf{I}$	$\mathbf{A} = \sqrt{\frac{P_T}{N_r N_d}}\mathbf{I}$ (include $\mathbf{a}_N$ and $\mathbf{a}_o$)
For each iteration:	For each iteration:
1. Compute $\mathbf{\Phi}$ and $\mathbf{Z}$ in (4.41) and (4.42).	1. Compute $\mathbf{\Phi}$ and $\mathbf{Z}$ in (4.60) and (4.61).
2. Use the QR algorithm or the power method to compute the dominant eigenvector of $\mathbf{Z}^{-1}\mathbf{\Phi}$, denoted as $\mathbf{w}_{\rm opt}$.	2. Use the QR algorithm or the power method to compute the dominant eigenvector of $\mathbf{Z}^{-1}\mathbf{\Phi}$, denoted as $\mathbf{w}_{\rm opt}$.
	3. Compute $\mathbf{T}$ in (4.75).
3. Compute $\mathbf{M}$ and $\mathbf{N}$ in (4.51) and (4.52).	4. Compute $\mathbf{M}$ and $\mathbf{N}$ in (4.77) and (4.72).
4. Use the QR algorithm or the power method to compute the dominant eigenvector of $\mathbf{N}^{-1}\mathbf{M}$, denoted as $\mathbf{a}$.	5. Use the QR algorithm or the power method to compute the dominant eigenvector of $\mathbf{N}^{-1}\mathbf{M}$, denoted as $\mathbf{a}_N$.
5. To ensure the power constraint $\mathbf{a}_{\rm opt}^H\mathbf{a}_{\rm opt} = \frac{P_T}{N_d}$, compute $\mathbf{a}_{\rm opt} = \sqrt{\frac{P_T}{N_d\mathbf{a}^H\mathbf{a}}}\mathbf{a}$.	6. To ensure the power constraint $\mathbf{a}_{N,\rm opt}^H\mathbf{a}_{N,\rm opt} = \frac{P_N}{N_d}$, compute $\mathbf{a}_{N,\rm opt} = \sqrt{\frac{P_N}{N_d\mathbf{a}_N^H\mathbf{a}_N}}\mathbf{a}_N$.

4.5 Analysis of the proposed algorithms

In this section, an analysis of the computational complexity and the convergence of the algorithms are developed. We first illustrate the computational complexity requirements of the proposed MMSE and MSR designs by tables and figures. Then, we make use of the convergence results for the alternating optimization algorithms in [85,86] and particularly present a set of sufficient conditions under which our proposed algorithms will converge to the optimal solutions.

4.5.1 Computational Complexity Analysis

Table 4.3 and Table 4.4 list the computational complexity per iteration in terms of the number of multiplications, additions and divisions for our proposed joint linear receiver design (MMSE and MSR) and power allocation strategies. For the joint MMSE designs, we use the QR algorithm to perform the eigendecomposition of the matrix. We set $M = \min\{N_s, N_r, N_d\} = 1$ and $M_N = \min\{N_s, N_N, N_d\} = 1$ to simplify the processing of solving the equations in (4.19) and (4.38). Please note that in this work the QR decomposition by Householder transformation [87, 88] is employed by the QR algorithms. The quantities n_Q and n_P denote the number of iterations of the QR algorithm and the power method, respectively. Because the multiplication dominates the computational complexity, in order to compare the computational complexity of our proposed joint MMSE and MSR designs, the number of multiplications versus the number of relay nodes for each iteration are displayed in Figure 4.2 and Figure 4.3. For the purpose of illustration, we set $N_s = 1$, $N_d = 2$ and $n_Q = n_P = 10$. R denotes the averaged ratio of the number of neighbour relay nodes to the number of relay nodes. It can be seen that our proposed MMSE and MSR receivers with a neighbour-based power constraint have a significant complexity reduction compared with the proposed receivers with a global power constraint. Obviously, a lower R will lead to a lower computational complexity. For the MMSE design, when the individual power constrains are considered, the computational complexity is lower than other constraints because there is no need to compute the eigendecomposition for it. For the MSR design, employing the power method to calculate the dominant eigenvectors has a lower computational complexity than employing the QR algorithm.

4.5.2 Sufficient Conditions for Convergence

To develop the analysis and proofs, we need to define a metric space and the Hausdorff distance that will extensively be used. A metric space is an ordered pair $(\mathcal{M}, d)$, where $\mathcal{M}$ is a nonempty set, and d is a metric on $\mathcal{M}$, i.e., a function $d : \mathcal{M} \times \mathcal{M} \to \mathbb{R}$ such that

Table 4.3: Computational Complexity per Iteration of the joint MMSE Designs for two-Hop WSNs

	Constraint	Multiplications	Additions	Divisions
W	All	$N_d(N_d-1)(4N_d+1)/6$ $+(N_s+N_r)N_d^2+N_r^2N_d$ $+N_sN_rN_d+N_rN_d$	$N_d(N_d-1)(4N_d+1)/6$ $+(N_s+N_r)N_d^2+N_r^2N_d+N_sN_rN_d$ $-(N_d^2+2N_sN_d+N_rN_d)+N_d$	$N_d(3N_d-1)/2$
λ	Global	$n_Q(\frac{13}{6}N_r^3+\frac{3}{2}N_r^2+\frac{1}{3}N_r-2)$ $-N_r^3+3N_sN_r^2+N_sN_rN_d$ $+N_r^2+N_sN_r+1$	$n_Q(\frac{13}{6}N_r^3-N_r^2-\frac{1}{6}N_r+1)$ $-N_r^3+3N_sN_r^2+N_sN_rN_d$ $-N_r^2-2N_sN_r-N_r+1$	$n_Q(N_r-1)+1$
	Individual	$N_sN_r^2+N_sN_rN_d+2N_r^2$ $+N_sN_r+N_r$	$N_sN_r^2+N_sN_rN_d-N_sN_r$	N_r
	Neighbour-based	$n_Q(\frac{13}{6}N_N^3+\frac{3}{2}N_N^2+\frac{1}{3}N_N-2)$ $-N_N^3+2N_sN_N^2+N_sN_rN_d$ $+N_sN_rN_N-N_N^2+2N_rN_N$ $+N_sN_N+1$	$n_Q(\frac{13}{6}N_N^3-N_N^2-\frac{1}{6}N_N+1)$ $-N_N^3+2N_sN_N^2+N_sN_rN_d$ $+N_sN_rN_N-N_N^2-N_sN_N$ $-N_sN_r-2N_N+2$	$n_Q(N_N-1)+1$
a	Global	$N_r(N_r-1)(4N_r+1)/6$ $+N_r^2+1$	$N_r(N_r-1)(4N_r+1)/6$ $+N_r^2$	$N_r(3N_r-1)/2$
	Individual	$2N_r$	N_r	N_r
	Neighbour-based	$N_N(N_N-1)(4N_N+1)/6$ $+N_N^2+1$	$N_N(N_N-1)(4N_N+1)/6$ $+N_N^2$	$N_N(3N_N-1)/2$

for any $x, y, z \in \mathcal{M}$, the following conditions hold:

1) $d(x, y) \geq 0$.

2) $d(x, y) = 0$ iff $x = y$.

3) $d(x, y) = d(y, x)$.

4) $d(x, y) \leq d(x, y) + d(y, z)$.

The Hausdorff distance measures how far two subsets of a metric space are from each

Table 4.4: Computational Complexity per Iteration of the joint MSR Designs for two-Hop WSNs

Constraint	Multiplications	Additions	Divisions
w			
Global/Neighbour-based	$n_Q(\frac{13}{6}N_d^3+\frac{3}{2}N_d^2+\frac{1}{3}N_d-2)$	$n_Q(\frac{13}{6}N_d^3-N_d^2-\frac{1}{6}N_d+1)$	$n_Q(N_d-1)$
QR Algorithm	$+N_d(N_d-1)(4N_d+1)/6$	$+N_d(N_d-1)(4N_d+1)/6$	$+N_d(3N_d-1)/2$
	$+N_rN_d^2+N_d^2+3N_rN_d$	$+N_rN_d^2-N_d^2+N_rN_d$	
Global/Neighbour-based	$n_PN_d^2$	$n_PN_d(N_d-1)$	
Power Method	$+N_d(N_d-1)(4N_d+1)/6$	$+N_d(N_d-1)(4N_d+1)/6$	$N_d(3N_d-1)/2$
	$+N_d^3+N_rN_d^2+N_d^2+3N_rN_d$	$+N_d^3+N_rN_d^2-2N_d^2+N_rN_d$	
Global	$n_Q(\frac{13}{6}N_r^3+\frac{3}{2}N_r^2+\frac{1}{3}N_r-2)$	$n_Q(\frac{13}{6}N_r^3-N_r^2-\frac{1}{6}N_r+1)$	$n_Q(N_r-1)$
QR Algorithm	$+N_r(N_r-1)(4N_r+1)/6$	$+N_r(N_r-1)(4N_r+1)/6$	$+N_r(3N_r-1)/2$
	$+N_r^2+N_rN_d+4N_r+N_d$	$+N_rN_d+N_r+N_d-2$	$+N_d+1$
Global	$n_PN_r^2$	$n_PN_r(N_r-1)$	
Power Method	$+N_r(N_r-1)(4N_r+1)/6$	$+N_r(N_r-1)(4N_r+1)/6$	$N_r(3N_r-1)/2$
	$+N_r^3+N_r^2+N_rN_d$	$+N_r^3-N_r^2+N_rN_d$	$+N_d+1$
	$+4N_r+N_d$	$+N_r+N_d-2$	
a			
	$n_Q(\frac{13}{6}N_N^3+\frac{3}{2}N_N^2+\frac{1}{3}N_N-2)$	$n_Q(\frac{13}{6}N_N^3-N_N^2-\frac{1}{6}N_N+1)$	$n_Q(N_N-1)$
Neighbour-based	$+N_N(N_N-1)(4N_N+1)/6$	$+N_N(N_N-1)(4N_N+1)/6$	$+N_N(3N_N-1)/2$
QR Algorithm	$-N_N^3+N_rN_N^2+2N_r^2+2N_N^2$	$-N_N^3+N_rN_N^2+N_r^2+2N_N^2$	$+N_d+1$
	$+N_d^2+N_rN_d-2N_rN_N$	$+N_d^2+N_rN_d-2N_rN_N$	
	$+2N_r+2N_N+N_d+1$	$-N_r+3N_N-3$	
	$n_PN_N^2$	$n_PN_r(N_r-1)$	
Neighbour-based	$+N_N(N_N-1)(4N_N+1)/6$	$+N_N(N_N-1)(4N_N+1)/6$	$N_N(3N_N-1)/2$
Power Method	$+N_rN_N^2+2N_r^2+2N_N^2+N_d^2$	$+N_rN_N^2+N_r^2+N_N^2+N_d^2$	$+N_d+1$
	$+N_rN_d-2N_rN_N+2N_r$	$+N_rN_d-2N_rN_N$	
	$+2N_N+N_d+1$	$-N_r+3N_N-3$	

other and is defined by

$$d_H(X,Y)=\max\left\{\sup_{x\in X}\inf_{y\in Y}d(x,y),\sup_{y\in Y}\inf_{x\in X}d(x,y)\right\}. \tag{4.79}$$

The proposed joint MMSE designs can be stated as an alternating minimization strategy based on the MSE defined in (4.5) and expressed as

$$\mathbf{W}_n\in\arg\min_{\mathbf{W}\in\underline{\mathbf{W}}_n}\mathrm{MSE}(\mathbf{W},\mathbf{a}_{n-1}) \tag{4.80}$$

$$\mathbf{a}_n\in\arg\min_{\mathbf{a}\in\underline{\mathbf{a}}_n}\mathrm{MSE}(\mathbf{W}_n,\mathbf{a}) \tag{4.81}$$

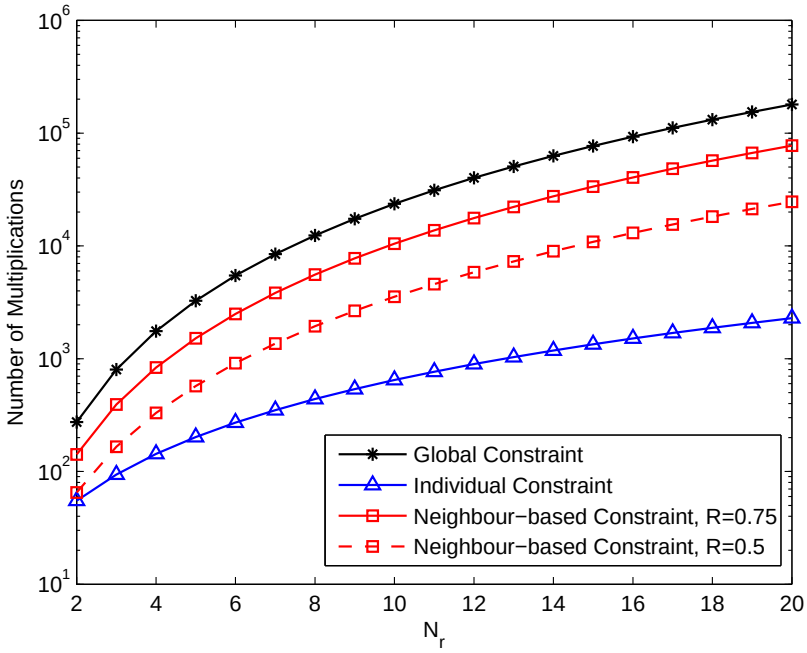

Figure 4.2: Number of multiplications versus the number of relay nodes of our proposed joint MMSE design of the receiver and power allocation strategies for two-hop WSNs.

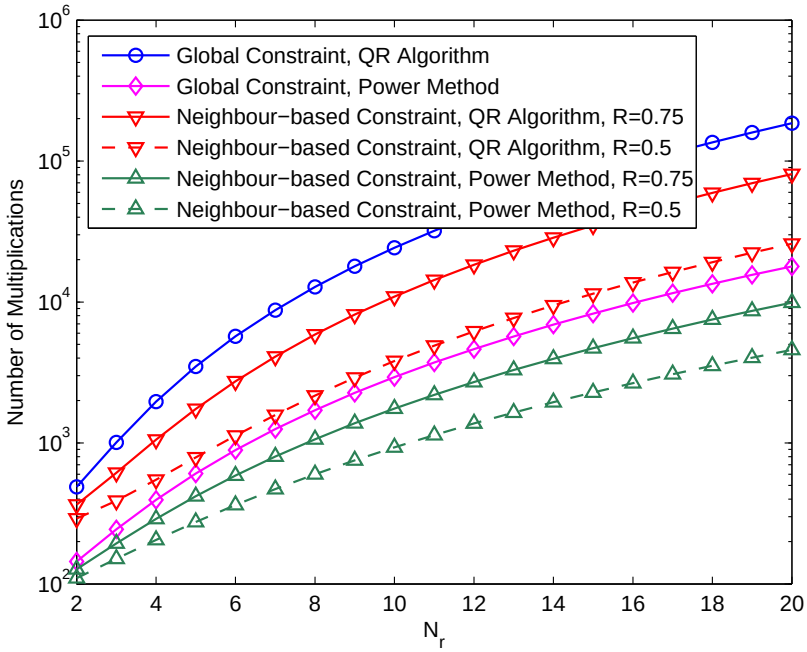

Figure 4.3: Number of multiplications versus the number of relay nodes of our proposed joint MSR design of the receiver and power allocation strategies for two-hop WSNs.

where the sets $\underline{\mathbf{W}}, \underline{\mathbf{a}} \subset \mathcal{M}$, and the sequences of compact sets $\{\underline{\mathbf{W}}_n\}_{n\geq 0}$ and $\{\underline{\mathbf{a}}_n\}_{n\geq 0}$ converge to the sets $\underline{\mathbf{W}}$ and $\underline{\mathbf{a}}$, respectively.

Although we are not given the sets $\underline{\mathbf{W}}$ and $\underline{\mathbf{a}}$ directly, we have the sequence of compact sets $\{\underline{\mathbf{W}}_n\}_{n\geq 0}$ and $\{\underline{\mathbf{a}}_n\}_{n\geq 0}$. The aim of our proposed joint MMSE designs is to find a sequence of $\mathbf{W}_n$ and $\mathbf{a}_n$ such that

$$\lim_{n\to\infty} \mathrm{MSE}(\mathbf{W}_n, \mathbf{a}_n) = \mathrm{MSE}(\mathbf{W}_{opt}, \mathbf{a}_{opt}) \tag{4.82}$$

where $\mathbf{W}_{opt}$ and $\mathbf{a}_{opt}$ correspond to the optimal values of $\mathbf{W}_n$ and $\mathbf{a}_n$, respectively. To present a set of sufficient conditions under which the proposed algorithms converge, we need the so-called three-point and four-point properties [85, 86]. Let us assume that there is a function $f : \mathcal{M} \times \mathcal{M} \to \mathbb{R}$ such that the following conditions are satisfied.

1) *Three-point property* $(\mathbf{W}, \widetilde{\mathbf{W}}, \mathbf{a})$:

For all $n \geq 1$, $\mathbf{W} \in \underline{\mathbf{W}}_n$, $\mathbf{a} \in \underline{\mathbf{a}}_{n-1}$, and $\widetilde{\mathbf{W}} \in \arg\min_{\mathbf{W}\in\underline{\mathbf{W}}_n} \mathrm{MSE}(\mathbf{W}, \mathbf{a})$, we have

$$f(\mathbf{W}, \widetilde{\mathbf{W}}) + \mathrm{MSE}(\widetilde{\mathbf{W}}, \mathbf{a}) \leq \mathrm{MSE}(\mathbf{W}, \mathbf{a}) \tag{4.83}$$

2) *Four-point property* $(\mathbf{W}, \mathbf{a}, \widetilde{\mathbf{W}}, \tilde{\mathbf{a}})$:

For all $n \geq 1$, $\mathbf{W}, \widetilde{\mathbf{W}} \in \underline{\mathbf{W}}_n$, $\mathbf{a} \in \underline{\mathbf{a}}_n$, and $\tilde{\mathbf{a}} \in \arg\min_{\mathbf{a}\in\underline{\mathbf{a}}_n} \mathrm{MSE}(\widetilde{\mathbf{W}}, \mathbf{a})$, we have

$$\mathrm{MSE}(\mathbf{W}, \tilde{\mathbf{a}}) \leq \mathrm{MSE}(\mathbf{W}, \mathbf{a}) + f(\mathbf{W}, \widetilde{\mathbf{W}}) \tag{4.84}$$

These two properties are the mathematical expressions of the sufficient conditions for the convergence of the alternating minimization algorithms which are stated in [85] and [86]. It means that if there exists a function $f(\mathbf{W}, \widetilde{\mathbf{W}})$ with the parameter $\mathbf{W}$ during two iterations that satisfies the two inequalities about the MSE in (4.83) and (4.84), the convergence of our proposed MMSE designs that make use of the alternating minimization algorithm can be proved by the theorem below.

Theorem: Let $\{(\underline{\mathbf{W}}_n, \underline{\mathbf{a}}_n)\}_{n\geq 0}$, $\underline{\mathbf{W}}, \underline{\mathbf{a}}$ be compact subsects of the compact metric space $(\mathcal{M}, d)$ such that

$$\underline{\mathbf{W}}_n \overset{d_H}{\to} \underline{\mathbf{W}} \quad \underline{\mathbf{a}}_n \overset{d_H}{\to} \underline{\mathbf{a}} \tag{4.85}$$

and let MSE : $\mathcal{M} \times \mathcal{M} \rightarrow \mathbb{R}$ be a continuous function. Let conditions 1) and 2) hold. Then, for the proposed algorithms we have

$$\lim_{n\rightarrow\infty} \mathrm{MSE}(\mathbf{W}_n, \mathbf{a}_n) = \mathrm{MSE}(\mathbf{W}_{opt}, \mathbf{a}_{opt}) \tag{4.86}$$

A general proof of this theorem is detailed in [85] and [86]. The proposed joint MSR designs can be stated as an alternating maximization strategy based on the SR defined in (4.40) that follow a similar procedure to the one above.

4.6 Simulations

In this section, we numerically study the performance of our proposed joint designs of the linear receiver and the power allocation parameters and compare them with the equal power allocation method [29] which allocates the same power level for all links between relay nodes and destination nodes. For the purpose of fairness, we assume that the total power for all relay nodes in the network is the same which can be indicated as $\sum_{i=1}^{N_r} P_{T,i} = P_T$. We consider a two-hop wireless sensor network. The number of source nodes (N_s), relay nodes (N_r) and destination nodes (N_d) are 1, 4 and 2 respectively. We consider an AF cooperation protocol. The quasi-static fading channel (block fading channel) is considered in our simulations whose elements are Rayleigh random variables (with zero mean and unit variance) and assumed to be invariant during the transmission of each packet. In our simulations, the channel is assumed to be known at the destination nodes. For channel estimation algorithms for WSNs and other low-complexity parameter estimation algorithms, one refers to [74] and [89]. During each phase, the source transmits the QPSK modulated packets with 1500 symbols. The noise at the relay and destination nodes is modeled as circularly symmetric complex Gaussian random variables with zero mean. A perfect (error free) feedback channel between the destination nodes and the relay nodes is assumed to transmit the amplification coefficients.

For the MMSE design, it can be seen from Figure 4.4 that our three proposed methods achieve a better BER performance than the equal power allocation method. Among them,

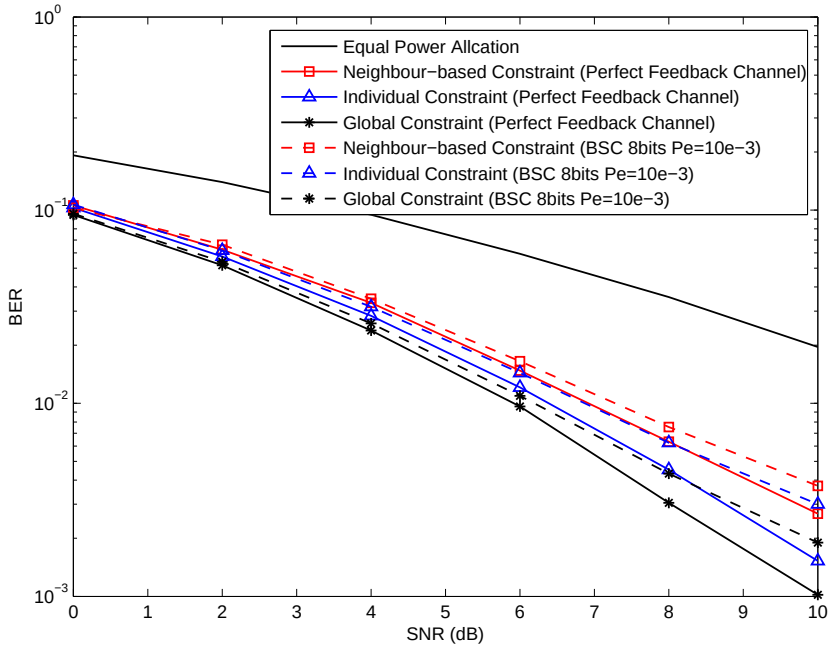

Figure 4.4: BER performance versus SNR of our proposed joint MMSE design of the receiver and power allocation strategies, compared to the equal power allocation method for two-hop WSNs.

the method with a global constraint has the best performance. This result is what we expected because a global constraint provides the largest degrees of freedom for allocating the power among the relay nodes. For the method with a neighbour-based constraint, we introduce a bound B, which is set to 0.6, for the channel power gain between the relay nodes and the destination nodes to choose the neighbour relay nodes. Although it has a higher BER compared to the method with a global constraint, the averaged ratio of the number of neighbour relay nodes to the number of relay nodes (R) is 0.7843 which indicates a reduced computational complexity. For the MSR design, it can be seen from Figure 4.5 and Figure 4.6 that our proposed methods achieve a better sum-rate performance than the equal power allocation method. Using the power method to calculate the dominant eigenvector yields a very similar result to the QR algorithm but requires a lower complexity. For the method with a neighbour-based constraint, when we introduce a bound B = 0.6, a similar performance to the method with a global constraint can be achieved with a reduced R (0.7830). To show the performance trend for other values of B, we fix the SNR at 10 dB and choose B ranging form 0 to 1.5. The performance

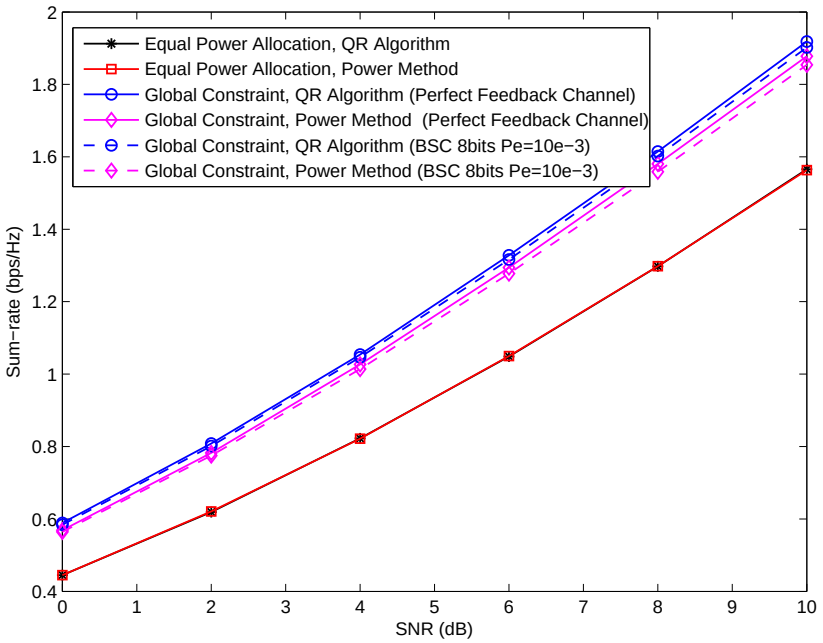

Figure 4.5: Sum-rate performance versus SNR of our proposed joint MSR design of the receiver and power allocation strategies with a global constraint, compared to the equal power allocation method for two-hop WSNs.

curves are shown in Figure 4.7 and Figure 4.8, which include the BER and sum-rate performance versus B and R versus B of the MMSE design and MSR design respectively with a neighbour-based power constraint. It can be seen that along with the increase in B, their performance becomes worse, and the R becomes lower. It demonstrates that for our joint designs of the receivers with a neighbour-based power constraint, the value of B can be varied to trade off achievable performance against computation complexity. In practice, the feedback channel cannot be error free. In order to study the impact of feedback channel errors on the performance, we employ the binary symmetric channel (BSC) as the model for the feedback channel and quantize each complex amplification coefficient to an 8-bit binary value (4 bits for the real part, 4 bits for the imaginary part). The error probability (Pe) of the BSC is fixed at 10^{-3}. The dashed curves in Figure 4.4, Figure 4.5 and Figure 4.6 show the performance degradation compared to the performance when using a perfect feedback channel. To show the performance trend of the BSC for other values of Pe, we fix the SNR at 10 dB and choose Pe ranging from 0 to 10^{-2}. The performance curves are shown in Figure 4.9, which illustrate the BER and the sum-rate performance

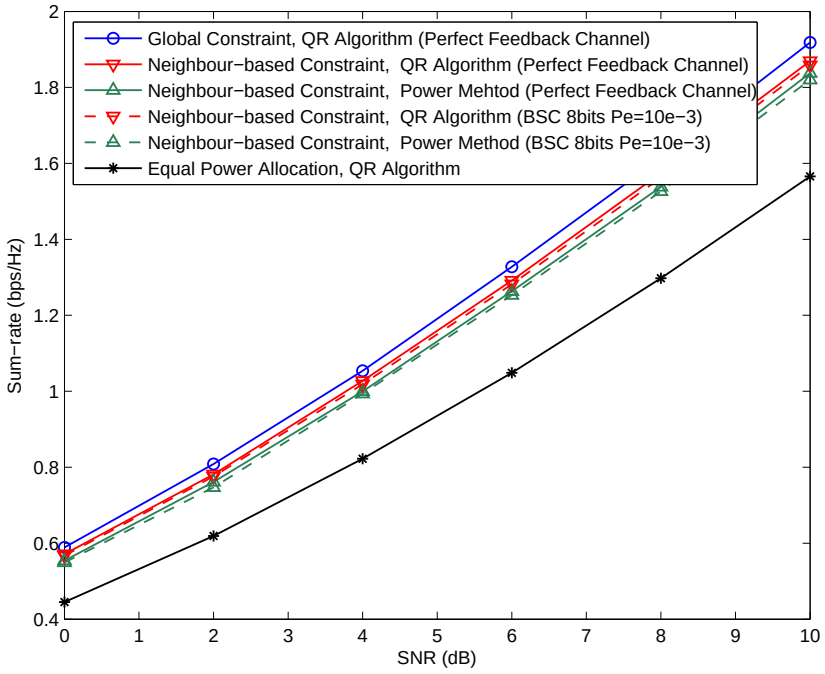

Figure 4.6: Sum-rate performance versus SNR of our proposed joint MSR design of the receiver and power allocation strategies with a neighbour-based constraint, compared to the equal power allocation method for two-hop WSNs.

versus Pe of our two proposed joint designs of the receivers with neighbour-based power constraints. It can be seen that along with the increase in Pe, their performance becomes worse.

Finally, we replace the perfect CSI with the estimated channel coefficients to compute the receive filters and power allocation parameters at the destinations. We employ the BEACON channel estimation which is proposed in [74]. Figure 4.10 illustrates the impact of the channel estimation on the performance of our proposed MMSE and MSR design with a global power constraint by comparing to the performance of perfect CSI. The quantity n_t denotes the number of training sequence symbols per data packet. Please note that in these simulations a perfect feedback channel is considered and the QR algorithm is used in the MSR design. For both the MMSE and MSR designs, it can be seen that when n_t is set to 10, the BEACON channel estimation lead to an obvious performance degradation compared to the perfect CSI. However, when n_t is increased to 50,

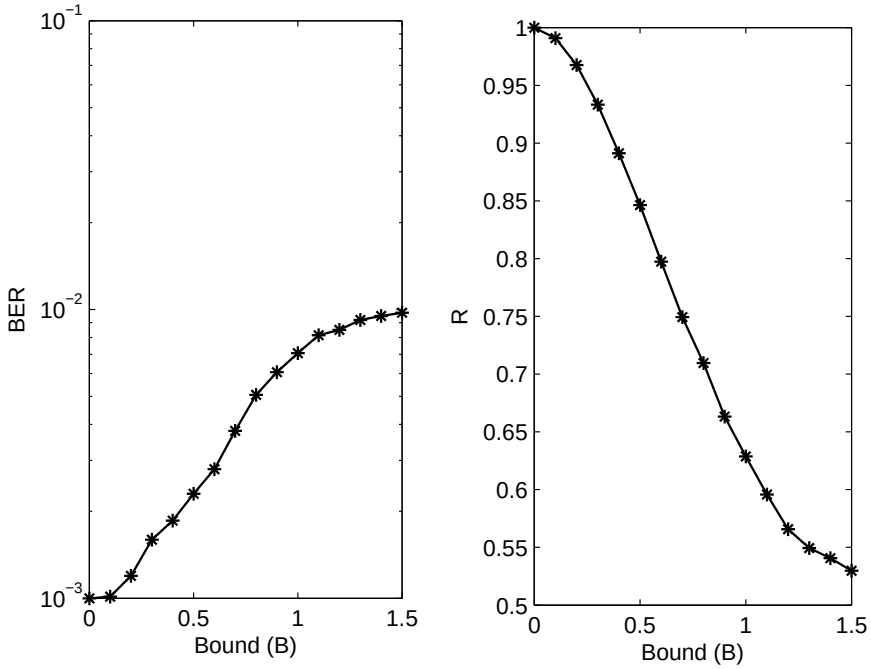

Figure 4.7: (a) BER performance versus the bound and (b) R versus the bound of the MMSE design with a neighbour-based power constraint for two-hop WSNs.

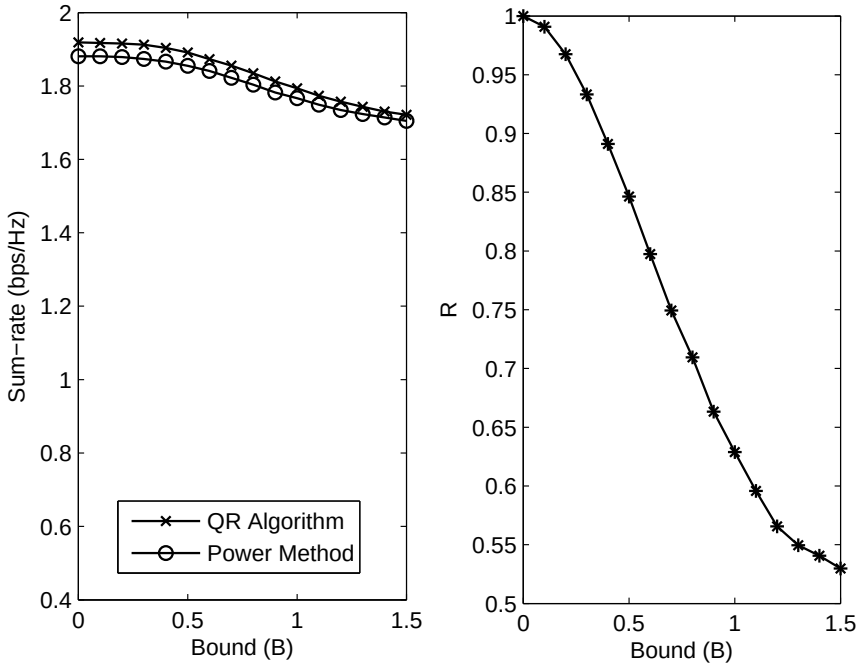

Figure 4.8: (a) Sum-rate performance versus the bound and (b) R versus the bound of the MSR design with a neighbour-based power constraint for two-hop WSNs.

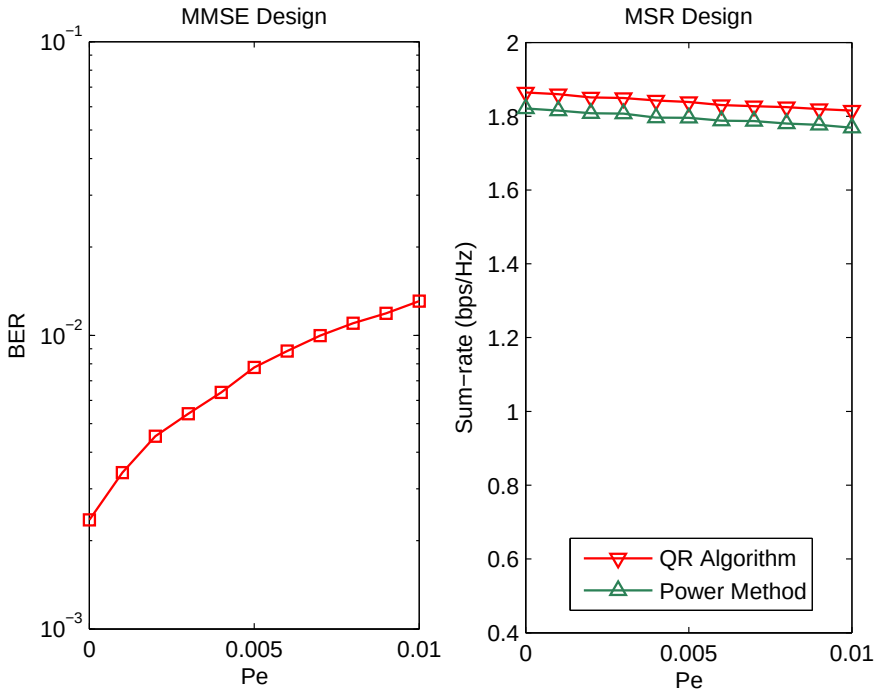

Figure 4.9: (a) BER performance versus Pe of our proposed MMSE design (b) Sum-rate performance versus Pe of our proposed MSR design with a neighbour-based power constraint when employing the BSC as the model for the feedback channel for two-hop WSNs.

the BEACON channel estimation can achieve a similar performance to the perfect CSI. Other scenarios and network topologies have been investigated and the results show that the proposed algorithms work very well with channel estimation algorithms and a small number of training symbols.

4.7 Summary

Two kinds of joint receiver design and power allocation strategies via an alternating optimization approach have been proposed for two-hop WSNs. The first one minimizes the mean-square error and the second one maximizes the sum-rate of the WSN. We derive constrained MMSE and constrained MSR expressions for the linear receivers and the power allocation parameters that contain the optimal complex amplification coefficients

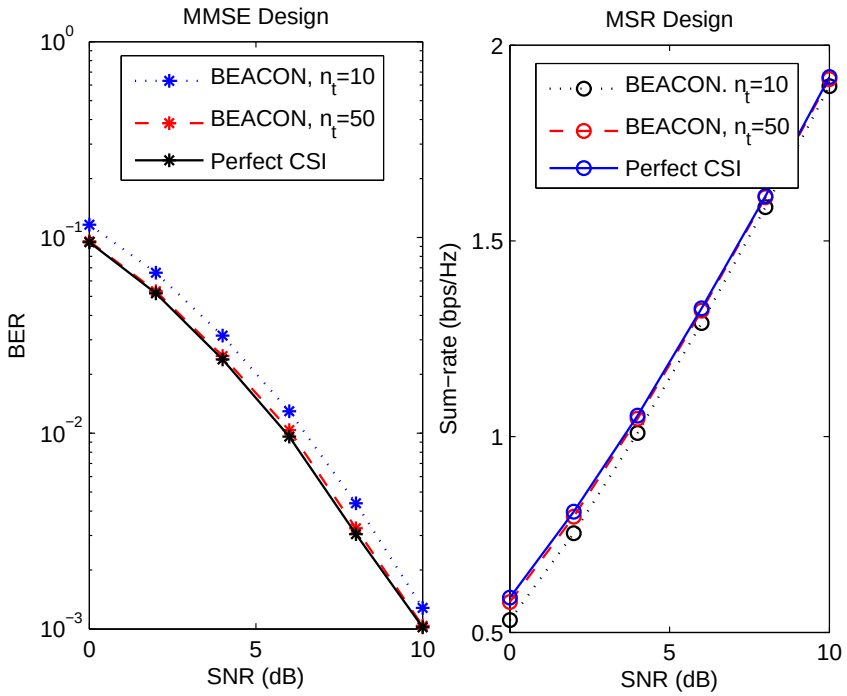

Figure 4.10: (a) BER performance versus SNR of our proposed MMSE design (b) Sum-rate performance versus SNR our proposed MSR design with a global power constraint when employing the BEACON channel estimation, compared to the performance of perfect CSI for two-hop WSNs

for each relay node. The power constraints include the global, individual and neighbour-based ones. An analysis of the computational complexity and the convergence of the algorithms is also presented. It has been shown that our proposed strategies achieve a significantly better performance than the equal power allocation method. Moreover, when the neighbour-based constraint is considered, it brings a feature to balance the performance against the computational complexity and the need for feedback information which is desirable for WSNs to extend their lifetime.

Chapter 5

Joint Linear Receiver Design and Power Allocation Using Alternating Optimization Algorithms for Multihop WSNs

Contents

5.1 Introduction

In this chapter, we consider a general multihop WSN where the AF relaying scheme is employed. The proposed strategy is to jointly design the linear receivers and the power allocation parameters that contain the optimal complex amplification coefficients for each relay nodes via an alternating optimization approach. Two kinds of linear receivers are designed, the minimum mean-square error (MMSE) receiver and the maximum sum-rate (MSR) receiver. They can be considered as solutions to constrained optimization problems where the objective function is the mean-square error (MSE) cost function or the sum-rate (SR) and the constraint is a bound on the power levels among the relay nodes. Then, the constrained MMSE or MSR expressions for the linear receiver and the power allocation parameter can be derived. The major novelty in these strategies presented here is that they are applicable to general multihop WSNs with multi source nodes and destination nodes, as opposed to the simple two-hop WSNs with one pair of source-destination nodes [27, 37, 82]. Unlike the previous works on the power allocation for multihop systems in [40]- [44], in our work, the power allocation and receiver coefficients are jointly optimized. For the MMSE receiver, we present three strategies where the allocation of power level across the relay nodes is subject to global, local and individual power constraints. Another fundamental contribution of this work is that a closed-form solution for the Lagrangian multiplier (λ) that arises in the expressions of the power allocation parameters can be achieved. For the MSR receiver, the local power constraints are considered. We propose a strategy that employs iterations with the Generalized Rayleigh Quotient [83] to solve the optimization problem in an alternating fashion.

The main contributions of this chapter can be summarized as:

1) Constrained MMSE expressions for the design of linear receivers and power allocation parameters for multihop WSNs. The constraints include the global, local and individual power constraints.

2) Constrained MSR expressions for the design of linear receivers and power allocation parameters for multihop WSNs subject to local power constraints.

3) Alternating optimization algorithms that compute the linear receivers and power allocation parameters in 1) and 2) to minimize the mean-square error or maximize the sum-rate of the WSN.

4) A study detailing the computational complexity and the convergence analysis of the proposed optimization algorithms.

The rest of this chapter is organized as follows. Section 5.2 describes the general multihop WSN system model. Section 5.3 develops three joint MMSE receiver design and power allocation strategies subject to three different power constraints. Section 5.4 develops the joint MSR receiver design and power allocation strategy subject to local power constraints. Section 5.5 contains the analysis of the computational complexity and the convergence. Section 5.6 presents and discusses the simulation results, while Section 5.7 provides some concluding remarks.

5.2 Multihop WSN System Model

Consider a general m-hop wireless sensor network (WSN) with multiple parallel relay nodes for each hop, as shown in Figure 5.1. The WSN consists of N_0 source nodes, N_m destination nodes and N_r relay nodes which are separated into $m-1$ groups: N_1,N_2, ... ,N_{m-1}. We concentrate on a time division scheme with perfect synchronization, for which all signals are transmitted and received in separate time slots. The sources first broadcast the $N_0 \times 1$ signal vector $\mathbf{s}$ to the first group of relay nodes. We consider an amplify-and-forward (AF) cooperation protocol in this work. Each group of relay nodes receives the signal, amplifies and rebroadcasts them to the next group of relay nodes (or the destination nodes). In practice, we need to consider the constraints on the transmission policy. For example, each transmitting node would transmit during only one phase. In our WSN system, we assume that each group of relay nodes transmits the signal to the nearest group of relay nodes (or the destination nodes) directly. We can use a block diagram to illustrate the multihop WSN system as shown in Figure 5.2.

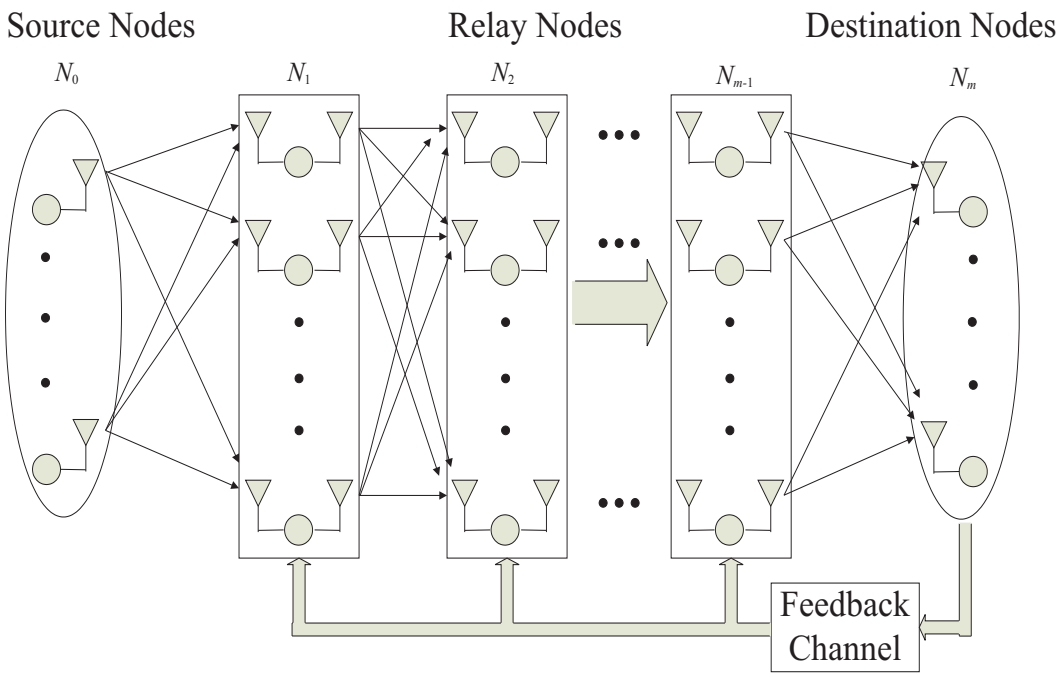

Figure 5.1: An m-hop WSN with N_0 source nodes, N_m destination nodes and N_r relay nodes.

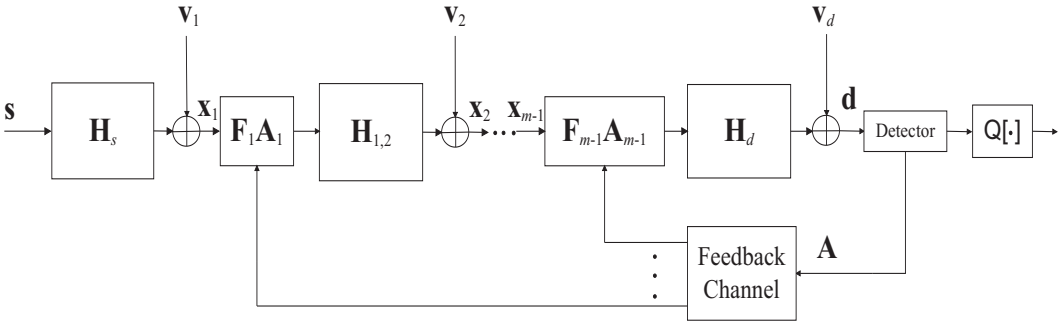

Figure 5.2: Block diagram of the multihop WSN system.

Let $\mathbf{H}_s$ denote the $N_1 \times N_0$ channel matrix between the source nodes and the first group of relay nodes, $\mathbf{H}_d$ denote the $N_m \times N_{m-1}$ channel matrix between the $(m-1)$th group of relay nodes and destination nodes, and $\mathbf{H}_{i-1,i}$ denote the $N_i \times N_{i-1}$ channel matrix

between two groups of relay nodes as described by

$$\mathbf{H}_s = \begin{bmatrix} \mathbf{h}_{s,1} \\ \mathbf{h}_{s,2} \\ \vdots \\ \mathbf{h}_{s,N_1} \end{bmatrix}, \quad \mathbf{H}_d = \begin{bmatrix} \mathbf{h}_{m-1,1} \\ \mathbf{h}_{m-1,2} \\ \vdots \\ \mathbf{h}_{m-1,N_m} \end{bmatrix}, \quad \mathbf{H}_{i-1,i} = \begin{bmatrix} \mathbf{h}_{i-1,1} \\ \mathbf{h}_{i-1,2} \\ \vdots \\ \mathbf{h}_{i-1,N_i} \end{bmatrix}, \tag{5.1}$$

where $\mathbf{h}_{s,j} = [h_{s,j,1}, h_{s,j,2}, ..., h_{s,j,N_0}]$ for $j = 1, 2, ..., N_1$ denote the channel coefficients between the source nodes and the jth relay of the first group of relay nodes, $\mathbf{h}_{m-1,j} = [h_{m-1,j,1}, h_{m-1,j,2}, ..., h_{m-1,j,N_{m-1}}]$ for $j = 1, 2, ..., N_m$ denote the channel coefficients between the $(m-1)$th group of relay nodes and the jth destination node and $\mathbf{h}_{i-1,j} = [h_{i-1,j,1}, h_{i-1,j,2}, ..., h_{i-1,j,N_{i-1}}]$ for $j = 1, 2, ..., N_i$ denote the channel coefficients between the $(i-1)$th group of relay nodes and the jth relay of the ith group of relay nodes. The received signal at the ith group of relay nodes ($\mathbf{x}_i$) for each phase can be expressed as:

Phase 1:

$$\mathbf{x}_1 = \mathbf{H}_s\mathbf{s} + \mathbf{v}_1, \tag{5.2}$$

$$\mathbf{y}_1 = \mathbf{F}_1\mathbf{x}_1, \tag{5.3}$$

Phase 2:

$$\mathbf{x}_2 = \mathbf{H}_{1,2}\mathbf{A}_1\mathbf{y}_1 + \mathbf{v}_2, \tag{5.4}$$

$$\mathbf{y}_2 = \mathbf{F}_2\mathbf{x}_2, \tag{5.5}$$

$\vdots$

Phase i: $(i = 3, 4, ..., m-1)$

$$\mathbf{x}_i = \mathbf{H}_{i-1,i}\mathbf{A}_{i-1}\mathbf{y}_{i-1} + \mathbf{v}_i, \tag{5.6}$$

$$\mathbf{y}_i = \mathbf{F}_i\mathbf{x}_i, \tag{5.7}$$

At the destination nodes, the received signal can be expressed as

$$\mathbf{d} = \mathbf{H}_d\mathbf{A}_{m-1}\mathbf{y}_{m-1} + \mathbf{v}_d, \tag{5.8}$$

where $\mathbf{v}$ is a zero-mean circularly symmetric complex additive white Gaussian noise (AWGN) vector with covariance matrix $\sigma^2\mathbf{I}$. The matrix $\mathbf{A}_i = \mathrm{diag}\{a_{i,1}, a_{i,2}, ..., a_{i,N_i}\}$ is a diagonal matrix whose elements represent the amplification coefficient of each relay of the ith group. The matrix $\mathbf{F}_i = \mathrm{diag}\{E(|x_{i,1}|^2), E(|x_{i,2}|^2), ..., E(|x_{i,N_i}|^2)\}^{-\frac{1}{2}}$ denotes the normalization matrix which can normalize the power of the received signal for each relay of the ith group of relays. Please note that the property of the matrix vector multiplication $\mathbf{Ay} = \mathbf{Ya}$ will be used in the next section, where $\mathbf{Y}$ is the diagonal matrix form of the vector $\mathbf{y}$ and $\mathbf{a}$ is the vector form of the diagonal matrix $\mathbf{A}$. In our proposed designs, the full CSI of the system is assumed to be known at all the destination nodes. In practice, a fusion centre [80] which contains the destination nodes is responsible for gathering the CSI, computing the optimal linear filters and the optimal amplification coefficients. The fusion centre also recovers the transmitted signal of the source nodes and transmits the optimal amplification coefficients to the relay nodes via a feedback channel.

5.3 Proposed Joint MMSE Design of the Receiver and Power Allocation

In this section, three constrained optimization problems are proposed to describe the joint design of the linear receiver ($\mathbf{W}$) and the power allocation parameter ($\mathbf{a}$) subject to a global, local and individual power constraints. They impose different power limitations on all the relay nodes, each group of relay nodes and each relay node, respectively. The assumptions of these power constraints could determine the degrees of freedom for allocating the power among the relay nodes which will affect the performance and the life time of the networks.

5.3.1 MMSE Design with a Global Power Constraint

We first consider the case where the total power of all the relay nodes is limited to P_T. The proposed method can be considered as the following optimization problem

$$\begin{aligned}[\mathbf{W}_{\text{opt}}, \mathbf{a}_{1,\text{opt}}, ..., \mathbf{a}_{m-1,\text{opt}}] &= \arg \min_{\mathbf{W}, \mathbf{a}_1, ..., \mathbf{a}_{m-1}} E[\|\mathbf{s} - \mathbf{W}^H \mathbf{d}\|^2], \\ &\text{subject to } \sum_{i=1}^{m-1} P_i = P_T\end{aligned} \tag{5.9}$$

where $(\cdot)^H$ denotes the complex-conjugate (Hermitian) transpose, P_i is the transmitted power of the ith group of relay nodes, and $P_i = N_{i+1}\mathbf{a}_i^H \mathbf{a}_i$.

To solve this constrained optimization problem, we modify the MSE cost function using the method of Lagrange multipliers [65] which yields the following Lagrangian function

$$\begin{aligned}\mathcal{L} =& E[\|\mathbf{s} - \mathbf{W}^H \mathbf{d}\|^2] + \lambda(\sum_{i=1}^{m-1} N_{i+1}\mathbf{a}_i^H \mathbf{a}_i - P_T) \\ =& E(\mathbf{s}^H \mathbf{s}) - E(\mathbf{d}^H \mathbf{W} \mathbf{s}) - E(\mathbf{s}^H \mathbf{W}^H \mathbf{d}) + E(\mathbf{d}^H \mathbf{W} \mathbf{W}^H \mathbf{d}) + \lambda(\sum_{i=1}^{m-1} N_{i+1}\mathbf{a}_i^H \mathbf{a}_i - P_T).\end{aligned} \tag{5.10}$$

By fixing $\mathbf{a}_1, ..., \mathbf{a}_{m-1}$ and setting the gradient of $\mathcal{L}$ in (5.10) with respect to the conjugate of the filter $\mathbf{W}$ equal to zero, we get

$$\begin{aligned}\mathbf{W}_{\text{opt}} =& [E(\mathbf{d}\mathbf{d}^H)]^{-1} E(\mathbf{d}\mathbf{s}^H) \\ =& \left[\mathbf{H}_d \mathbf{A}_{m-1} E(\mathbf{y}_{m-1}\mathbf{y}_{m-1}^H)\mathbf{A}_{m-1}^H \mathbf{H}_d^H + \sigma_n^2 \mathbf{I}\right]^{-1} \mathbf{H}_d \mathbf{A}_{m-1} E(\mathbf{y}_{m-1}\mathbf{s}^H).\end{aligned} \tag{5.11}$$

The optimal expression for $\mathbf{a}_{m-1}$ is obtained by equating the partial derivative of $\mathcal{L}$ with respect to $\mathbf{a}_{m-1}^*$ to zero

$$\begin{aligned}\frac{\partial \mathcal{L}}{\partial \mathbf{a}_{m-1}^*} =& - E(\frac{\partial \mathbf{d}^H}{\partial \mathbf{a}_{m-1}^*} \mathbf{W} \mathbf{s}) + E(\frac{\partial \mathbf{d}^H}{\partial \mathbf{a}_{m-1}^*} \mathbf{W} \mathbf{W}^H \mathbf{d}) + N_m \lambda \mathbf{a}_{m-1} \\ =& - E(\mathbf{Y}_{m-1}^H \mathbf{H}_d^H \mathbf{W} \mathbf{s}) + E[\mathbf{Y}_{m-1}^H \mathbf{H}_d^H \mathbf{W} \mathbf{W}^H (\mathbf{H}_d \mathbf{Y}_{m-1} \mathbf{a}_{m-1} + \mathbf{v}_d)] + N_m \lambda \mathbf{a}_{m-1} \\ =& \mathbf{0}.\end{aligned} \tag{5.12}$$

where $(\cdot)^*$ denotes the complex-conjugate. Therefore, we obtain

$$\begin{aligned}\mathbf{a}_{m-1,\text{opt}} =&[E(\mathbf{Y}_{m-1}^H\mathbf{H}_d^H\mathbf{W}\mathbf{W}^H\mathbf{H}_d\mathbf{Y}_{m-1}) + N_m\lambda\mathbf{I}]^{-1}E(\mathbf{Y}_{m-1}^H\mathbf{H}_d^H\mathbf{W}\mathbf{s})\\ =&[\mathbf{H}_d^H\mathbf{W}\mathbf{W}^H\mathbf{H}_d \odot E(\mathbf{y}_{m-1}\mathbf{y}_{m-1}^H)^* + N_m\lambda\mathbf{I}]^{-1}[\mathbf{H}_d^H\mathbf{W} \odot E(\mathbf{y}_{m-1}\mathbf{s}^H)^*\mathbf{u}]\end{aligned} \tag{5.13}$$

where $\odot$ denotes the Hadamard (element-wise) product and $\mathbf{u} = [1, 1, ..., 1]^T$.

Similarly, for $i = 2, 3, ...m-1$, we have

$$\begin{aligned}\frac{\partial\mathcal{L}}{\partial\mathbf{a}_{i-1}^*} &= -E(\frac{\partial\mathbf{d}^H}{\partial\mathbf{a}_{i-1}^*}\mathbf{W}\mathbf{s}) + (\frac{\partial\mathbf{d}^H}{\partial\mathbf{a}_{i-1}^*}\mathbf{W}\mathbf{W}^H\mathbf{d}) + N_i\lambda\mathbf{a}_{i-1}\\ &= \mathbf{0}\end{aligned} \tag{5.14}$$

where

$$\frac{\partial\mathbf{d}^H}{\partial\mathbf{a}_{i-1}^*} = \mathbf{Y}_{i-1}^H\left(\prod_{k=i}^{m-1}\mathbf{H}_{k-1,k}^H\mathbf{F}_k^H\mathbf{A}_k^H\right)\mathbf{H}_d^H. \tag{5.15}$$

Let

$$\mathbf{B}_{i-1} = \prod_{k=i}^{m-1}\mathbf{H}_{k-1,k}^H\mathbf{F}_k^H\mathbf{A}_k^H. \tag{5.16}$$

Then, we get

$$\begin{aligned}\mathbf{a}_{i-1,\text{opt}} =&[E(\mathbf{Y}_{i-1}^H\mathbf{B}_{i-1}\mathbf{H}_d^H\mathbf{W}\mathbf{W}^H\mathbf{H}_d\mathbf{B}_{i-1}^H\mathbf{Y}_{i-1}) + N_i\lambda\mathbf{I}]^{-1}E(\mathbf{Y}_{i-1}^H\mathbf{B}_{i-1}\mathbf{H}_d^H\mathbf{W}\mathbf{s})\\ =&[\mathbf{B}_{i-1}\mathbf{H}_d^H\mathbf{W}\mathbf{W}^H\mathbf{H}_d\mathbf{B}_{i-1}^H \odot E(\mathbf{y}_{i-1}\mathbf{y}_{i-1}^H)^* + N_i\lambda\mathbf{I}]^{-1}[\mathbf{B}_{i-1}\mathbf{H}_d^H\mathbf{W} \odot E(\mathbf{y}_{i-1}\mathbf{s}^H)^*\mathbf{u}].\end{aligned} \tag{5.17}$$

From (5.13) and (5.17), we conclude that

$$\begin{aligned}\mathbf{a}_{i,\text{opt}} =&[E(\mathbf{Y}_i^H\mathbf{B}_i\mathbf{H}_d^H\mathbf{W}\mathbf{W}^H\mathbf{H}_d\mathbf{B}_i^H\mathbf{Y}_i) + N_{i+1}\lambda\mathbf{I}]^{-1}E(\mathbf{Y}_i^H\mathbf{B}_i\mathbf{H}_d^H\mathbf{W}\mathbf{s})\\ =&[\mathbf{B}_i\mathbf{H}_d^H\mathbf{W}\mathbf{W}^H\mathbf{H}_d\mathbf{B}_i^H \odot E(\mathbf{y}_i\mathbf{y}_i^H)^* + N_{i+1}\lambda\mathbf{I}]^{-1}[\mathbf{B}_i\mathbf{H}_d^H\mathbf{W} \odot E(\mathbf{y}_i\mathbf{s}^H)^*\mathbf{u}]\end{aligned} \tag{5.18}$$

where

$$\mathbf{B}_i = \begin{cases}\prod_{k=i+1}^{m-1}\mathbf{H}_{k-1,k}^H\mathbf{F}_k^H\mathbf{A}_k^H, & \text{for } i = 1, 2, ..., m-2,\\ \mathbf{I}, & \text{for } i = m-1.\end{cases} \tag{5.19}$$

Please see the Appendix C to find the expressions of $\mathbf{F}_i$, $E(\mathbf{y}_i\mathbf{y}_i^H)$, and $E(\mathbf{y}_i\mathbf{s}^H)$. The expressions in (5.11) and (5.18) depend on each other. Thus, it is necessary to iterate them with an initial value of $\mathbf{a}_i$ ($i = 1, 2, ..., m-1$) to obtain the solutions.

The Lagrange multiplier λ can be determined by solving

$$\sum_{i=1}^{m-1}N_{i+1}\mathbf{a}_{i,\text{opt}}^H\mathbf{a}_{i,\text{opt}} = P_T. \tag{5.20}$$

Let

$$\boldsymbol{\phi}_i = E(\mathbf{Y}_i^H \mathbf{B}_i \mathbf{H}_d^H \mathbf{W}\mathbf{W}^H \mathbf{H}_d \mathbf{B}_i^H \mathbf{Y}_i) \tag{5.21}$$

and

$$\mathbf{z}_i = E(\mathbf{Y}_i^H \mathbf{B}_i \mathbf{H}_d^H \mathbf{W}\mathbf{s}). \tag{5.22}$$

Then, we get

$$\mathbf{a}_i = (\boldsymbol{\phi}_i + N_{i+1}\lambda \mathbf{I})^{-1} \mathbf{z}_i. \tag{5.23}$$

When λ is a real value,

$$[(\boldsymbol{\phi}_i + N_{i+1}\lambda \mathbf{I})^{-1}]^H = [(\boldsymbol{\phi}_i + N_{i+1}\lambda \mathbf{I})^H]^{-1} = (\boldsymbol{\phi}_i + N_{i+1}\lambda \mathbf{I})^{-1}. \tag{5.24}$$

Equation (5.20) becomes

$$\sum_{i=1}^{m-1} N_{i+1} \mathbf{z}_i^H (\boldsymbol{\phi}_i + N_{i+1}\lambda \mathbf{I})^{-1} (\boldsymbol{\phi}_i + N_{i+1}\lambda \mathbf{I})^{-1} \mathbf{z}_i = P_T. \tag{5.25}$$

Using an EVD, we have

$$\boldsymbol{\phi}_i = \mathbf{Q}_i \boldsymbol{\Lambda}_i \mathbf{Q}_i^{-1} \tag{5.26}$$

where $\boldsymbol{\Lambda}_i = \text{diag}\{\alpha_{i,1}, \alpha_{i,2}, ..., \alpha_{i,M_i}, 0, ..., 0\}$ consists of eigenvalues of $\boldsymbol{\phi}_i$ and $M_i = \min\{N_0, N_i, N_m\}$. Then, we get

$$\boldsymbol{\phi}_i + N_{i+1}\lambda \mathbf{I} = \mathbf{Q}_i (\boldsymbol{\Lambda}_i + N_{i+1}\lambda \mathbf{I}) \mathbf{Q}_i^{-1}. \tag{5.27}$$

Therefore, (5.25) can be expressed as

$$\sum_{i=1}^{m-1} N_{i+1} \mathbf{z}_i^H \mathbf{Q}_i (\boldsymbol{\Lambda}_i + N_{i+1}\lambda \mathbf{I})^{-2} \mathbf{Q}_i^{-1} \mathbf{z}_i = P_T. \tag{5.28}$$

Using the properties of the trace operation, (5.28) can be written as

$$\sum_{i=1}^{m-1} N_{i+1} tr\left((\boldsymbol{\Lambda}_i + N_{i+1}\lambda \mathbf{I})^{-2} \mathbf{Q}_i^{-1} \mathbf{z}_i \mathbf{z}_i^H \mathbf{Q}_i\right) = P_T. \tag{5.29}$$

Defining $\mathbf{C}_i = \mathbf{Q}_i^{-1} \mathbf{z}_i \mathbf{z}_i^H \mathbf{Q}_i$, (5.29) becomes

$$\sum_{i=1}^{m-1} \sum_{j=1}^{N_i} N_{i+1} (\alpha_{i,j} + N_{i+1}\lambda)^{-2} \mathbf{C}_i(j,j) = P_T. \tag{5.30}$$

Since $\boldsymbol{\phi}_i$ is a matrix with at most rank M_i, only the first M_i columns of $\mathbf{Q}_i$ span the column space of $E(\mathbf{Y}_i^H \mathbf{B}_i \mathbf{H}_d^H \mathbf{W}\mathbf{s})^H$ which causes the last $(N_i - M_i)$ columns of $\mathbf{z}_i^H \mathbf{Q}_i$ to become zero vectors and the last $(N_i - M_i)$ diagonal elements of $\mathbf{C}_i$ are zero. Therefore, we obtain the $\{\sum_{i=1}^{m-1} 2M_i\}$th-order polynomial in λ

$$\sum_{i=1}^{m-1} \sum_{j=1}^{M_i} N_{i+1} (\alpha_{i,j} + N_{i+1}\lambda)^{-2} \mathbf{C}_i(j,j) = P_T. \tag{5.31}$$

5.3.2 MMSE Design with Local Power Constraints

Secondly, we consider the case where the total power of the relay nodes in each group is limited to some value $P_{T,i}$. The proposed method can be considered as the following optimization problem

$$\begin{aligned}[\mathbf{W}_{\text{opt}}, \mathbf{a}_{1,\text{opt}}, ..., \mathbf{a}_{m-1,\text{opt}}] = \arg \min_{\mathbf{W}, \mathbf{a}_1, ..., \mathbf{a}_{m-1}} E[\|\mathbf{s} - \mathbf{W}^H \mathbf{d}\|^2], \\ \text{subject to } P_i = P_{T,i},\ i = 1, 2, ..., m-1,\end{aligned} \tag{5.32}$$

where P_i as defined above is the transmitted power of the ith group of relays, and $P_i = N_{i+1}\mathbf{a}_i^H \mathbf{a}_i$. Using the method of Lagrange multipliers again, we obtain the following Lagrangian function

$$\mathcal{L} = E[\|\mathbf{s} - \mathbf{W}^H \mathbf{d}\|^2] + \sum_{i=1}^{m-1} \lambda_i (N_{i+1}\mathbf{a}_i^H \mathbf{a}_i - P_{T,i}). \tag{5.33}$$

Following the same steps described in Section 5.3.1, we get the same optimal expression for $\mathbf{W}$ as in (5.11). The optimal expression for the power allocation vector $\mathbf{a}_i$ is different from (5.18) and given by

$$\mathbf{a}_{i,\text{opt}} = [\mathbf{B}_i \mathbf{H}_d^H \mathbf{W}\mathbf{W}^H \mathbf{H}_d \mathbf{B}_i^H \odot E(\mathbf{y}_i \mathbf{y}_i^H)^* + N_{i+1}\lambda_i \mathbf{I}]^{-1} [\mathbf{B}_i \mathbf{H}_d^H \mathbf{W} \odot E(\mathbf{y}_i \mathbf{s}^H)^* \mathbf{u}], \tag{5.34}$$

where

$$\mathbf{B}_i = \begin{cases} \prod_{k=i+1}^{m-1} \mathbf{H}_{k-1,k}^H \mathbf{F}_k^H \mathbf{A}_k^H, & \text{for } i = 1, 2, ..., m-2, \\ \mathbf{I}, & \text{for } i = m-1. \end{cases} \tag{5.35}$$

The Lagrange multiplier λ_i can be determined by solving

$$N_{i+1}\mathbf{a}_{i,\text{opt}}^H \mathbf{a}_{i,\text{opt}} = P_{T,i}\ \ i = 1, 2, ..., m-1. \tag{5.36}$$

Following the same steps as in Section 5.3.1, we obtain $(m-1)$ $\{2M_i\}$th-order polynomials in λ_i

$$\sum_{j=1}^{M_i} N_{i+1}(\alpha_{i,j} + N_{i+1}\lambda_i)^{-2} \mathbf{C}_i(j,j) = P_{T,i},\ \ i = 1, 2, ..., m-1. \tag{5.37}$$

5.3.3 MMSE Design with Individual Power Constraints

Thirdly, we consider the case where the power of each relay node is limited to some value $P_{T,i,j}$. The proposed method can be considered as the following optimization problem

$$\begin{aligned}[\mathbf{W}_{\rm opt}, \mathbf{a}_{1,\rm opt}, ..., \mathbf{a}_{m-1,\rm opt}] &= \arg \min_{\mathbf{W},\mathbf{a}_1,...,\mathbf{a}_{m-1}} E[\|\mathbf{s} - \mathbf{W}^H\mathbf{d}\|^2], \\ \text{subject to } P_{i,j} &= P_{T,i,j},\ i = 1, 2, ..., m-1,\ j = 1, 2, ..., N_i,\end{aligned} \tag{5.38}$$

where $P_{i,j}$ is the transmitted power of the jth relay node in the ith group, and $P_{i,j} = N_{i+1}a_{i,j}^* a_{i,j}$. Using the method of Lagrange multipliers once again, we have the following Lagrangian function

$$\mathcal{L} = E[\|\mathbf{s} - \mathbf{W}^H\mathbf{d}\|^2] + \sum_{i=1}^{m-1}\sum_{j=1}^{N_i} \lambda_{i,j}(N_{i+1}a_{i,j}^* a_{i,j} - P_{T,i,j}). \tag{5.39}$$

Following the same steps as described in Section 5.3.1, we get the same optimal expression for the $\mathbf{W}$ as in (5.11), and the optimal expression for the $a_{i,j}$

$$a_{i,j,\rm opt} = [\boldsymbol{\phi}_i(j,j) + N_{i+1}\lambda_{i,j}]^{-1}[\mathbf{z}_i(j) - \sum_{l\in I, l\neq j} \boldsymbol{\phi}_i(j,l)a_{i,l}], \tag{5.40}$$

where $I = \{1, 2, ..., N_i\}$, $\boldsymbol{\phi}_i$ and $\mathbf{z}_i$ have the same expression as in (5.21) and (5.22). The Lagrange multiplier $\lambda_{i,j}$ can be determined by solving

$$N_{i+1}a_{i,j,\rm opt}^* a_{i,j,\rm opt} = P_{T,i,j}\ \ i = 1, 2, ..., m-1,\ \ j = 1, 2, ...N_i. \tag{5.41}$$

Table 5.1 shows a summary of our proposed MMSE designs with global, local and individual power constraints which will be used for the simulations. If the quasi-static fading channel (block fading) is considered in the simulations, we only need two iterations. Alternatively, low-complexity adaptive algorithms can be used to compute the linear receiver $\mathbf{W}_{\rm opt}$ and the power allocation parameter vector $\mathbf{a}_{i,\rm opt}$.

5.4 Proposed Joint Maximum Sum-Rate Design of the Receiver and the Power Allocation

In this section, we detail the proposed joint MSR design of the receiver and the power allocation. By the MSR designs, the best possible SNR and QoS can be obtained at

Table 5.1: Summary of the Proposed MMSE Design with Global, local and individual Power Constraints for Multihop WSNs

Global Power Constraint	Local Power Constraints	Individual Power Constraint
Initialize the algorithm by setting: $\mathbf{A} = \sqrt{\frac{P_T}{\sum_{i=1}^{m-1} N_i N_{i+1}}}\mathbf{I}$	Initialize the algorithm by setting: $\mathbf{A}_i = \sqrt{\frac{P_{T,i}}{N_i N_{i+1}}}\mathbf{I}$ for $i = 1, 2, ..., m-1$	Initialize the algorithm by setting: $a_{i,j} = \sqrt{\frac{P_{T,i,j}}{N_{i+1}}}$ for $i = 1, 2, ..., m-1, j = 1, 2, ..., N_i$
For each iteration:	For each iteration:	For each iteration:
1. Compute $\mathbf{W}_{\text{opt}}$ in (5.11).	1. Compute $\mathbf{W}_{\text{opt}}$ in (5.11).	1. Compute $\mathbf{W}_{\text{opt}}$ in (5.11).
2. For $i = 1, 2, ..., m-1$	2. For $i = 1, 2, ..., m-1$	2. For $i = 1, 2, ..., m-1$
a) Compute $\boldsymbol{\phi}_i$ and $\mathbf{z}_i$ in (5.21) and (5.22).	a) Compute $\boldsymbol{\phi}_i$ and $\mathbf{z}_i$ in (5.21) and (5.22).	a) Compute $\boldsymbol{\phi}_i$ and $\mathbf{z}_i$ in (5.21) and (5.22).
b) Calculate the EVD of $\boldsymbol{\phi}_i$ in (5.26).	b) Calculate the EVD of $\boldsymbol{\phi}_i$ in (5.26).	b) For $j = 1, 2, ..., N_i$
c) Solve λ in (5.31).	c) Solve λ_i in (5.37).	i) Solve $\lambda_{i,j}$ in (5.41).
d) Compute $\mathbf{a}_{i,\text{opt}}$ in (5.18).	d) Compute $\mathbf{a}_{i,\text{opt}}$ in (5.34).	ii) Compute $a_{i,j,\text{opt}}$ in (5.40).

the destinations. They will improve the spectrum efficiency which is desirable for the WSNs with the limitation in the sensor node computational capacity. Only the local constraints are considered here, because of the MSR receiver we make use of the Generalized Rayleigh Quotient which is only suitable to solve optimization problems with vectors. It limits the types of power constraints. By substituting (5.2)-(5.7) into (5.8), we get

$$\begin{aligned}\mathbf{d} =& \mathbf{C}_{0,m-1}\mathbf{s} + \mathbf{C}_{1,m-1}\mathbf{v}_1 + \mathbf{C}_{2,m-1}\mathbf{v}_2 + ... + \mathbf{C}_{m-1,m-1}\mathbf{v}_{m-1} + \mathbf{v}_d \\ =& \mathbf{C}_{0,m-1}\mathbf{s} + \sum_{i=1}^{m-1} \mathbf{C}_{i,m-1}\mathbf{v}_i + \mathbf{v}_d,\end{aligned} \tag{5.42}$$

where

$$\mathbf{C}_{i,j} = \begin{cases} \prod_{k=i}^{j} \mathbf{B}_k, & \text{if } i \leqslant j, \\ \mathbf{I}, & \text{if } i > j, \end{cases} \tag{5.43}$$

and

$$\mathbf{B}_0 = \mathbf{H}_s, \tag{5.44}$$

$$\mathbf{B}_i = \mathbf{H}_{i,i+1}\mathbf{A}_i\mathbf{F}_i \quad \text{for } i = 1,\ 2,\ ...,\ m-2, \tag{5.45}$$

$$\mathbf{B}_{m-1} = \mathbf{H}_d\mathbf{A}_{m-1}\mathbf{F}_{m-1}. \tag{5.46}$$

We focus on a system with one source node for simplicity. The generalization to multiple sources amounts to performing the optimization of the additional filters. Therefore, the expression of the sum-rate (SR) in terms of bps/Hz for our m-hop WSN is expressed as

$$\mathrm{SR} = \frac{1}{m}\log_2\left[1+\frac{\sigma_s^2}{\sigma_n^2}\frac{\mathbf{w}^H\mathbf{C}_{0,m-1}\mathbf{C}_{0,m-1}^H\mathbf{w}}{\mathbf{w}^H(\sum_{i=1}^{m}\mathbf{C}_{i,m-1}\mathbf{C}_{i,m-1}^H)\mathbf{w}}\right] \text{ (bps/Hz)}, \tag{5.47}$$

where $\mathbf{w}$ is the linear receiver, and $(\cdot)^H$ denotes the complex-conjugate (Hermitian) transpose. Let

$$\mathbf{\Phi} = \mathbf{C}_{0,m-1}\mathbf{C}_{0,m-1}^H \tag{5.48}$$

and

$$\mathbf{Z} = \sum_{i=1}^{m}\mathbf{C}_{i,m-1}\mathbf{C}_{i,m-1}^H. \tag{5.49}$$

The expression for the sum-rate can be written as

$$\mathrm{SR} = \frac{1}{m}\log_2\left(1+\frac{\sigma_s^2}{\sigma_n^2}\frac{\mathbf{w}^H\mathbf{\Phi}\mathbf{w}}{\mathbf{w}^H\mathbf{Z}\mathbf{w}}\right) = \frac{1}{m}\log_2(1+ax), \tag{5.50}$$

where

$$a = \frac{\sigma_s^2}{\sigma_n^2} \tag{5.51}$$

and

$$x = \frac{\mathbf{w}^H\mathbf{\Phi}\mathbf{w}}{\mathbf{w}^H\mathbf{Z}\mathbf{w}}. \tag{5.52}$$

Since $\frac{1}{m}\log_2(1+ax)$ is a monotonically increasing function of x ($a>0$), the problem of maximizing the sum-rate is equivalent to maximizing x. In this section, we consider the case where the total power of the relay nodes in each group is limited to some value $P_{T,i}$ (local constraints). The proposed method can be considered as the following optimization problem:

$$\begin{gathered}[\mathbf{w}_{\mathrm{opt}}, \mathbf{a}_{1,\mathrm{opt}}, ..., \mathbf{a}_{m-1,\mathrm{opt}}] = \arg\max_{\mathbf{w},\mathbf{a}_1,...,\mathbf{a}_{m-1}} \frac{\mathbf{w}^H\mathbf{\Phi}\mathbf{w}}{\mathbf{w}^H\mathbf{Z}\mathbf{w}}, \\ \text{subject to } P_i = P_{T,i},\ i=1,2,...,m-1\end{gathered} \tag{5.53}$$

where P_i as defined above is the transmitted power of the ith group of relays, and $P_i = N_{i+1}\mathbf{a}_i^H\mathbf{a}_i$. We note that the expression $\frac{\mathbf{w}^H\mathbf{\Phi}\mathbf{w}}{\mathbf{w}^H\mathbf{Z}\mathbf{w}}$ in (5.53) is the Generalized Rayleigh Quotient. Thus, the optimal solution of our maximization problem can be obtained: $\mathbf{w}_{\mathrm{opt}}$ is any eigenvector corresponding to the dominant eigenvalue of $\mathbf{Z}^{-1}\mathbf{\Phi}$.

In order to obtain the optimal power allocation vector $\mathbf{a}_{\text{opt}}$, we rewrite $\frac{\mathbf{w}^H\mathbf{\Phi}\mathbf{w}}{\mathbf{w}^H\mathbf{Z}\mathbf{w}}$ and the expression is given by

$$\frac{\mathbf{w}^H\mathbf{\Phi}\mathbf{w}}{\mathbf{w}^H\mathbf{Z}\mathbf{w}} = \frac{\mathbf{a}_i^H\mathbf{M}_i\mathbf{a}_i}{\mathbf{a}_i^H\mathbf{P}_i\mathbf{a}_i + \mathbf{w}_i^H\mathbf{T}_i\mathbf{w}_i}, \text{ for } i = 1,\ 2, ...,\ m-1, \tag{5.54}$$

where

$$\mathbf{M}_i = \text{diag}\{\mathbf{w}_i^H\mathbf{C}_{i+1,m-1}\mathbf{H}_{i,i+1}\mathbf{F}_i\}\mathbf{C}_{0,i-1}\mathbf{C}_{0,i-1}^H\text{diag}\{\mathbf{F}_i^H\mathbf{H}_{i,i+1}^H\mathbf{C}_{i+1,m-1}^H\mathbf{w}_i\}, \tag{5.55}$$

$$\mathbf{P}_i = \text{diag}\{\mathbf{w}_i^H\mathbf{C}_{i+1,m-1}\mathbf{H}_{i,i+1}\mathbf{F}_i\}(\sum_{k=1}^{i}\mathbf{C}_{k,i-1}\mathbf{C}_{k,i-1}^H)\text{diag}\{\mathbf{F}_i^H\mathbf{H}_{i,i+1}^H\mathbf{C}_{i+1,m-1}^H\mathbf{w}_i\}, \tag{5.56}$$

and

$$\mathbf{T}_i = \sum_{k=i+1}^{m}\mathbf{C}_{k,m-1}\mathbf{C}_{k,m-1}^H. \tag{5.57}$$

Since the multiplication of any constant value and an eigenvector is still an eigenvector of the matrix, we express the receive filter as

$$\mathbf{w}_i = \frac{\mathbf{w}_{\text{opt}}}{\sqrt{\mathbf{w}_{\text{opt}}^H\mathbf{T}_i\mathbf{w}_{\text{opt}}}}. \tag{5.58}$$

Hence, we obtain

$$\mathbf{w}_i^H\mathbf{T}_i\mathbf{w}_i = 1 = \frac{N_{i+1}\mathbf{a}_i^H\mathbf{a}_i}{P_{T,i}}. \tag{5.59}$$

By substituting (5.59) into (5.54), we obtain

$$\frac{\mathbf{w}^H\mathbf{\Phi}\mathbf{w}}{\mathbf{w}^H\mathbf{Z}\mathbf{w}} = \frac{\mathbf{a}_i^H\mathbf{M}_i\mathbf{a}_i}{\mathbf{a}_i^H\mathbf{N}_i\mathbf{a}_i} \quad \text{for } i = 1,\ 2, ...,\ m-1, \tag{5.60}$$

where

$$\mathbf{N}_i = \mathbf{P}_i + \frac{N_{i+1}}{P_{T,i}}\mathbf{I}. \tag{5.61}$$

Likewise, we note that the expression $\frac{\mathbf{a}^H\mathbf{M}_i\mathbf{a}}{\mathbf{a}_i^H\mathbf{N}_i\mathbf{a}_i}$ in (5.60) is the Generalized Rayleigh Quotient. Thus, the optimal solution of our maximization problem can be solved: $\mathbf{a}_{i,\text{opt}}$ is any eigenvector corresponding to the dominant eigenvalue of $\mathbf{N}_i^{-1}\mathbf{M}_i$ and satisfies $\mathbf{a}_{i,\text{opt}}^H\mathbf{a}_{i,\text{opt}} = \frac{P_{T,i}}{N_{i+1}}$. Here, the local power constraints can be satisfied by employing a normalization. When considering the global power constraint P_T, there is no unique solution of $\mathbf{a}_{i,\text{opt}}$ $(i = 1, 2, ..., m-1)$ that satisfy $\sum_{i=1}^{m-1} N_{i+1}\mathbf{a}_{i,\text{opt}}^H\mathbf{a}_{i,\text{opt}} = P_T$. Thus, for this reason, we do not consider the global power constraint. The solutions of $\mathbf{w}_{\text{opt}}$ and $\mathbf{a}_{i,\text{opt}}$ depend on each other. Therefore it is necessary to iterate them with an initial value of $\mathbf{a}_i$ $(i = 1, 2, ..., m-1)$ to obtain the optimum solutions.

In this section, two methods are employed to calculate the dominant eigenvectors. The first one is the QR algorithm [87] which calculates all the eigenvalues and eigenvectors of a matrix. We can choose the dominant eigenvector among them. The second one is the power method [87] which only calculates the dominant eigenvector of a matrix. Hence, the computational complexity can be reduced. Table 5.2 shows a summary of our proposed MSR design with local power constraint which will be used for the simulations. If the quasi-static fading channel (block fading) is considered in the simulations, we only need two iterations.

Table 5.2: Summary of the Proposed MSR Design with Local Power Constraints for Multihop WSNs

Initialize the algorithm by setting

$$\mathbf{A}_i = \sqrt{\frac{P_{T,i}}{N_i N_{i+1}}}\mathbf{I} \quad \text{for } i = 1, 2, ..., m-1$$

For each iteration:

1. Compute $\mathbf{\Phi}$ and $\mathbf{Z}$ in (5.48) and (5.49).
2. Using the QR algorithm or the power method to compute the dominant eigenvector of $\mathbf{Z}^{-1}\mathbf{\Phi}$, denoted as $\mathbf{w}_{\rm opt}$.
3. For $i = 1, 2, ..., m-1$
   a) Compute $\mathbf{M}_i$ and $\mathbf{N}_i$ in (5.55) and (5.61).
   b) Using the QR algorithm or the power method to compute the dominant eigenvector of $\mathbf{N}_i^{-1}\mathbf{M}_i$, denoted as $\mathbf{a}_i$.
   c) To ensure the local power constraint $\mathbf{a}_{i,\rm opt}^H \mathbf{a}_{i,\rm opt} = \frac{P_{T,i}}{N_{i+1}}$, compute $\mathbf{a}_{i,\rm opt} = \sqrt{\frac{P_{T,i}}{N_{i+1}\mathbf{a}_i^H\mathbf{a}_i}}\mathbf{a}_i$.

5.5 Analysis of the proposed algorithms

In this section, an analysis of the computational complexity and the convergence of the algorithms are developed. We first illustrate the computational complexity requirements of the proposed MMSE and MSR designs by tables and figures. Then, we make use of the convergence results for the alternating optimization algorithms in [85,86] and particularly present a set of sufficient conditions under which our proposed algorithms will converge

to the optimal solutions.

5.5.1 Computational Complexity Analysis

Table 5.3 and Table 5.4 list the computational complexity per iteration in terms of the number of multiplications, additions and divisions for our proposed joint linear receiver design (MMSE and MSR) and power allocation strategies. For the joint MMSE designs, we use the QR algorithm to perform the eigendecomposition of the matrix. Please note that in this work the QR decomposition by the Householder transformation [87, 88] is employed by the QR algorithms. The quantities n_Q and n_P denote the number of iterations of the QR algorithm and the power method, respectively. For the computational complexity of λ in Table 5.3, it does not include the processing of solving the equation in (5.31), (5.37) and (5.41), because of the method with a global power constraint, equation (5.31) is a higher order polynomial whose complexity is difficult to be summarized. As the multiplication dominates the computational complexity, in order to compare the computational complexity of our proposed joint MMSE and MSR designs, the number of multiplications versus the number of relay nodes in each group for each iteration are displayed in Figure 5.3 and Figure 5.4. For the purpose of illustration, we set $m = 3$, $N_0 = 1$, $N_3 = 2$ and $n_Q = n_P = 10$. For the MMSE design, it can be seen that our proposed receiver with a global constraint has the same complexity as the receiver with local constraints. In practice, when considering the processing of solving the equation in (5.31), (5.37), the method with a global constraint will require higher computational complexity than the local constraints and the difference will become larger along with the increase of the number of hops (m). When the individual power constraints are considered, the computational complexity is lower than other constraints because there is no need to compute the eigendecomposition for it. For the MSR design, employing the power method to calculate the dominant eigenvectors has a lower computational complexity than employing the QR algorithm.

Table 5.3: Computational Complexity per Iteration of the joint MMSE Designs for Multihop WSNs

	Constraint	Multiplications	Additions	Divisions
$\mathbf{W}$	All	$N_m(N_m-1)(4N_m+1)/6$ $+(N_0+N_{m-1})N_d^2+N_{m-1}^2N_m$ $+N_0N_{m-1}N_m+N_{m-1}N_m$ $+\sum_{i=2}^{m-1}\{2N_{i-1}^2N_i+N_{i-1}N_i^2$ $+N_0N_{i-1}N_i+4N_{i-1}N_i+2N_i\}$	$N_m(N_m-1)(4N_m+1)/6+N_m$ $+(N_0+N_{m-1})N_m^2+N_{m-1}^2N_m$ $+N_0N_{m-1}N_m-N_m^2+2N_0N_m$ $+N_{m-1}N_m+\sum_{i=2}^{m-1}\{2N_{i-1}N_i^2$ $+N_0(N_{i-1}-1)N_i-N_i^2+N_i\}$	$N_m(3N_m-1)/2$
λ	Global	$\sum_{i=1}^{m-1}\{n_Q(\frac{13}{6}N_i^3+\frac{3}{2}N_i^2$ $+\frac{1}{3}N_i-2)-N_i^3$ $+3N_0N_i^2+N_0N_iN_{i+1}+N_i^2\}$ $+\sum_{i=1}^{m-2}\{N_iN_{i+1}+N_{i+1}\}$	$\sum_{i=1}^{m-1}\{n_Q(\frac{13}{6}N_i^3-N_i^2$ $-\frac{1}{6}N_i+1)-N_i^3$ $+3N_0N_i^2+N_0N_iN_{i+1}$ $-N_i^2-N_0N_i-N_i\}$	$\sum_{i=1}^{m-1}\{n_Q(N_i-1)\}$
	Local	$\sum_{i=1}^{m-1}\{n_Q(\frac{13}{6}N_i^3+\frac{3}{2}N_i^2$ $+\frac{1}{3}N_i-2)-N_i^3$ $+3N_0N_i^2+N_0N_iN_{i+1}+N_i^2\}$ $+\sum_{i=1}^{m-2}\{N_iN_{i+1}+N_{i+1}\}$	$\sum_{i=1}^{m-1}\{n_Q(\frac{13}{6}N_i^3-N_i^2$ $-\frac{1}{6}N_i+1)-N_i^3$ $+3N_0N_i^2+N_0N_iN_{i+1}$ $-N_i^2-N_0N_i-N_i\}$	$\sum_{i=1}^{m-1}\{n_Q(N_i-1)\}$
	Individual	$\sum_{i=1}^{m-1}\{N_0N_i^2+N_0N_iN_{i+1}$ $+N_i^2+N_0N_i\}$ $+\sum_{i=1}^{m-2}\{N_iN_{i+1}+N_{i+1}\}$	$\sum_{i=1}^{m-1}\{N_0N_i^2+N_0N_iN_{i+1}$ $-N_i^2-N_i\}$	
$\mathbf{a}$	Global	$\sum_{i=1}^{m-1}\{N_i(N_i-1)(4N_i+1)/6$ $+N_i^2+1\}$	$\sum_{i=1}^{m-1}\{N_i(N_i-1)(4N_i+1)/6$ $+N_i^2\}$	$\sum_{i=1}^{m-1}\{N_i(3N_i-1)/2\}$
	Local	$\sum_{i=1}^{m-1}\{N_i(N_i-1)(4N_i+1)/6$ $+N_i^2+1\}$	$\sum_{i=1}^{m-1}\{N_i(N_i-1)(4N_i+1)/6$ $+N_i^2\}$	$\sum_{i=1}^{m-1}\{N_i(3N_i-1)/2\}$
	Individual	$2\sum_{i=1}^{m-1}N_i$	$\sum_{i=1}^{m-1}N_i$	$\sum_{i=1}^{m-1}N_i$

5.5.2 Sufficient Conditions for Convergence

Following the similar statements in section 4.5.2, the proposed joint MMSE designs can be stated as an alternating minimization strategy based on the MSE defined in (5.9) and expressed as

$$\mathbf{W}_n \in \arg\min_{\mathbf{W}\in\underline{\mathbf{W}}_n} \mathrm{MSE}(\mathbf{W}, \mathbf{a}_{i,n-1}) \tag{5.62}$$

$$\mathbf{a}_{i,n} \in \arg\min_{\mathbf{a}\in\underline{\mathbf{a}}_{i,n}} \mathrm{MSE}(\mathbf{W}_n, \mathbf{a}_i) \text{ for } i = 1, 2, ..., m-1 \tag{5.63}$$

Table 5.4: Computational Complexity per Iteration of the joint MSR Designs for Multihop WSNs

		Multiplications	Additions	Divisions
w	QR Algorithm	$n_Q(\frac{13}{6}N_m^3+\frac{3}{2}N_m^2+\frac{1}{3}N_m-2)+N_m^2$ $+N_m(N_m-1)(4N_m+1)/6+N_1N_m$ $+\sum_{i=1}^{m-1}\{N_iN_m^2+N_iN_{i+1}+N_i\}$ $+\sum_{i=2}^{m-1}\{2N_{i-1}^2N_i+N_{i-1}N_i^2$ $+N_{i-1}N_iN_m+4N_{i-1}N_i+2N_i\}$	$n_Q(\frac{13}{6}N_d^3-N_d^2-\frac{1}{6}N_d+1)$ $+N_m(N_m-1)(4N_m+1)/6$ $-N_m^2+N_1N_m+\sum_{i=1}^{m-1}N_iN_m^2$ $+\sum_{i=2}^{m-1}\{2N_{i-1}N_i^2$ $+N_{i-1}(N_i-1)N_m-N_i^2+N_i\}$	$n_Q(N_m-1)$ $+N_m(3N_m-1)/2$
	Power Method	$n_PN_m^2+N_m(N_m-1)(4N_m+1)/6$ $+N_m^3+N_m^2+N_1N_m$ $+\sum_{i=1}^{m-1}\{N_iN_m^2+N_iN_{i+1}+N_i\}$ $+\sum_{i=2}^{m-1}\{2N_{i-1}^2N_i+N_{i-1}N_i^2$ $+N_{i-1}N_iN_m+4N_{i-1}N_i+2N_i\}$	$n_PN_m(N_m-1)$ $+N_m(N_m-1)(4N_m+1)/6+N_m^3$ $-2N_m^2+N_1N_m+\sum_{i=1}^{m-1}N_iN_m^2$ $+\sum_{i=2}^{m-1}\{2N_{i-1}N_i^2$ $+N_{i-1}(N_i-1)N_m-N_i^2+N_i\}$	$N_m(3N_m-1)/2$
a	QR Algorithm	$\sum_{i=1}^{m-1}\{n_Q(\frac{13}{6}N_i^3+\frac{3}{2}N_i^2$ $+\frac{1}{3}N_i-2)$ $+N_i(N_i-1)(4N_i+1)/6$ $+\sum_{k=1}^{i}N_kN_i^2+3N_i^2+2N_iN_{i+1}$ $+N_{i+1}N_m+3N_i+2\}+2N_m^2$	$\sum_{i=1}^{m-1}\{n_Q(\frac{13}{6}N_i^3-N_i^2$ $-\frac{1}{6}N_i+1)+N_iN_{i+1}$ $+N_i(N_i-1)(4N_i+1)/6$ $+N_{i+1}N_m-N_{i+1}+N_i-1\}$ $+\sum_{i=2}^{m-1}\{\sum_{k=1}^{i-1}(N_k-1)N_i^2$ $+N_i^2(i-2)+N_i\}+2N_m^2-2N_m$	$\sum_{i=1}^{m-1}\{n_Q(N_i-1)$ $+N_i(3N_i-1)/2\}$ $+N_m+m-1$
	Power Method	$\sum_{i=1}^{m-1}\{n_PN_i^2$ $+N_i(N_i-1)(4N_i+1)/6$ $+\sum_{k=1}^{i}N_kN_i^2+N_i^3+3N_i^2$ $+2N_iN_{i+1}+N_{i+1}N_m$ $+3N_i+2\}+2N_m^2$	$\sum_{i=1}^{m-1}\{n_PN_r(N_r-1)$ $+N_i(N_i-1)(4N_i+1)/6+N_i^3$ $-N_i^2+N_iN_{i+1}+N_{i+1}N_m$ $-N_{i+1}+N_i-1\}$ $+\sum_{i=2}^{m-1}\{\sum_{k=1}^{i-1}(N_k-1)N_i^2$ $+N_i^2(i-2)+N_i\}+2N_m^2-2N_m$	$\sum_{i=1}^{m-1}\{N_i(3N_i-1)/2\}$ $+N_m+m-1$

where the sets $\underline{\mathbf{W}}, \underline{\mathbf{a}}_i \subset \mathcal{M}$, and the sequences of compact sets $\{\underline{\mathbf{W}}_n\}_{n\geq 0}$ and $\{\underline{\mathbf{a}}_{i,n}\}_{n\geq 0}$ converge to the sets $\underline{\mathbf{W}}$ and $\underline{\mathbf{a}}_i$, respectively.

Although we are not given the sets $\underline{\mathbf{W}}$ and $\underline{\mathbf{a}}_i$ directly, we have the sequence of compact sets $\{\underline{\mathbf{W}}_n\}_{n\geq 0}$ and $\{\underline{\mathbf{a}}_{i,n}\}_{n\geq 0}$. The aim of our proposed joint MMSE designs is to find a sequence of $\mathbf{W}_n$ and $\mathbf{a}_{i,n}(i=1,2,...,m-1)$ such that

$$\lim_{n\to\infty} \mathrm{MSE}(\mathbf{W}_n, \mathbf{a}_{1,n}, \mathbf{a}_{2,n}, ..., \mathbf{a}_{m-1,n}) = \mathrm{MSE}(\mathbf{W}_{opt}, \mathbf{a}_{1,opt}, \mathbf{a}_{2,opt}, ..., \mathbf{a}_{m-1,opt}) \quad (5.64)$$

where $\mathbf{W}_{opt}$ and $\mathbf{a}_{i,opt}$ correspond to the optimal values of $\mathbf{W}_n$ and $\mathbf{a}_{i,n}$, respectively. The

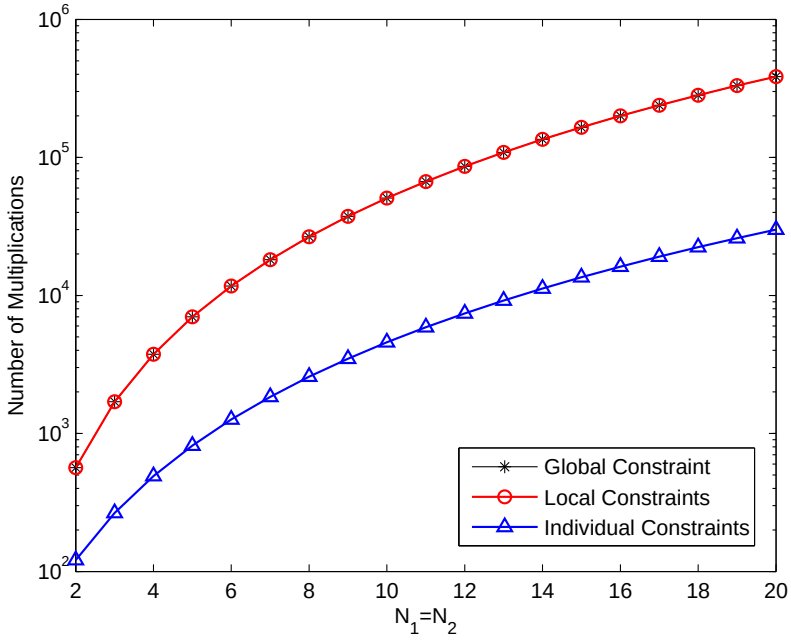

Figure 5.3: Number of multiplications versus the number of relay nodes of our proposed joint MMSE design of the receiver and the power allocation strategies for multihop WSNs.

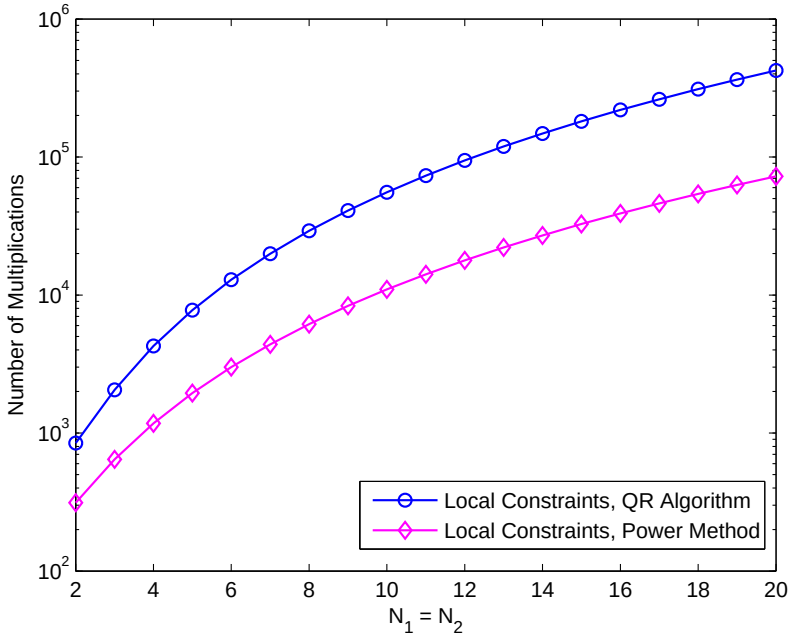

Figure 5.4: Number of multiplications versus the number of relay nodes of our proposed joint MSR design of the receiver and the power allocation strategies for multihop WSNs.

equation (5.64) can be considered as the necessary condition of the following equations

$$\lim_{n\to\infty} \mathrm{MSE}(\mathbf{W}_n, \mathbf{a}_{i,n}) = \mathrm{MSE}(\mathbf{W}_{opt}, \mathbf{a}_{i,opt}) \text{ for } i = 1, 2, ..., m-1 \tag{5.65}$$

if the other power allocation parameters $\mathbf{a}_{j,n}(j \neq i)$ are kept constant when computing $\mathbf{a}_{i,n}$ during the iterations. To present a set of sufficient conditions under which the proposed algorithms converge, we need the so-called three-point and four-point properties [85, 86]. Let us assume that there is a function $f : \mathcal{M} \times \mathcal{M} \to \mathbb{R}$ such that the following conditions are satisfied.

1) *Three-point property* $(\mathbf{W}, \widetilde{\mathbf{W}}, \mathbf{a}_i)$:

For all $n \geq 1$, $\mathbf{W} \in \underline{\mathbf{W}}_n$, $\mathbf{a}_i \in \underline{\mathbf{a}}_{i,n-1}$, and $\widetilde{\mathbf{W}} \in \arg\min_{\mathbf{W}\in\underline{\mathbf{W}}_n} \mathrm{MSE}(\mathbf{W}, \mathbf{a}_i)$, we have

$$f(\mathbf{W}, \widetilde{\mathbf{W}}) + \mathrm{MSE}(\widetilde{\mathbf{W}}, \mathbf{a}_i) \leq \mathrm{MSE}(\mathbf{W}, \mathbf{a}_i) \tag{5.66}$$

2) *Four-point property* $(\mathbf{W}, \mathbf{a}_i, \widetilde{\mathbf{W}}, \tilde{\mathbf{a}}_i)$:

For all $n \geq 1$, $\mathbf{W}, \widetilde{\mathbf{W}} \in \underline{\mathbf{W}}_n$, $\mathbf{a}_i \in \underline{\mathbf{a}}_{i,n}$, and $\tilde{\mathbf{a}}_i \in \arg\min_{\mathbf{a}_i\in\underline{\mathbf{a}}_{i,n}} \mathrm{MSE}(\widetilde{\mathbf{W}}, \mathbf{a}_i)$, we have

$$\mathrm{MSE}(\mathbf{W}, \tilde{\mathbf{a}}_i) \leq \mathrm{MSE}(\mathbf{W}, \mathbf{a}_i) + f(\mathbf{W}, \widetilde{\mathbf{W}}) \tag{5.67}$$

These two properties are the mathematical expressions of the sufficient conditions for the convergence of the alternating minimization algorithms which are stated in [85] and [86]. It means that if there exists a function $f(\mathbf{W}, \widetilde{\mathbf{W}})$ with the parameter $\mathbf{W}$ during two iterations that satisfies the two inequalities about the MSE in (5.66) and (5.67), the convergence of our proposed MMSE designs that make use of the alternating minimization algorithm can be proved by the theorem below.

Theorem: Let $\{(\underline{\mathbf{W}}_n, \underline{\mathbf{a}}_{i,n})\}_{n\geq 0}$, $\underline{\mathbf{W}}, \underline{\mathbf{a}}_i$ be compact subsects of the compact metric space $(\mathcal{M}, d)$ such that

$$\underline{\mathbf{W}}_n \overset{d_H}{\to} \underline{\mathbf{W}} \quad \underline{\mathbf{a}}_{i,n} \overset{d_H}{\to} \underline{\mathbf{a}}_i \tag{5.68}$$

and let MSE : $\mathcal{M} \times \mathcal{M} \to \mathbb{R}$ be a continuous function. Let conditions 1) and 2) hold. Then, for the proposed algorithms, we have

$$\lim_{n\to\infty} \mathrm{MSE}(\mathbf{W}_n, \mathbf{a}_{i,n}) = \mathrm{MSE}(\mathbf{W}_{opt}, \mathbf{a}_{i,opt}) \text{ for } i = 1, 2, ..., m-1. \tag{5.69}$$

Thus, equation (5.64) can be satisfied. A general proof of this theorem is detailed in [85] and [86]. The proposed joint MSR designs can be stated as an alternating maximization strategy based on the SR defined in (5.47) that follow a similar procedure to the one above.

5.6 Simulations

In this section, we assess the performance of our proposed joint MMSE designs of the linear receiver and power allocation methods and compare them with the equal power allocation method which allocates the same power level equally for all links from the relay nodes. For the purpose of fairness, we assume that the total power for all relay nodes in the network is the same which can be indicated as $\sum_{i=1}^{m-1} P_{T,i} = \sum_{i=1}^{m-1} \sum_{j=1}^{N_i} P_{T,i,j} = P_T$. We consider a 3-hop ($m$=3) wireless sensor network as an example even though the algorithms can be used with any number of hops. The number of source nodes (N_0), two groups of relay nodes (N_1, N_2) and destination nodes (N_3) are 1, 4, 4 and 2, respectively. We consider an AF cooperation protocol. The quasi-static fading channel (block fading channel) is considered in our simulations whose elements are Rayleigh random variables (with zero mean and unit variance) and assumed to be invariant during the transmission of each packet. In our simulations, the channel is assumed to be known at the destination nodes. For channel estimation algorithms for WSNs and other low-complexity parameter estimation algorithms, one refers to [74] and [89]. During each phase, the sources transmit the QPSK modulated packets with 1500 symbols. The noise at the destination nodes is modeled as circularly symmetric complex Gaussian random variables with zero mean. A perfect (error free) feedback channel between destination nodes and relay nodes is assumed to transmit the amplification coefficients.

For the MMSE design, it can be seen from Figure 5.5 that our three proposed methods achieve a better performance than the equal power allocation method. Among them, the method with a global constraint has the best performance whereas the method with individual constraints has the worst performance. This result is what we expect because a global constraint provides the largest degrees of freedom for allocating the power among

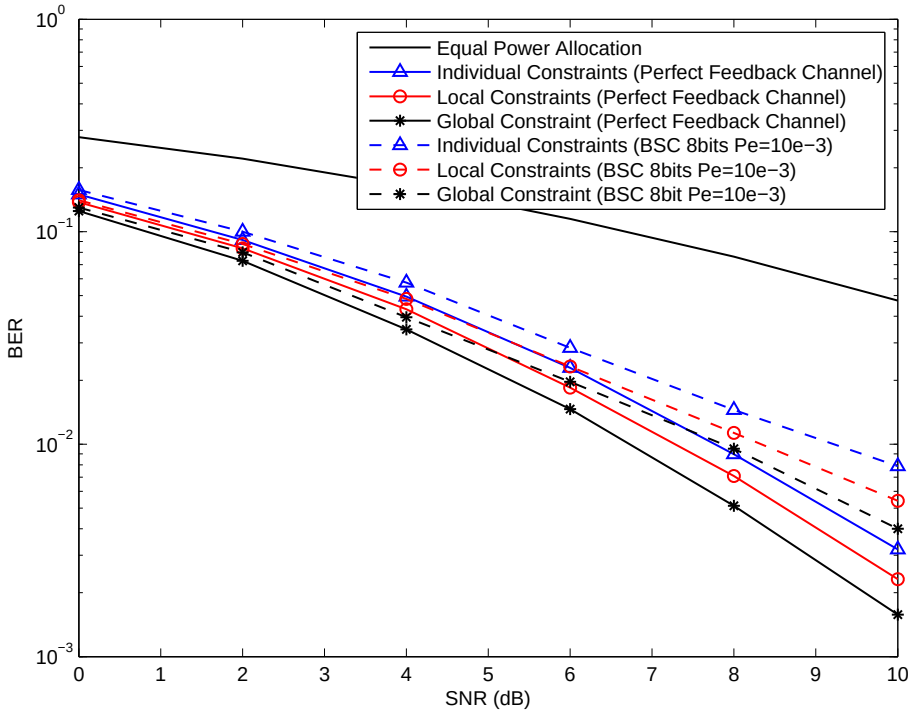

Figure 5.5: BER performance versus SNR of our proposed joint MMSE design of the receiver and power allocation strategies, compared to the equal power allocation method for multihop WSNs.

the relay nodes whereas an individual constraint provides the least. For the MSR design, it can be seen from Figure 5.6 that our proposed method achieves a better sum-rate performance than the equal power allocation method. Using the power method to calculate the dominant eigenvector yields a very similar result to the QR algorithm but requires a lower complexity. In practice, the feedback channel cannot be error free. In order to study the impact of feedback channel errors on the performance, we employ the binary symmetric channel (BSC) as the model for the feedback channel and quantize each complex amplification coefficient to an 8-bit binary value (4 bits for the real part, 4 bits for the imaginary part). The error probability (Pe) of the BSC is fixed at 10^{-3}. The dashed curves in Figure 5.5 and Figure 5.6 show the performance degradation compared to the performance when using a perfect feedback channel. To show the performance tendency of the BSC for other values of Pe, we fix the SNR at 10 dB and choose Pe ranging from 0 to 10^{-2}. The performance curves are shown in Figure 5.7 and Figure 5.8 , which illustrate

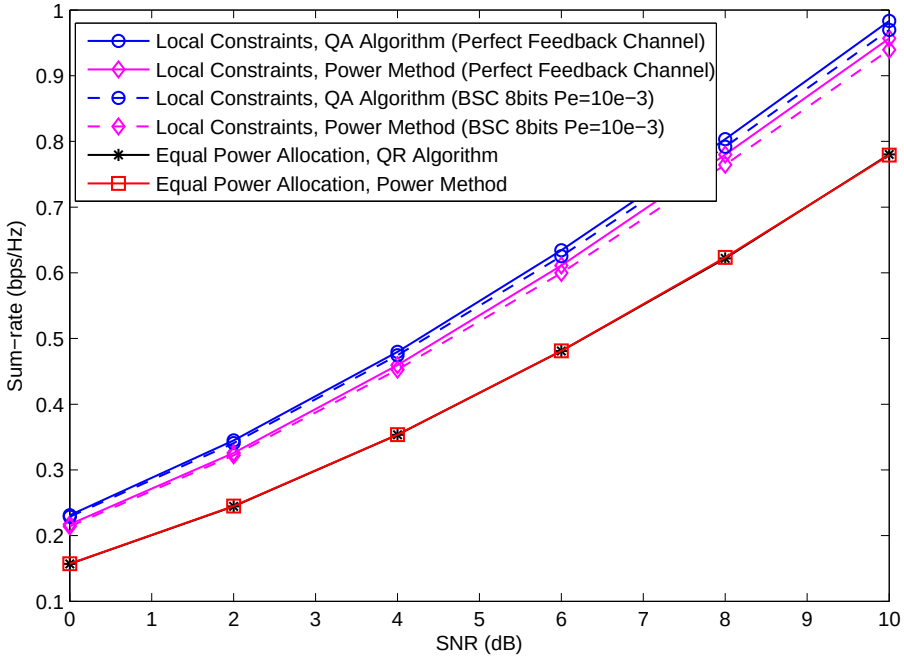

Figure 5.6: Sum-rate performance versus SNR of our proposed joint MSR design of the receiver and power allocation strategies with local constraints, compared to the equal power allocation method for multihop WSNs.

the BER and the sum-rate performance versus Pe of our two proposed joint designs of the receivers. It can be seen that along with the increase in Pe, their performance becomes worse.

Finally, we replace the perfect CSI with the estimated channel coefficients to compute the receive filters and power allocation parameters at the destinations. We employ the BEACON channel estimation which is proposed in [74]. Figure 5.9 illustrates the impact of the channel estimation on the performance of our proposed MMSE and MSR design with local constraints by comparing to the performance of perfect CSI. The quantity n_t denotes the number of training sequence symbol per data packet. Please note that in these simulations perfect feedback channel is considered and the QR algorithm is used in the MSR design. For both the MMSE and MSR designs, it can be seen that when n_t is set to 10, the BEACON channel estimation lead to an obvious performance degradation compared to the perfect CSI. However, when n_t is increased to 50, the BEACON channel estimation can achieve a similar performance to the perfect CSI. Other scenarios and

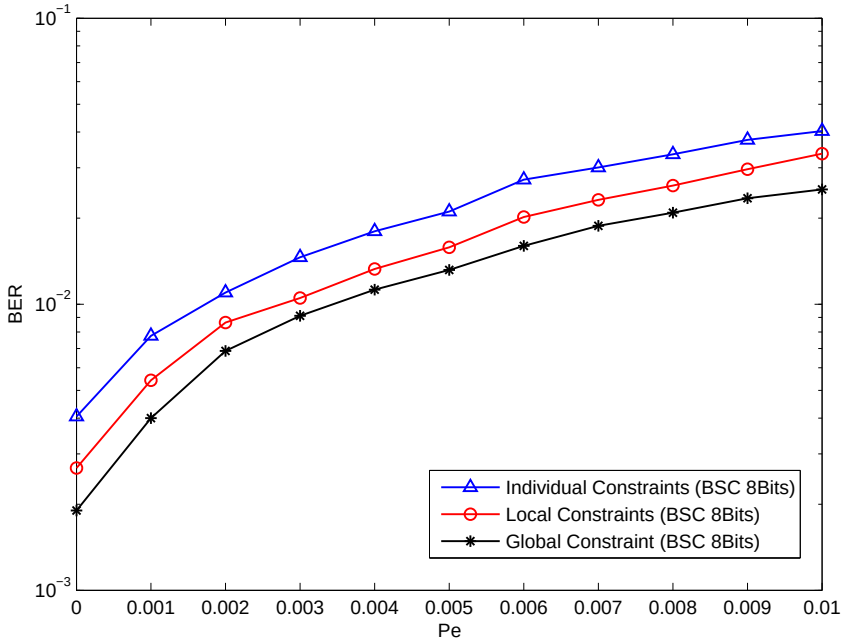

Figure 5.7: BER performance versus Pe of our proposed MMSE designs when employing the BSC as the model for the feedback channel for multihop WSNs.

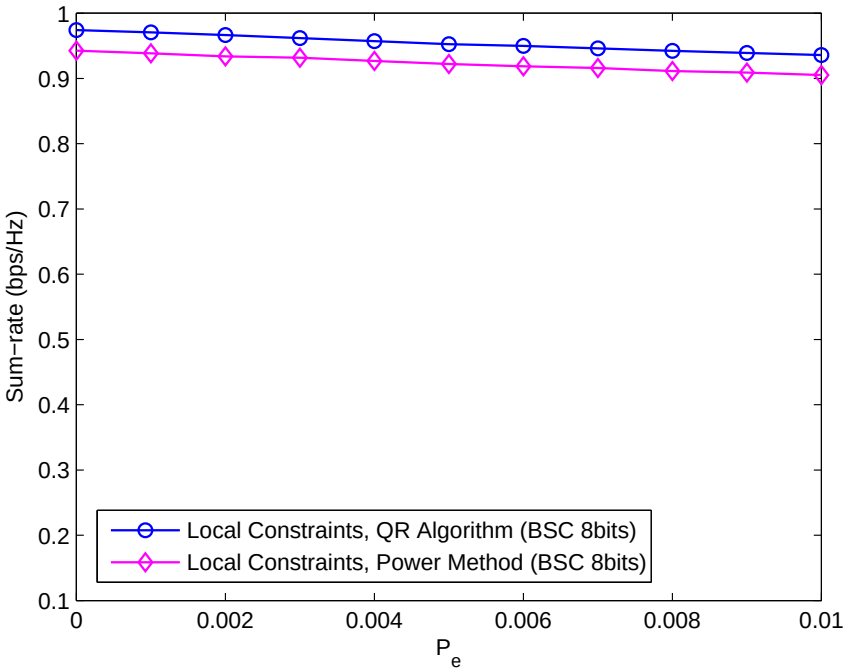

Figure 5.8: Sum-rate performance versus Pe of our proposed MSR design when employing the BSC as the model for the feedback channel for multihop WSNs.

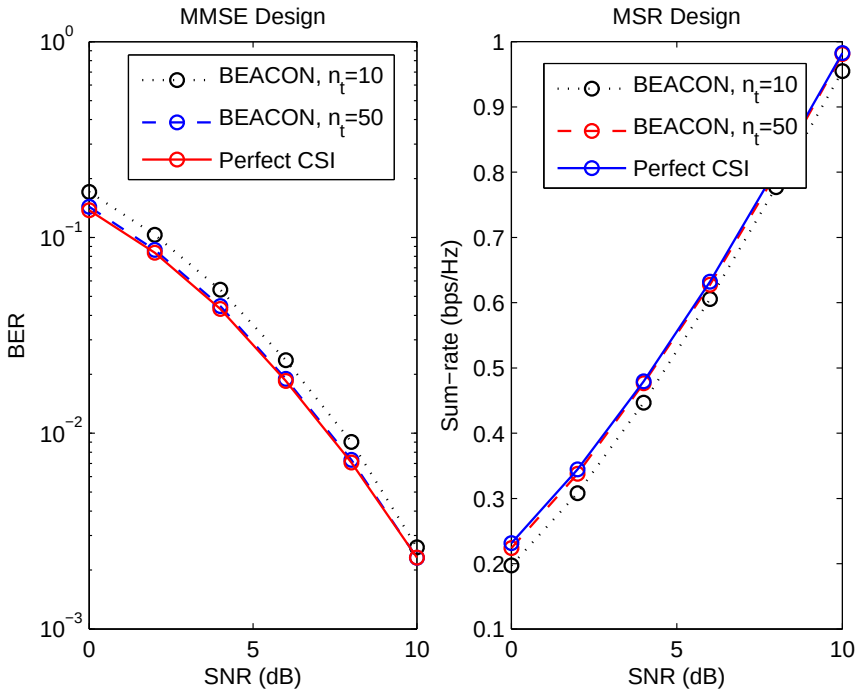

Figure 5.9: (a) BER performance versus SNR of our proposed MMSE design (b) Sum-rate performance versus SNR our proposed MSR design with local power constraints when employing the BEACON channel estimation, compared to the performance of perfect CSI for multihop WSNs

network topologies have been investigated and the results show that the proposed algorithms work very well with channel estimation algorithms and a small number of training symbols.

5.7 Summary

In this chapter, we present a study of the alternating optimization algorithms for receive filter design and power adjustment which can be applied to general multihop WSNs. MMSE and MSR criteria have been considered in the development of the algorithmic solutions. They can be considered as an extension of the strategies proposed for the two-hop WSNs in Chapter 4 and more complex mathematical derivations are presented. Three different power constraints are considered which include the global, local and individual

ones. Simulations have shown that our proposed algorithms achieve a significantly better performance than the equal power allocation method. The major advantage is that they are applicable to general multihop WSNs which can provide larger coverage than the two-hop WSNs.

Chapter 6

Conclusions and Further Work

Contents

6.1 Conclusions

In this thesis, our research focused on the development of low-complexity signal processing algorithms for the physical layer and cross layer designs for WSNs. For the physical layer design, low-complexity SM channel estimation algorithms have been investigated. For the cross layer design, strategies to jointly design linear receivers and the power allocation parameters via an alternating optimization approach have been proposed.

In Chapter 3, the SM-NLMS and BEACON channel estimation algorithms have been proposed based on time-varying bound for cooperative WSNs. It has been shown that our proposed algorithms can achieve better or similar performance to conventional NLMS and RLS channel estimation, offering reduced computational complexity. Analyses of the steady-state MSE and computational complexity are presented for the two channel estimation and closed-form expressions of the excess MSE and the probability of update

are provided. Furthermore, the incorporation of the time-varying bound function makes it robust to changes in the environment. These features are desirable for WSNs and bring about a significant reduction in energy consumption.

In Chapter 4, two kinds of joint receiver design and power allocation strategies have been proposed for two-hop WSNs. Firstly, the constrained MMSE expressions for the design of linear receivers and power allocation parameters are derived. The constraints include the global, individual and neighbour-based power constraints. Secondly, the constrained MSR expressions for the design of linear receivers and power allocation parameters are derived. The constraints include the global and neighbour-based power constraints. Finally, computational complexity and convergence analysis of the proposed optimization algorithms are presented. It has been shown that our proposed strategies achieve a significantly better performance than the equal power allocation method. Moreover, when the neighbour-based constraint is considered, it brings a feature to balance the performance against the computational complexity and the need for feedback information which is desirable for WSNs to extend their lifetime.

In Chapter 5, two kinds of joint receiver design and power allocation strategies have been proposed for general multihop WSNs. They can be considered as the extension work of the strategies proposed for the two-hop WSNs in Chapter 4 and more complex mathematical derivations are presented. Firstly, the constrained MMSE expressions for the design of linear receivers and power allocation parameters are derived. The constraints include the global, local and individual power constraints. Secondly, the constrained MSR expressions for the design of linear receivers and power allocation parameters subject to local power constraints. Finally, computational complexity and convergence analysis of the proposed optimization algorithms are also presented. It has been shown that our proposed strategies achieve a significantly better performance than the equal power allocation method. The major advantage is that they are applicable to general multihop WSNs which can provide larger coverage than the two-hop WSNs.

6.2 Further Work

Some suggestions for further work based on this thesis are given below:

- For Chapter 3, we can extend the family of set-membership channel estimation methods by applying the SMF framework to other algorithms such as the conjugate gradient (CG) algorithm and affine projection (AP) algorithm. It will increase the flexibility for us to address the trade off between the performance and computational complexity. These SM algorithms can be very attractive for the WSNs where by avoiding unnecessary computation the battery life is increased.

- For Chapter 4 and Chapter 5, we can employ low-complexity adaptive algorithms (i.e. the RLS, CG and SM algorithms) to compute the linear receiver and power allocation parameters. Compared with the MMSE design, these adaptive algorithms can bring a significant reduction in energy consumption which is desirable for WSNs. Other possible extensions to these work may include the design of non-linear receivers [90–97] and the reduced-rank processing for reduced complexity and data compression [98–115].

Also, two topics for WSNs that we are interested in investigating in our future research are follows:

- Relay selection: For WSNs, various protocols are proposed to choose the best relay to forward the information from all the available nodes. The best relay is usually selected depending on its geographic position [116], mean SNR to the destination node [117], or CSI at the source and relay nodes [118]. The relay selection can help to improve the symbol error probability [119, 120], increase the data transmission rate [121], and reduce the energy consumption [122] which is important for WSNs. One idea for our future work is to jointly design the relay selection and the power allocation to improve the performance for two-hop and general multihop WSNs.

- Energy harvesting [123]- [128]: It is refereed as the process that captures the energy from the environment (i.e. solar power, thermal energy, wind energy) and converts it to electricity. By employing the energy harvesting techniques, the lifetime of the sensor nodes can be extended significantly compared with the battery-powered sensor nodes. During the energy harvesting interval, some system parameters of the node can be tuned to increase the performance of the network with the support of more power. Therefore, how to exploit the energy harvesting opportunities to dynamically tune system parameters and decide which parameters should be tuned become the future challenges of energy harvesting techniques.

Appendix A

The Derivation of the Proposed BEACON Channel Estimation Algorithm

By setting the gradient of $\mathcal{L}$ in (3.24) with respect to $\mathbf{H}(n)$ equal to zero, we have

$$\begin{aligned}\frac{\partial \mathcal{L}}{\partial \mathbf{H}(n)} =& 2\sum_{l=1}^{n-1}\lambda(n)^{n-l}\left[\mathbf{r}(l)-\mathbf{H}(n)\mathbf{s}(l)\right]\left[-\mathbf{s}^H(l)\right] \\ &+ 2\lambda(n)[\|\mathbf{r}(n)-\mathbf{H}(n)\mathbf{s}(n)][-\mathbf{s}^H(n)] = 0.\end{aligned} \tag{A.1}$$

Therefore,

$$\mathbf{H}(n)\left[\sum_{l=1}^{n-1}\lambda(n)^{n-l}\mathbf{s}(l)\mathbf{s}^H(l)+\lambda(n)\mathbf{s}(n)\mathbf{s}^H(n)\right] = \sum_{l=1}^{n-1}\lambda(n)^{n-l}\mathbf{r}(l)\mathbf{s}^H(l)+\lambda(n)\mathbf{r}(n)\mathbf{s}^H(n). \tag{A.2}$$

Then we can get

$$\begin{aligned}\mathbf{H}(n) =& \left[\sum_{l=1}^{n-1}\lambda(n)^{n-l}\mathbf{r}(l)\mathbf{s}^H(l)+\lambda(n)\mathbf{r}(n)\mathbf{s}^H(n)\right] \\ &\cdot\left[\sum_{l=1}^{n-1}\lambda(n)^{n-l}\mathbf{s}(l)\mathbf{s}^H(l)+\lambda(n)\mathbf{s}(n)\mathbf{s}^H(n)\right]^{-1}.\end{aligned} \tag{A.3}$$

Let:

$$\boldsymbol{\phi}(n) = \sum_{l=1}^{n-1}\lambda(n)^{n-l}\mathbf{s}(l)\mathbf{s}^H(l)+\lambda(n)\mathbf{s}(n)\mathbf{s}^H(n), \tag{A.4}$$

and

$$\mathbf{Z}(n) = \sum_{l=1}^{n-1} \lambda(n)^{n-l} \mathbf{r}(l)\mathbf{s}^H(l) + \lambda(n)\mathbf{r}(n)\mathbf{s}^H(n). \tag{A.5}$$

Equation (A.3) becomes:

$$\mathbf{H}(n) = \mathbf{Z}(n)\boldsymbol{\phi}^{-1}(n). \tag{A.6}$$

Isolating the term corresponding to $l = n-1$ from the rest of the summation on the right-hand side of (A.4), we may write:

$$\boldsymbol{\phi}(n) = \left[\sum_{l=1}^{n-2} \lambda(n)^{n-l}\mathbf{s}(l)\mathbf{s}^H(l) + \lambda(n)\mathbf{s}(n-1)\mathbf{s}^H(n-1)\right] + \lambda(n)\mathbf{s}(n)\mathbf{s}^H(n). \tag{A.7}$$

The expression inside the brackets on the right-hand side of (A.7) equals $\boldsymbol{\phi}(n-1)$ assuming the forgetting factor of the cost function is close to 1. Hence, we have the following recursion for updating the value of $\boldsymbol{\phi}(n)$:

$$\boldsymbol{\phi}(n) = \boldsymbol{\phi}(n-1) + \lambda(n)\mathbf{s}(n)\mathbf{s}^H(n). \tag{A.8}$$

Similarly, we may use (A.5) to derive the following recursion for updating $\mathbf{Z}(n)$:

$$\mathbf{Z}(n) = \mathbf{Z}(n-1) + \lambda(n)\mathbf{r}(n)\mathbf{s}^H(n). \tag{A.9}$$

Then, using the matrix inversion lemma [65], we obtain the following recursive equation for the inverse of $\boldsymbol{\phi}(n)$:

$$\boldsymbol{\phi}^{-1}(n) = \boldsymbol{\phi}^{-1}(n-1) - \frac{\lambda(n)\boldsymbol{\phi}^{-1}(n-1)\mathbf{s}(n)\mathbf{s}^H(n)\lambda(n)\boldsymbol{\phi}^{-1}(n-1)}{1+\lambda(n)\mathbf{s}^H(n)\boldsymbol{\phi}^{-1}(n-1)\mathbf{s}(n)}. \tag{A.10}$$

For convenience of computation, let:

$$\mathbf{P}(n) = \boldsymbol{\phi}^{-1}(n), \tag{A.11}$$

and

$$\mathbf{k}(n) = \frac{\mathbf{s}^H(n)\mathbf{P}(n-1)}{1+\lambda(n)\mathbf{s}^H(n)\mathbf{P}(n-1)\mathbf{s}(n)}. \tag{A.12}$$

Therefore, we may rewrite (A.6) and (A.10) as:

$$\mathbf{H}(n) = \mathbf{Z}(n)\mathbf{P}(n), \tag{A.13}$$

$$\mathbf{P}(n) = \mathbf{P}(n-1) - \lambda(n)\mathbf{P}(n-1)\mathbf{s}(n)\mathbf{k}(n). \tag{A.14}$$

Then we substitute (A.9) and (A.14) into (A.13) to obtain a recursive equation for updating the channel matrix $\mathbf{H}(n)$:

$$\mathbf{H}(n) = \mathbf{H}(n-1) - \lambda(n)\mathbf{H}(n-1)\mathbf{s}(n)\mathbf{k}(n) + \lambda(n)\mathbf{r}(n)\mathbf{s}^H(n)\mathbf{P}(n). \tag{A.15}$$

By rearranging (A.12) , we can get:

$$\begin{aligned} \mathbf{k}(n) &= \mathbf{s}^H(n)\mathbf{P}(n-1) - \lambda(n)\mathbf{s}^H(n)\mathbf{P}(n-1)\mathbf{s}(n)\mathbf{k}(n) \\ &= \mathbf{s}^H(n)\left[\mathbf{P}(n-1) - \lambda(n)\mathbf{P}(n-1)\mathbf{s}(n)\mathbf{k}(n)\right] \\ &= \mathbf{s}^H(n)\mathbf{P}(n). \end{aligned} \tag{A.16}$$

Using (A.16) above, we get the desired recursive equation for updating the channel matrix $\mathbf{H}(n)$:

$$\begin{aligned} \mathbf{H}(n) &= \mathbf{H}(n-1) - \lambda(n)\mathbf{H}(n-1)\mathbf{s}(n)\mathbf{k}(n) + \lambda(n)\mathbf{r}(n)\mathbf{k}(n) \\ &= \mathbf{H}(n-1) + \lambda(n)\left[\mathbf{r}(n) - \mathbf{H}(n-1)\mathbf{s}(n)\right]\mathbf{k}(n) \\ &= \mathbf{H}(n-1) + \lambda(n)\boldsymbol{\epsilon}(n)\mathbf{k}(n), \end{aligned} \tag{A.17}$$

where $\boldsymbol{\epsilon}(n) = \mathbf{r}(n) - \mathbf{H}(n-1)\mathbf{s}(n)$ denotes the prediction error vector at time instant n.

Appendix B

Analysis of the Proposed SM-NLMS Channel Estimation Algorithm

From (3.41), the update equation of the channel estimation error is:

$$\Delta\mathbf{H}(n+1) = \Delta\mathbf{H}(n) - \frac{1}{N\sigma_s^2}\mathbf{e}(n)\mathbf{s}^H(n) + \frac{\gamma}{N\sigma_s^2}\frac{\mathbf{e}(n)}{\|\mathbf{e}_0(n)\|}\mathbf{s}^H(n). \tag{B.1}$$

Let:

$$\mathbf{A} = \Delta\mathbf{H}(n) - \frac{1}{N\sigma_s^2}\mathbf{e}(n)\mathbf{s}^H(n), \tag{B.2}$$

and

$$\mathbf{B} = \frac{\gamma}{N\sigma_s^2}\frac{\mathbf{e}(n)}{\|\mathbf{e}_0(n)\|}\mathbf{s}^H(n). \tag{B.3}$$

Equation (B.1) becomes:

$$\Delta\mathbf{H}(n+1) = \mathbf{A} + \mathbf{B}. \tag{B.4}$$

From (3.38), we can get the output excess MSE at time instant $n+1$:

$$\begin{aligned} J_{ex}(n+1) &= tr\{E[\mathbf{s}(n+1)\mathbf{s}^H(n+1)\Delta\mathbf{H}^H(n+1)\Delta\mathbf{H}(n+1)]\} \\ &= tr\{E[\mathbf{s}(n)\mathbf{s}^H(n)\Delta\mathbf{H}^H(n+1)\Delta\mathbf{H}(n+1)]\} \\ &= \psi_1 + \psi_2 + \psi_3 + \psi_4. \end{aligned} \tag{B.5}$$

Then we analyze each term separately:

$$\psi_1 = tr\{E[\mathbf{s}(n)\mathbf{s}^H(n)\mathbf{A}^H\mathbf{A}]\} = \rho_1 + \rho_2, \tag{B.6}$$

$$\rho_1 = J_{ex}(n) - 2N\sigma_s^2 \frac{1}{N\sigma_s^2} J_{ex}(n) + N^2\sigma_s^4 \frac{1}{N^2\sigma_s^4} J_{ex}(n) = 0, \tag{B.7}$$

$$\rho_2 = N^2\sigma_s^4 M\sigma_n^2 \frac{1}{N^2\sigma_s^4} = M\sigma_n^2, \tag{B.8}$$

$$\begin{aligned}
\psi_2 =& tr\{E[\mathbf{s}(n)\mathbf{s}^H(n)\mathbf{A}^H\mathbf{B}]\} \\
=& tr\{E[\mathbf{s}(n)\mathbf{s}^H(n)\Delta\mathbf{H}^H(n)\frac{\gamma}{N\sigma_s^2}\frac{\mathbf{e}(n)}{\|\mathbf{e}_0(n)\|}\mathbf{s}^H(n)]\} \\
& - tr\{E[\mathbf{s}(n)\mathbf{s}^H(n)\frac{\gamma}{N^2\sigma_s^4}\mathbf{s}(n)\frac{\mathbf{e}^H(n)\mathbf{e}(n)}{\|\mathbf{e}_0(n)\|}\mathbf{s}^H(n)]\} \\
=& \gamma tr\{E[\mathbf{s}^H(n)\Delta\mathbf{H}^H(n)\frac{\mathbf{e}(n)}{\|\mathbf{e}_0(n)\|}]\} - \gamma E\left[\frac{\|\mathbf{e}(n)\|^2}{\|\mathbf{e}_0(n)\|}\right] \\
=& \gamma tr\{E[\mathbf{s}^H(n)\Delta\mathbf{H}^H(n)\frac{\mathbf{n}(n)+\Delta\mathbf{H}(n)\mathbf{s}(n)}{\|\mathbf{e}_0(n)\|}]\} - \gamma E\left[\frac{\|\mathbf{e}(n)\|^2}{\|\mathbf{e}_0(n)\|}\right] \\
=& \gamma tr\{E[\mathbf{s}^H(n)\Delta\mathbf{H}^H(n)\frac{\Delta\mathbf{H}(n)\mathbf{s}(n)}{\|\mathbf{e}_0(n)\|}]\} - \gamma E\left[\frac{\|\mathbf{e}(n)\|^2}{\|\mathbf{e}_0(n)\|}\right] \\
=& \gamma E\left[\frac{1}{\|\mathbf{e}_0(n)\|}\right] J_{ex}(n) - \gamma E\left[\frac{\|\mathbf{e}(n)\|^2}{\|\mathbf{e}_0(n)\|}\right],
\end{aligned} \tag{B.9}$$

$$\psi_3 = tr\{E[\mathbf{s}(n)\mathbf{s}^H(n)\mathbf{B}^H\mathbf{A}]\} = \psi_2, \tag{B.10}$$

$$\begin{aligned}
\psi_4 =& tr\{E[\mathbf{s}(n)\mathbf{s}^H(n)\mathbf{B}^H\mathbf{B}]\} \\
=& tr\{E[\mathbf{s}(n)\mathbf{s}^H(n)\frac{\gamma^2}{N^2\sigma_s^4}\mathbf{s}(n)\frac{\mathbf{e}^H(n)\mathbf{e}(n)}{\|\mathbf{e}_0(n)\|^2}\mathbf{s}^H(n)]\} \\
=& \gamma^2 E\left[\frac{\|\mathbf{e}(n)\|^2}{\|\mathbf{e}_0(n)\|^2}\right].
\end{aligned} \tag{B.11}$$

Finally, we can obtain the update equation of the output excess MSE:

$$J_{ex}(n+1) = M\sigma_n^2 + 2\gamma E\left[\frac{1}{\|\mathbf{e}_0(n)\|}\right] J_{ex}(n) - 2\gamma E\left[\frac{\|\mathbf{e}(n)\|^2}{\|\mathbf{e}_0(n)\|}\right] + \gamma^2 E\left[\frac{\|\mathbf{e}(n)\|^2}{\|\mathbf{e}_0(n)\|^2}\right]. \tag{B.12}$$

Appendix C

The Expressions of $\mathbf{F}_i$, $E(\mathbf{y}_i\mathbf{y}_i^H)$, and $E(\mathbf{y}_i\mathbf{s}^H)$

Here, we derive the the expressions of $\mathbf{F}_i$, $E(\mathbf{y}_i\mathbf{y}_i^H)$, and $E(\mathbf{y}_i\mathbf{s}^H)$ that are used in Sections 5.2, 5.3 and 5.4.

$$\mathbf{F}_i = \text{diag}\{E(|x_{i,1}|^2), E(|x_{i,2}|^2), ..., E(|x_{i,N_i}|^2)\}^{-\frac{1}{2}} \tag{C.1}$$

where

$$E(|x_{i,j}|^2 = \begin{cases} \sigma_s^2|\mathbf{h}_{s,j}|^2 + \sigma_n^2, & \text{for } i = 1, \\ \mathbf{h}_{i-1,j}\mathbf{A}_{i-1}E(\mathbf{y}_{i-1}\mathbf{y}_{i-1}^H)\mathbf{A}_{i-1}^H\mathbf{h}_{i-1,j}^H + \sigma_n^2, & \text{for } i = 2, 3, ..., m. \end{cases} \tag{C.2}$$

$$E(\mathbf{y}_i\mathbf{y}_i^H) = \begin{cases} \mathbf{F}_i(\sigma_s^2\mathbf{H}_s\mathbf{H}_s^H + \sigma_n^2\mathbf{I})\mathbf{F}_i^H, & \text{for } i = 1, \\ \mathbf{F}_i[\mathbf{H}_{i-1,i}\mathbf{A}_{i-1}E(\mathbf{y}_{i-1}\mathbf{y}_{i-1}^H)\mathbf{A}_{i-1}^H\mathbf{H}_{i-1,i}^H + \sigma_n^2\mathbf{I}]\mathbf{F}_i^H, & \text{for } i = 2, 3, ..., m. \end{cases} \tag{C.3}$$

$$E(\mathbf{y}_i\mathbf{s}^H) = \begin{cases} \sigma_s^2\mathbf{F}_i\mathbf{H}_s, & \text{for } i = 1, \\ \mathbf{F}_i\mathbf{H}_{i-1,i}\mathbf{A}_{i-1}E(\mathbf{y}_{i-1}\mathbf{s}^H), & \text{for } i = 2, 3, ..., m. \end{cases} \tag{C.4}$$

Glossary

AF	Amplify-and-Forward
AP	Affine Projection
AWGN	Additional White Gaussian Noise
BER	Bit Error Rate
bps	Bit per Second
BSC	Binary Symmetric Channel
C-CE	Cascaded Channel Estimation
CF	Compress-and-Forward
CSI	Channel State Information
dB	Decibel
D-CE	Disintegrated Channel Estimation
DF	Decode-and-Forward
ECD	Effective Configuration Duration
EVD	Eigenvalue Decomposition
Hz	Hertz
LMS	Least Mean Square
LS	Least Squares
MMSE	Minimum Mean Square Error
MSE	Mean Square Error
MSR	Maximum Sum-Rate
NBC	Biological and Chemical
NLMS	Normalized Least Mean Square
QoS	Quality of Service
OBE	Optimal Bounding Ellipsoidal
QPSK	Quadrature Phase Shift Keying
RLS	Recursive Least Squares
SM	Set-Membership
SM-AP	Set-Membership Affine Projection
SM-BNDRLMS	Set-Membership Date-Reusing Least Mean Square
SMF	Set-Membership Filtering

SM-NLMS	Set-Membership Normalized Least Mean Square
SNR	Signal to Noise Ratio
SORA	Self-Organizing Resource Allocation
SR	Sum-Rate
STC	Space Time Coding
UR	Update Rate
WSNs	Wireless Sensor Networks
WZC	Wyner-Ziv Coding

Bibliography

[1] I. F. Akyildiz, W. Su, Y. Sankarasubramaniam, and E. Cayirci, "A Survey on Sensor Networks," *IEEE Communications Magazine*, vol. 40, pp. 102-114, August 2002.

[2] J. N. Laneman and G. W. Wornell, "Cooperative diversity in wireless networks: Efficient protocols and outage behavior," *IEEE Transactions on Information Theory*, vol. 50, no. 12, pp. 3062-3080, December 2004.

[3] H. Li and P. D. Mitchell, "Reservation packet medium access control for wireless sensor networks," *IEEE Personal, Indoor and Mobile Radio Communications Conference (PIMRC)*, September 2008.

[4] Y. W. Hong, W. J. Huang, F. H. chiu, and C. C. J. Kuo, "Cooperative Communications in Resource-Constrained Wireless Networks," *IEEE Signal Processing Magazine*, vol. 24, pp. 47-57, May 2007.

[5] A. Manikas, Y. I. Kamil, and P. Karaminas, "Positioning in Wireless Sensor Networks using Array Processing," *Proceedings of IEEE GLOBECOM*, 2008.

[6] G. Elissaios and A. Manikas, "Array formation in Arrayed Wireless Sensor Networks," *HERMIS-mu-pi International Journal of Computer Mathematics and its Applications*, vol.6, pp.122-134, March 2006.

[7] N. Khajehnouri and A.H. Sayed, "Distributed MMSE Relay Strategies for Wireless Sensor Networks," *IEEE Transactions on Signal Processing*, vol. 55, no. 7, pp. 3336-3348, July 2007.

[8] R. Krishna, Z. Xiong, and S. Lambotharan, "A Cooperative MMSE Relay Strategy for Wireless Sensor Networks," *IEEE Signal Processing Letters*, vol. 15, pp. 549-552, 2008.

[9] S. Gollamudi, S. Nagaraj, S. Kapoor, and Y. F. Huang, "Set-Membership Filtering and a Set-Membership Normalized LMS Algorithm with an Adaptive Step Size," *IEEE Signal Processing Letters*, vol. 5, no. 5, pp. 111-114, May 1998.

[10] S. Nagaraj, S. Gollamudi, S. Kapoor, and Y. F. Huang, "BEACON: An Adaptive Set-Membership Filtering Technique with Sparse Updates," *IEEE Transactions on Signal Processing*, vol. 47, no. 11, pp. 2928-2941, November 1999.

[11] S. Dasgupta and Y. F. Huang, "Asymptotically Convergent Modified Recursive Least-Squares with Data Dependent Updating and Forgetting Factor," *IEEE Conference on Decision and Control*, December 1985.

[12] P. S. R. Diniz, "Analysis of a set-membership affine projection algorithm in nonstationary environment," *European Signal Processing Conference*, 2009.

[13] M. V. S. Lima and P. S. R. Diniz, "Steady-state Analysis of the set-membership of a set-membership affine projection algorithm," *IEEE International Conference on Acoustics, and Speech Signal Processing (ICASSP)*, March 2010.

[14] P. S. R. Diniz and S. Werner, "Set-Membership Binormalized Data-Reusing LMS Algorithms," *IEEE Transactions on Signal Processing*, vol. 51, no.1, pp. 124-134, January 2003.

[15] W. Ye, J. Heidemann, and D. Estrin, "An Energy-Efficient MAC Protocol for Wireless Sensor Networks," *in Proceedings of the IEEE Infocom*, pp. 1567-1576, June, 2002.

[16] A. Bachir, M. Dohler, T. Watteyne and K. K. Leung, "MAC Essentials for Wireless Sensor Networks," *IEEE Communications Surveys & Tutorials*, vol. 12, no. 2, pp. 222-248, 2010.

[17] A. Sendonaris, E. Erkip, and B. Aazhang, "User cooperation diversity. Part I. System Description," *IEEE Transactions on Communications*, vol. 51, no. 11, pp. 1927-1938, November 2003.

[18] A. Sendonaris, E. Erkip, and B. Aazhang, "User cooperation diversity. Part II. Implementation aspects and performance analysis," *IEEE Transactions on Communications*, vol. 51, no. 11, pp. 1939-1948, November 2003.

[19] S. Yang and J.C. Belfiore, "Towards the Optimal Amplify-and-Forward Cooperative Diversity Scheme," *IEEE Transactions on Information Theory*, vol. 53, no. 9, pp. 3114-3126, September 2007.

[20] P. Clarke, R. C. de Lamare, "Transmit Diversity and Relay Selection Algorithms for Multirelay Cooperative MIMO Systems", *IEEE Transactions on Vehicular Technology*, vol. 61 , no. 3, pp. 1084-1098, 2012.

[21] K. J. R. Liu, A. K. Sadek, W. Su, and A. Kwasinski, *Cooperative Communications and Networking*, Cambridge University Press, 2009.

[22] A. Host-Madsen, "Capacity bounds for cooperative diversity," *IEEE Transactions on Information Theory*, vol. 52, pp. 1522-1544, April 2006.

[23] A. Host-Madsen and J. Zhang, "Capacity bounds and power allocation for wireless relay channels," *IEEE Transactions on Information Theory*, vol. 51, no. 6, pp. 2020-2040, June 2005.

[24] J. Jiang, J. Thompson, P. Grant, and N. Goertz, "Practical compress-and-forward cooperation for the classical relay network," *European Signal Processing Conference*, Glasgow, Scotland, pp. 2421-2425, August 2009.

[25] A. Wyner and J. Ziv, "The rate-distortion function for source coding with side information at the decoder," *IEEE Transactions on Information Theory*, vol. 22, no. 1, pp. 1-10, January 1976.

[26] G. Mainland, D. C. Parkes, and M. Welsh, "Decentralized, Adaptive Resource Allocation for Sensor Networks," *Proceedings of the 2nd conference on Symposium on Networked Systems Design & Implementation*, 2005.

[27] T. Q. S. Quek, H. Shin, and M. Z. Win, "Robust Wireless Relay Networks: Slow Power Allocation With Guaranteed QoS," *IEEE Journal of Selected Topics in Signal Processing*, vol. 1, no. 4, pp. 700-713, December 2007.

[28] K. Vardhe, D. Reynolds, and B. D. Woerner "Joint Power Allocation and Relay Selection for Multiuser Cooperative Communication" *IEEE Transactions on Wireless Communications*, vol. 9, no. 4, pp. 1255-1260, April 2010.

[29] J. Luo, R. S. Blum, L. J. Cimini, L. J. Greenstein, and A. M. Haimovich "Decode-Forward Cooperative Diversity with Power Allocation in Wireless Networks" *IEEE Transactions on Wireless Communications*, vol. 6, no. 3, pp. 793-799, March 2007.

[30] W. Su, A. K. Sadek, and K. J. R. Liu, "Ser performance analysis and optimum power allocation for decode and forward cooperation protocol in wireless networks," *IEEE Wireless Communications and Networking Conference (WCNC)*, pp. 984-989, March 2005.

[31] D. Gunduz and E. Erkip, "Opportunisti cooperation by dynamic resource allocation," *IEEE Transactions on Wireless Communications*, vol. 6, pp. 1446-1454, April 2007.

[32] M. Dohler, A. Gkelias, and H. Aghvami, "Resource Allocation for FDMA-Based Regenerative Multihop Links," *IEEE Transactions on Wireless Communications*, vol. 3, no. 6, November 2004.

[33] J. Adeane, M. R. D. Rodrigues, and I. J. Wassell, "Centralised and distributed power allocation algorithms in cooperative networks" *IEEE 6th Workshop on Signal Processing Advances in Wireless Communications*, 2005.

[34] M. Chen, S. Serbetli, and A. Yener, "Distributed Power Allocation Strategies for Parallel Relay Networks," *IEEE Transactions on Wireless Communications*, vol. 7, no. 2, Feb. 2008.

[35] Y. Li, B. Vucetic, Z. Zhou, and M. Dohler, "Distributed Adaptive Power Allocation for Wireless Relay Networks," *IEEE Transactions on Wireless Communications*, vol. 6, no. 3, pp. 948-958, March 2007.

[36] R. C. de Lamare and S. Li, "Joint Iterative Power Allocation and Linear Interference Suppression Algorithms for Cooperative DS-CDMA Networks," *IEEE Vehicular Technology Conference (VTC)*, May 2010.

[37] X. Deng and A. Haimovich, "Power allocation for cooperative relaying in wireless networks," *IEEE Transactions on Communications*, vol. 50, no. 12, pp. 3062-3080, July 2005.

[38] J. Boyer, D. D. Falconer, and H. Yanikomeroglu, "Multihop Diversity in Wireless Relaying Channels," *IEEE Transactions on Communications*, vol. 52, no. 10, pp. 1820-1830, October 2004.

[39] H. Gharavi and K. Ban, "Multihop sensor network design for wide-band communications," *Proceedings of the IEEE*, vol. 91, no. 8, pp. 1221-1234, August 2003.

[40] Z. Shelby, C. Pomalaza-Raez, and J. Haapola, "Energy Optimization in Multihop Wireless Embedded and Sensor Networks," *IEEE International Symposium on Personal, Indoor and Mobile Radio Communications (PIMRC)*, September. 2004.

[41] B. Maham and A. Hjorungnes, "Near-Optimum Power Allocation for BER Restricted Multihop Cooperative Networks," *IEEE International Conference on Communications (ICC)*, May 2010.

[42] A. P. T. Lau and S. Cui, "Joint Power Minimization in Wireless Relay Channels," *IEEE Transactions on Wireless Communications*, vol. 6, no. 8, pp. 2820-2824, August 2007.

[43] G. Farhadi and N. C. Beaulieu, "Power-Optimized Amplify-and-Forward Multi-Hop Relaying Systems," *IEEE Transactions on Wireless Communications*, vol. 8, no. 9, pp. 4634-4643, September 2009.

[44] M. O. Hasna and M. Alouini, "Optimal Power Allocation for Relayed Transmissions Over Rayleigh-Fading Channels," *IEEE Transactions on Wireless Communications*, vol. 3, no. 6, pp. 1999-2004, November 2004.

[45] G. Yu, Z. Zhang, Y. Chen, and P. Qiu, "Adaptive Power Allocation for Cooperative Relaying System in Fading Wireless Channel" *International Conference on Wireless Communications, Networking and Mobile Computing*, September 2007.

[46] Y. Zhao, R. Adve, and T. J. Lim, "Improving amplify-and-forward relay networks: optimal power allocation versus selection," *IEEE Trans. on Wireless Commun.*, vol. 6, no. 8, pp. 3114-3123, August 2007.

[47] X. Deng and A. M. Haimovich, "Power Allocation for Cooperative Relaying in Wireless Network," *IEEE Communications Letters*, vol. 9, no. 11, pp. 994-996, November 2005.

[48] C. Yang, W. Wang, G. Yuan and M. Peng, "A Power Allocation Method with Maximum Effective Configuration Duration in Wireless Sensor Networks" *5th International Conference on Broadband Communications, Networks and Systems*, 2008.

[49] B. Gedik and M. Uysal, "Two Channel Estimation Methods for Amplify-and-Forward Relay Networks" *Canadian Conference on Electrical and Computer Engineering (CCECE)*, pp. 615-618, May 2008.

[50] C. S. Patel and G. L. Stuber, "Channel Estimation for Amplify and Forward Relay Based Cooperation Diversity Systems," *IEEE Transactions on Wireless Communications*, vol. 6, no. 6, pp. 2348-2356, June 2007.

[51] F. Gao, T. Cui, and A. Nallanathan, "On Channel Estimation and Optimal Training Design for Amplify and Forward Relay Networks" *IEEE Transactions on Wireless Communications*, vol. 7, no. 5, pp. 1907-1916, May 2008.

[52] J.-L. Yu, I.-T. Lee, "MIMO Capon receiver and channel estimation for space-time coded CDMA systems," *IEEE Transactions on Wireless Communications*, vol. 5, no. 11, pp. 3023-3028, November 2006.

[53] R. C. de Lamare and R. Sampaio-Neto, "Blind adaptive MIMO receivers for space-time block-coded DS-CDMA systems in multipath channels using the constant modulus criterion," *IEEE Transactions on Communications*, vol. 58, no. 1, pp, January 2010. 21-27.

[54] A. S. Lalos, A. A. Rontogiannis, K. Berberidis, "Channel Estimation Techniques in Amplify and Forward Relay Networks" *IEEE 9th Workshop on Signal Processing Advances in Wireless Communications (SPAWC)*, pp. 446-450, July, 2008,

[55] B. Widrow and S. D. Stearns, *Adaptive Signal Processing*, Prentice Hall, Englewood Cliffs, NJ, 1985.

[56] J. R. Treichler, C. R. Johnson, Jr., and M. G. Larimore, *Theory and Design of Adaptive Filters*, JohnWiley & Sons, NewYork, NY, 1987.

[57] B. Farhang-Boroujeny, *Adaptive Filters: Theory and Applications*, John Wiley & Sons, New York, NY, 1998.

[58] A. H. Sayed, *Fundamentals of Adaptive Filtering*, John Wiley & Sons, Hoboken, NJ, 2003.

[59] L. R. Rabiner and R. W. Schaffer, *Digital Processing of Speech Signals*, Prentice Hall, Englewood Cliffs, NJ, 1978.

[60] D. H. Johnson and D. E. Dudgeon, *Array Signal Processing, Prentice Hall*, Englewood Cliffs, NJ, 1993.

[61] P. S. R. Diniz, *Adaptive Filtering: Algorithms and Practical Implementation*, Springer, Boston, MA, 3rd ed, 2008.

[62] D. G. Luenberger, *Introduction to Linear and Nonlinear Programming*, Addison Wesley, Reading, MA, 2nd edition, 1984.

[63] R. Fletcher, *Practical Methods of Optimization*, John Wiley & Sons, NewYork, NY, 2nd edition, 1990.

[64] A. Antoniou and W. S. Lu, *Practical Optimization: Algorithms and Engineering Applications*, Springer, NewYork, NY, 2007.

[65] S. Haykin, *Adaptive Filter Theory*, 4th ed. Englewood Cliffs, NJ: Prentice-Hall, 2002.

[66] S. Gollamudi, S. Nagaraj, S. Kapoor, and Y. F. Huang, "Set-Membership Adaptive Equalization and Updator-Shared Implementation for Multiple Channel Communications Systems" *IEEE Transactions on Signal Processing*, vol. 46, pp. 2372-2384, September 1998.

[67] R. C. de Lamare and P. S. R. Diniz, "Set-Membership Adaptive Algorithms Based on Time-Varying Error Bounds for CDMA Interference Suppression," *IEEE Transactions on Vehicular Technology*, vol. 58, no. 2, pp. 644-654, February 2009.

[68] S. Werner and P. S. R. Diniz, "Set-Membership Affine Projection Algorithm" *IEEE Signal Processing Letters*, vol. 8, pp. 231-235, August 2001.

[69] P. S. R. Diniz and S. Werner, "Set-Membership Binormalized Data-Reusing LMS Algorithms" *IEEE Transactions on Signal Processing*, vol. 51, pp. 124-134, January 2003.

[70] T. Wang, R. C. de Lamare and P. D. Mitchell, "BEACON Channel Estimation for Cooperative Wireless Sensor Networks Based on Data Selection," *IEEE International Symposium on Wireless Communication Systems (ISWCS)*, September 2010.

[71] L. Guo and Y. F. Huang, "Set-Membership Adaptive Filtering with Parameter-Dependent Error Bound Tuning," *IEEE International Conference on Acoustics, and Speech Signal Processing (ICASSP)*, March 2005.

[72] J. F. Galdino, J.A.Apolinario, and M. L. R. de Campos, "A Set-Membership NLMS Algorithm with Time-Varying Error Bound," *IEEE International Symposium on Circuits and Systems*, May 2006.

[73] M. Z. A. Bhotto and A. Antoniou, "A set-membership NLMS algorithm with adaptive error bound," *IEEE Canadian Conference on Electrical and Computer Engngineering*, pp. 2007-2010, May 2008.

[74] T. Wang, R. C. de Lamare, and P. D. Mitchell, "Low-Complexity Set-Membership Channel Estimation for Cooperative Wireless Sensor Networks," *IEEE Transactions on Vehicular Technology (VTC)*, vol. 60, no. 6, May, 2011.

[75] J. G. Proakis, *Digital Communications*, 4th ed. McGraw-Hill, 2000.

[76] S. M. Kay, *Fundumentals of Statistical Signal Processing: Estimation Theory*. Englewood Cliffs, NJ: Prentice-Hall, 1993.

[77] M. Biguesh and A. B. Gershman, "Training-based MIMO channel estimation: a study of estimator tradeoffs and optimal training signals," *IEEE Transactions on Signal Processing*, vol. 54, no. 3, March 2006.

[78] A. Papoulis and S. U. Pillai, *probability random variables and stochastic processes*, 4th ed. McGraw-Hill Education Pvt Ltd, 2002.

[79] T. S. Rappaport, *Wireless Communications*. Englewood Cliffs, NJ:Prentice-Hall, 1996.

[80] P. K. Varshney, Distributed Detection and Data Fusion, Springer-Verlag, 1997.

[81] M. Yu, J. Li, "Is amplify-and-forward practically better than decode-and-forward or vice versa?" *IEEE International Conference on Acoustics, Speech, and Signal Processing (ICASSP)*, March 2005.

[82] J. Huang, Z. Han, M. Chiang, and H. V. Poor, "Auction-Based Resource Allocation for Cooperative Communications," *IEEE Journal on Selected Areas in Communications*, vol. 26, no. 7, pp. 1226-1237, September 2008.

[83] R. D. Juday, "Generalized Rayleigh quotient approach to filter optimization" *Journal of the Optical Society of America*, vol. 15, no. 4, pp. 777-790, April 1998.

[84] T. Wang and R. C. de Lamare, "Joint Receiver Design and Power Allocation Strategies for Wireless Sensor Networks," *Sensor Signal Processing for Defence(SSPD)*, September 2011.

[85] I. Csiszar and G. Tusnady, "Information geometry and alternating minimization procedure," *Statistics and Decisions*, no. 1, pp. 205-237, 1984.

[86] U. Niesen, D. Shah, and G. W. Wornell, "Adaptive alternating minimization algorithms," *IEEE Transactions on Information Theory*, vol. 55, no. 3, pp. 1423-1429, March 2009.

[87] D. S. Watkins, *Fundamentals of Matrix Computations*, 2nd ed. John Wiley & Sons, New York, 2002.

[88] G. H. Golub and C. F. V. Loan, *Matrix Computations*, 3rd ed. Baltimore, MD: Johns Hopkins Univ. Press, 1996.

[89] R. C. de Lamare and P. S. R. Diniz, "Set-Membership Adaptive Algorithms based on Time-Varying Error Bounds for CDMA Interference Suppression," *IEEE Transactions on Vehicular Technology (VTC)*, vol. 58, no. 2, February 2009.

[90] R. C. de Lamare and R. Sampaio-Neto, "Minimum Mean Squared Error Iterative Successive Parallel Arbitrated Decision Feedback Detectors for DS-CDMA Systems," *IEEE Transactions on Communications.* vol. 56, no. 5, May, 2008.

[91] G. D. Golden, C. J. Foschini, R. A. Valenzuela and P. W. Wolniansky, "Detection algorithm and initial laboratory results using V-BLAST space-time communication architecture," *Electronics Letters*, vol. 35, no.1, January 1999.

[92] A. Rontogiannis, V. Kekatos, and K. Berberidis, "A Square-Root Adaptive V-BLAST Algorithm for Fast Time-Varying MIMO Channels," *IEEE Signal Processing Letters*, Vol. 13, No. 5, pp. 265-268, May 2006.

[93] J. H. Choi, H. Y. Yu, Y. H. Lee, "Adaptive MIMO decision feedback equalization for receivers with time-varying channels," *IEEE Transactions on Signal Processing*, 2005, vol. 53, no. 11, pp. 4295-4303, 2005.

[94] R. C. de Lamare, R. Sampaio-Neto, "Adaptive MBER decision feedback multiuser receivers in frequency selective fading channels," *IEEE Communications Letters*, vol. 7, no. 2, pp. 73-75, February 2003.

[95] R. C. de Lamare, R. Sampaio-Neto, A. Hjorungnes, "Joint iterative interference cancellation and parameter estimation for cdma systems," *IEEE Communications Letters*, vol. 11, no. 12, pp. 916-918, December 2007.

[96] P. Li, R. C. de Lamare and R. Fa, "Multiple Feedback Successive Interference Cancellation Detection for Multiuser MIMO Systems," *IEEE Transactions on Wireless Communications*, vol.10, no.8, pp.2434-2439, August 2011.

[97] P. Li, R. C. de Lamare, "Adaptive Decision-Feedback Detection With Constellation Constraints for MIMO Systems," *IEEE Transactions on Vehicular Technology*, vol. 61 , no. 2, pp. 853 - 859, 2012.

[98] I. T. Jolliffe, *Principal component analysis*, New York, Springer Verlag, 1986 (2 ed., 2002).

[99] J. S. Goldstein, I. S. Reed, and L. L. Scharf, "A multistage representation of the Wiener filter based on orthogonal projections," *IEEE Transactions on Information Theory*, vol. 44, November 1998.

[100] M. L. Honig and J. S. Goldstein, "Adaptive reduced-rank interference suppression based on the multistage Wiener filter," *IEEE Transactions on Communications*, vol. 50, pp. 986-994, June 2002.

[101] R. C. de Lamare, M. Haardt and R. Sampaio-Neto, Blind Adaptive Constrained Reduced-Rank Parameter Estimation based on Constant Modulus Design for CDMA Interference Suppression," *IEEE Transactions on Signal Processing*, vol. 56., no. 6, June 2008.

[102] R. C. de Lamare and R. Sampaio-Neto, "Reduced-rank Interference Suppression for DS-CDMA based on Interpolated FIR Filters," *IEEE Communications Letters*, vol. 9, no. 3, March 2005.

[103] R. C. de Lamare and R. Sampaio-Neto, "Adaptive Reduced-Rank MMSE Filtering with Interpolated FIR Filters and Adaptive Interpolators," *IEEE Signal Processing Letters*, vol. 12, no. 3, March, 2005.

[104] R. C. de Lamare and R. Sampaio-Neto, "Adaptive Interference Suppression for DS-CDMA Systems based on Interpolated FIR Filters with Adaptive Interpolators in Multipath Channels", *IEEE Transactions on Vehicular Technology*, vol. 56, no. 6, September 2007.

[105] R. C. de Lamare and R. Sampaio-Neto, "Adaptive Reduced-Rank MMSE Parameter Estimation based on an Adaptive Diversity Combined Decimation and Interpolation Scheme," *IEEE International Conference on Acoustics, Speech and Signal Processing*, vol. 3, pp. III-1317-III-1320, April 2007.

[106] R. C. de Lamare and R. Sampaio-Neto, "Reduced-Rank Adaptive Filtering Based on Joint Iterative Optimization of Adaptive Filters", *IEEE Signal Processing Letters*, vol. 14, no. 12, December 2007.

[107] D. A. Pados and G. N. Karystinos, "An iterative algorithm for the computation of the MVDR filter," *IEEE Transactions on Signal Processing*, vol. 49, no. 2, February, 2001.

[108] H. Qian and S.N. Batalama, "Data record-based criteria for the selection of an auxiliary vector estimator of the MMSE/MVDR filter," *IEEE Transactions on Communications*, vol. 51, no. 10, pp. 1700-1708, October 2003.

[109] Y. Hua, M. Nikpour, and P. Stoica, "Optimal reduced-rank estimation and filtering," *IEEE Transactions on Signal Processing*, vol.49, pp. 457-469, 2001.

[110] R. C. de Lamare and R. Sampaio-Neto, "Reduced-Rank Adaptive Filtering Based on Joint Iterative Optimization of Adaptive Filters," *IEEE Signal Processing Letters*, vol. 14, no. 12, pp. 980-983, December 2007.

[111] R. C. de Lamare and R. Sampaio-Neto, "Adaptive Reduced-Rank Processing Based on Joint and Iterative Interpolation, Decimation and Filtering," *IEEE Transactions on Signal Processing*, vol. 57, no. 7, pp. 2503-2514, July 2009.

[112] R. C. de Lamare, L. wang and R. Fa, "Adaptive Reduced-Rank LCMV Beamforming Algorithm Based on Joint Iterative Optimization of Filters: Design and Analysis," *Elsevier Journal on Signal Processing*, vol. 90, no 2, pp. 640-652, February 2010.

[113] R. C. de Lamare and R. Sampaio-Neto, "Reduced-Rank Space-Time Adaptive Interference Suppression With Joint Iterative Least Squares Algorithms for Spread-Spectrum Systems," *IEEE Transactions on Vehicular Technology*, vol. 59, no. 3, pp. 1217-1228, March 2010.

[114] R. C. de Lamare, R. Sampaio-Neto, M. Haardt, "Blind Adaptive Constrained Constant-Modulus Reduced-Rank Interference Suppression Algorithms Based on Interpolation and Switched Decimation," *IEEE Trans. on Signal Processing*, vol. 59, no. 2, pp. 681-695, February 2011.

[115] R. C. de Lamare and R. Sampaio-Neto, "Adaptive Reduced-Rank Equalization Algorithms Based on Alternating Optimization Design Techniques for MIMO Systems," *IEEE Transactions on Vehicular Technology*, vol. 60, no. 6, pp. 2482-2494, July 2011.

[116] B. Zhao and M. C. Valenti, "Practical relay networks: A generalization of hybrid-ARQ", *IEEE Journal on Selected Areas in Communications*, vol. 23, no. 1, pp. 7-18, January 2005.

[117] J. Luo, R. S. Blum, L. J. Greenstein, L. J. Cimini, and A. M. Haimovich, "New approaches for cooperative use of multiple antennas in ad hoc wireless networks," *IEEE Transactions on Vehicular Technology (VTC)*, vol. 4, pp. 2769-2773, September 2004.

[118] A. S. Ibrahim, A. K. Sadek, W. Su, and K. J. R. Liu, "Cooperative communications with partial channel state information: when to cooperate?" *IEEE Global Telecommunications Conference (Globecom05)*, pp. 3068-3072, vol. 5, November 2005.

[119] Y. Zhao, R. Adve, and T. J. Lim, "symbol error rate of selection amplify-and-forward relay systems," *IEEE Communications Letters*, vol. 10, pp. 757-759, November 2006.

[120] P. Clarke and R. C. de Lamare, "Joint Transmit Diversity Optimization and Relay Selection for Multi-relay Cooperative MIMO Systems Using Discrete Stochastic Algorithms", *IEEE Communications Letters*, vol. 15, no .10, pp. 1035-1037, October 2011.

[121] Y. Zhao, R. Adve, and T. J. Lim, "Improving amplify-and-forward relay networks: optimal power allocation versus selection," *IEEE International Symposium on Information Theory*, pp. 1234-1238, 2006.

[122] Z. Zhou, S. Zhou, J.-H. Cui, and S. Cui, "Energy-efficient cooperative communication based on power control and selective single-relay in wireless sensor networks," *IEEE Transactions on Wireless Communications*, vol. 7, pp. 3066-3078, August 2008.

[123] S. Sudevalayam and P. Kulkarni, "Energy harvesting sensor nodes: Survey and implications," *IEEE Communications Surveys & Tutorials*, vol. 13, no. 3, pp. 443-461, 2011.

[124] A. Kansal, J. Hsu, S. Zahedi, and M. B. Srivastava, "Power Management in Energy Harvesting Sensor Networks," *ACM Transactions on Embedded Computing Systems*, vol. 6, no. 4, 2007.

[125] V. Raghunathan, A. Kansal, J. Hsu, J. Friedman, and M. Srivastava, "Design Considerations for Solar Energy Harvesting Wireless Embedded Systems," *4th International Symposium on Information Processing in Sensor Networks*, pp. 457-462, April 2005.

[126] C. Park and P. Chou, "AmbiMax: Autonomous Energy Harvesting Platform for Multi-Supply Wireless Sensor Nodes," *3rd Annual IEEE Communications Society on Sensor and Ad Hoc Communications and Networks*, vol. 1, pp. 168-177, September 2006.

[127] M. Weimer, T. Paing, and R. Zane, "Remote Area Wind Energy Harvesting for Low-power Autonomous Sensors," *37th IEEE Power Electronics Specialists Conference*, pp. 1-5, June 2006.

[128] S. Chalasani and J. Conrad, "A Survey of Energy Harvesting Sources for Embedded Systems," *IEEE Southeastcon*, pp. 442-447, April 2008.